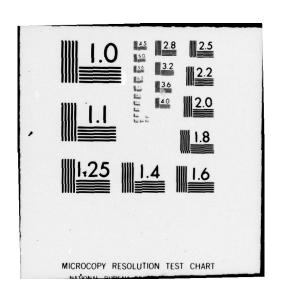
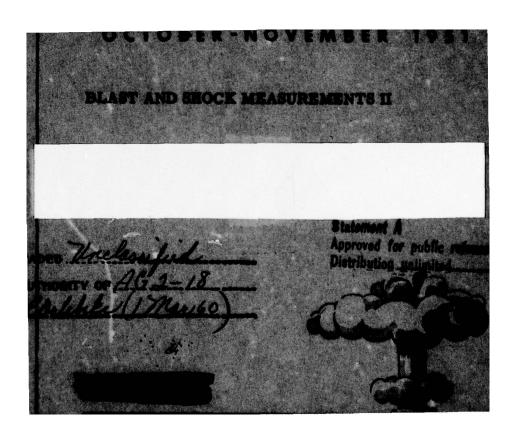
DEFENSE ATOMIC SUPPORT AGENCY WASHINGTON DC F/6 18/3 OPERATION JANGLE. NEVADA PROVING GROUNDS, OCTOBER - NOVEMBER 19-ETC(U) MAR 52 AD-A078 577 AEC-WT-367 UNCLASSIFIED NL 1 OF 3 AD A 078577 *** 0.



PHOTOGRAPH THIS SHEET ADA 0 7857 AEC WT-367 DOCUMENT IDENTIFICATION DISTRIBUTION STATEMENT A Approved for public release; Distribution Unlimited **DISTRIBUTION STATEMENT ACCESSION FOR** NTIS GRAMI DTIC TAB UNANNOUNCED JUSTIFICATION DISTRIBUTION / AVAILABILITY CODES AVAIL AND/OR SPECIAL DATE ACCESSIONED DISTRIBUTION STAMP 79 12 18 556 DATE RECEIVED IN DTIC PHOTOGRAPH THIS SHEET AND RETURN TO DTIC-DDA-2



UNULASSIFIED





This document consists of 227 plus 4 pages (counting all preliminary pages in all reports and all unnumbered blanks)

.. Copy 209 of 243 copies, Series B

OPERATION JANGLE

BLAST AND SHOCK MEASUREMENTS II

Project 1.2b Close-in Ground Measurements (WT-364)

Project 1.3a Free Air Shock Arrival Times (WT-324)

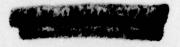
Project 1.3b Free Air Peak Pressure Measurements (WT-389)

Project 1.3c The Measurement of Free Air Atomic Blast Pressures (WT-325)

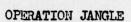
Project 1.4 Air Pressure vs Time (WT-306)

UNULASSIFIED - 53-53-67

Reproduced Direct from Manuscript Copy by AEC Technical Information Service Oak Ridge, Tennessee







PROJECT 1.2b

CLOSE IN GROUND MEASUREMENTS

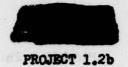
by

CHRELE William F. Gannon, USN



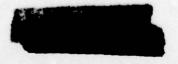
NSWU 471, Field Command, AFSWP Sandia Base, Albuquerque, New Mexico

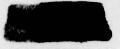




CONTENTS

ABSTRACT .		V
SECTION 1	EARLY WORK OF PROJECT 1.2b	. 1
	L.1 General	. 1
SECTION 2	INSTRUMENTATION	. 2
	2.1 Method of Measurement	. 6
	2.3 Detailed Description of Instruments Employed 2.3.1 Blast Switches 2.3.2 Thyratrons 2.3.3 Electronic Chronograph and Associated Circuits 2.3.4 Drum Camera 2.3.5 Type 250AH Dumont Oscillograph	10
SECTION 3	ESULTS	
	3.1 General	22
SECTION 4	CONCLUSIONS AND RECOMMENDATIONS	24
	.1 General Conclusions	24 26 26



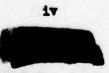


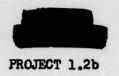
PROJECT 1.2b

ILLUSTRATIONS

SECTION 2	INSTRUMENTATION
	2.1 Electronic Chronograph System
	2.2 Marker Circuit for Drum Camera
	2.3 Blast Switch (Normally Open)
	2.4 Open Switch Thyratron Circuit
	2.3 Blast Switch (Normally Open)
	2.6 Laboratory Hookup for Determining
	Switch Closing Time
	Switch Closing Time
	2.8 Thyratron Chassis (Bottom)
	2.9 Synchro-Thyratron Chassis (Top)
	2.10 Synchro-Thyratron Chassis (Bottom)
	2.11 Synchro-Thyratron Circuit
	2.12 Electronic Chronograph (Signal Side)
	2.13 Electronic Chronograph (Power Side)
	2.14 Electronic Chronograph Signal Amplifier
	and Marker Circuit
	2.15 Electronic Chronograph Amplifier, Marker
	and Control Relays (Top)
	2.16 Electronic Chronograph Amplifier, Marker
	and Control Relays (Bottom)
	2.17 Remote Control Circuit for Electronic
	Chronograph and Amplifiers
	2.18 Drum Camera System
SECTION 4	CONCLUSIONS AND RECOMMENDATIONS
	4.1 Project 1.2b Time of Arrival
	4.2 Chronograph Record
	TABLES
3.1 Data	TABLES on First Arrival in Ground at 17 Foot
	on Underground Shot







ABSTRACT

At the time of the JANGLE underground shot the rate of progression of the underground wave was measured. In addition, an attempt was made to record the rate of expansion of the fireball and the point of break-away of the shock front from the fireball.

In obtaining close-in measurements of blast phenomena, recording is difficult because of ionization in cables produced by gamma radiation and electrical differences in potential set up by ground currents produced at the time of detonation. To overcome these difficulties and derive a suitable system, several methods were considered, tested, rejected, or modified, some as late as two weeks before the blast. Some of the methods considered and rejected were (1) the Wiancko accelerometers (variable reluctance type), (2) the closed loop resistance method, and (3) the open switch (light recording) method.

The two methods finally decided upon were the normally closed thyratron switch and the normally open thyratron switch. For the first method a diaphram—actuated switch was developed, the opening of which removed a fixed bias on a thyratron tube, permitting it to conduct. The switch for the second method was basically the same as that for the first except that the action of the diaphram closed the switch and shorted out the bias on a thyratron tube, causing it to conduct.

The results of the close-in ground measurements showed that, for the first few feet, there was a very large expansion with a velocity of the order of 10⁵ feet per second. From 25 to 100 feet the velocity was approximately 2700 feet per second. During the second hundred feet the average velocity was reduced to 2500 feet per second. Beyond 200 feet the velocity increased to more than 4000 feet per second.

Although the time of arrival data presented in Figure 4.1 is subject to correction, the tests have definitely proved that the velocity of a shock wave traveling through the earth can be measured by using a closed-diaphram switch in conjunction with a thyratron-pulsing circuit. As pointed out in the body of this report, the chronograph employed is subject to improvement.





EARLY WORK OF PROJECT 1.2b

1.1 GENERAL

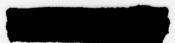
Historically, Project 1.2b had its origin in Program 5 of an operation which was planned to be conducted in the Amchitka area. As WIND-STORM (Secret) Projects 5.5a and 5.5b work on testing, rejecting, or accepting instruments for the required test progressed satisfactorily at the Sandia Corporation "West Lab." Tests were also made on various equipment at the Coyote Canyon firing range. With the indefinite post-ponement of the Amchitka operation all work on these two projects ceased, test equipment and material that was borrowed was returned and all undelivered orders were cancelled.

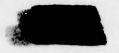
Immediately after all equipment was returned to Sandia Corporation, word was received that the program had been reactivated. Because of limited personnel and time, a meeting was called at Los Alamos in June, 1951, and Dr. Ogle agreed to take over Project 5.5a, then known as The Measurement of the Rate of Expansion of the Fireball and the Point of Breakaway of the Shockwave from the Fireball. It was also decided then to complete the abolishment of Program 5 and transfer the remaining Project 5.5b to Program 1, to be renamed Project 1.2b. CHRELE Gannon assumed duties as Project Officer, Project 1.2b, and with the assistance of G. R. Hunt, ETC, USN designed and built equipment for and completed project measurements at the Nevada Test Site.

1.2 OBJECTIVE

The measurement required of Project 1.2b was the rate of progression of the first underground wave from zero to 333 feet during the underground test. These measurements were to be made at a 17-foot depth which corresponded to the depth of burial of the center of gravity of the weapon.







SECTION 2

INSTRUMENTATION

2.1 METHOD OF MEASUREMENT

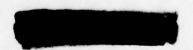
Because equipment which measures the effects of an underground atomic blast should be designed to compensate for the effects caused by ionization and ground currents, the two methods used, one to backup the other, were derived only after considerable experimentation. One method was the normally closed thyratron switch, the other a normally open thyratron switch. Figure 2.1 shows the overall block diagram of both methods.

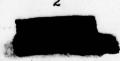
Thirty-one holes, 6 inches in diameter and 17 feet deep, were drilled, and two switches, one normally closed and the other normally open, were placed at 17-foot and 16-foot depths. The cutputs of these switches were connected electrically by RG-8/U coaxial cables to the inputs of type 2D21 thyratrons. Excepting Switch 1, which was used as a fiducial mark for both systems, separate thyratron circuits were used for the different types of switches to reduce the possibility of failure.

The thyratron circuits were in a structure located 350 feet from the bomb along the main blast line. This structure was built 12 feet under the earth's surface to minimize the possibility that the thyratrons would fire prematurely from the effects of ionization. An entrance to the structure was made by a vertical shaft placed adjacent to the shelter. This shaft was filled with sand bags just prior to the blast. The output of each circuit was carried by 8000 feet of RG-8/U coaxial cable to the 8000-foot station and the camera truck revetment, and the ouputs terminated in the input to the chronograph amplifier and the oscillograph in the camera truck.

In the 8000-foot shelter were the electronic-chronograph amplifier and shaper and a marker amplifier and clipper on the same chassis to give reference marks on the 35mm film of the chronograph; the General Radio tuning fork, type 723, to furnish a 1000-cycle input to the marker; two externally driven sweep oscillographs, Dumont type 250AH, with marker circuits to modulate the Z input; various batteries for power and cameras for recording the oscillographs.

The camera truck contained a drum camera for recording and a dual beam ETC oscillograph. The markers for the oscillograph were obtained from a secondary standard oscillator of 100 kilocycles and a clipper marker circuit (Fig. 2.2). The signal appeared on the other half of the dual beam tube, and the action was photographed by the rotating drum camera.





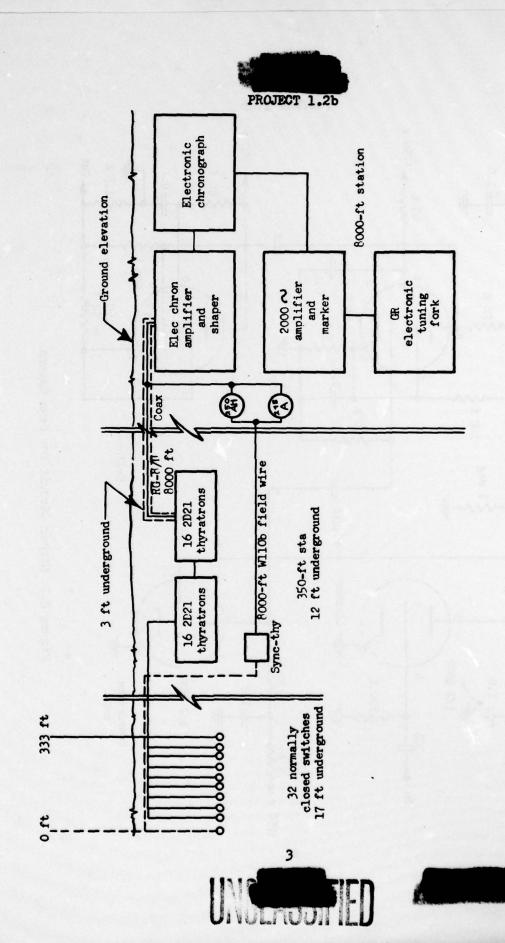


Figure 2.1 Electronic Chronograph System

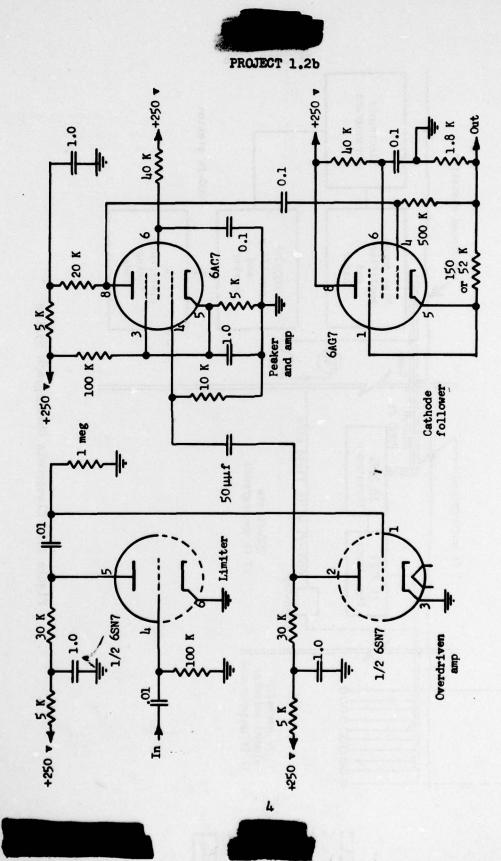
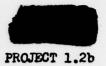


Figure 2.2 Marker Circuit for Drum Camera



2.2 METHODS CONSIDERED AND REJECTED

Methods other than those finally selected include Wiancko accelerometers (variable reluctance type), the closed loop resistance method, and the open switch (light recording) method. Of these the Wiancko accelerometers were rejected because of their slow response time. A brief description of the other two methods, along with the reason for their rejection is presented in the following sub-paragraphs.

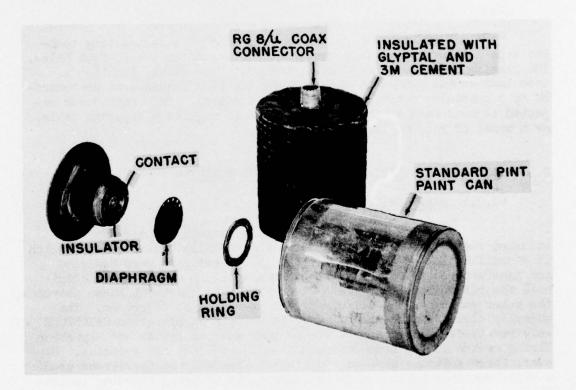
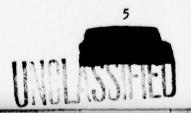
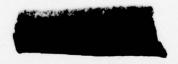
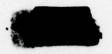


Figure 2.3 Blast Switch (Normally Open)







PROJECT 1.2b

2.2.1 Closed Loop Resistance

This method employs a resistance wire placed in a metal tube, the resistance wire being insulated from the tube. The fireball progressively burns the tube, and the wire thereby changes the resistance against time, the change being recorded on an oscillograph. This method was to be used for the Amchitka test to record the point of breakaway of the shock wave from the fireball. It was rejected for the JANGLE test because it was believed that a 1 KT weapon would not produce sufficient heat to burn the shield required to minimize gamma radiation effects. It was further believed that reducing the diameter of the tube would permit the ionization to short across the tube.

2.2.2 Open Switch

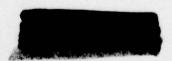
fhe open switch method consisted of a fast-acting tumbler type switch mounted in a container and placed in the 17-foot holes. The passing shock wave would cause the switch to close, lighting a neon lamp at the 8000-foot station, the lighting sequence to be recorded by a specially constructed moving film camera. This method was rejected because each of the 32 switches would require a separate cable, or a total of 256,000 feet of cable.

2.3 DETAILED DESCRIPTION OF INSTRUMENTS EMPLOYED

2.3.1 Blast Switches

Figures 2.3 and 2.4 show the normally open diaphramactuated switch, and Figure 2.5 shows the normally closed switch, which is a modification of the open switch. These switches were designed and manufactured to give a fast-acting electrical contact. To eliminate the possibility that ground currents would short out these switches, the outer container and all wiring was insulated above ground. The normally closed switch was built after reports on Operation SANDSTONE were received. These reports stated that an open switch and thyratron firing method failed because ionization shorted out the switches. However, these switches were of a different type and the thyratrons used a high-impedance input, which is susceptible to being fired by ionization.

As shown in Figure 2.4, the open switches can be adjusted by varying the distance of the contact from the diaphram. This distance was set with a micrometer to 0.015 inch. The thickness of the diaphram was determined by test. It was designed to close the switch upon application of 11 psi of which 9 psi would be the static ground pressure. After the switch was mounted in the container, the container was filled with transformer oil to give a shock-wave transfer medium and to prevent shorting in case of switch leakage.





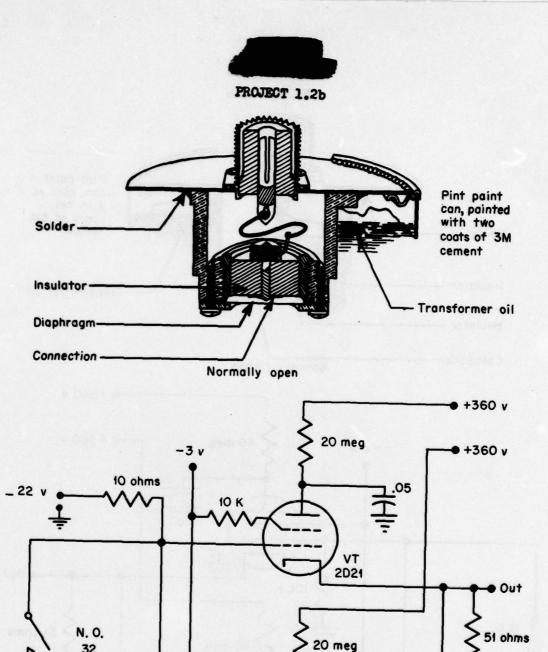
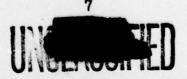


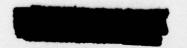
Figure 2.4 Open-Switch Thyratron Circuit

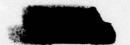
VT 2D21

10 K

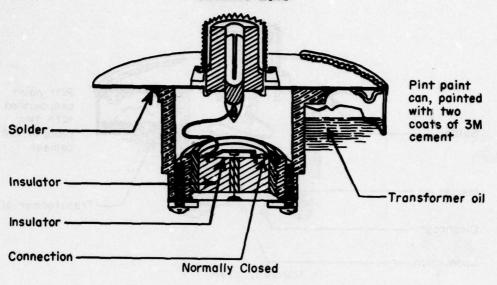
blast switches







PROJECT 1.2b



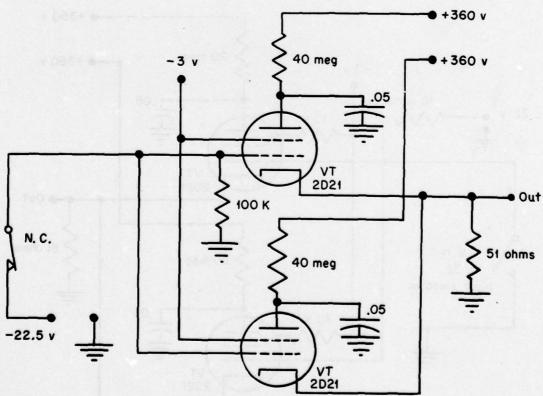
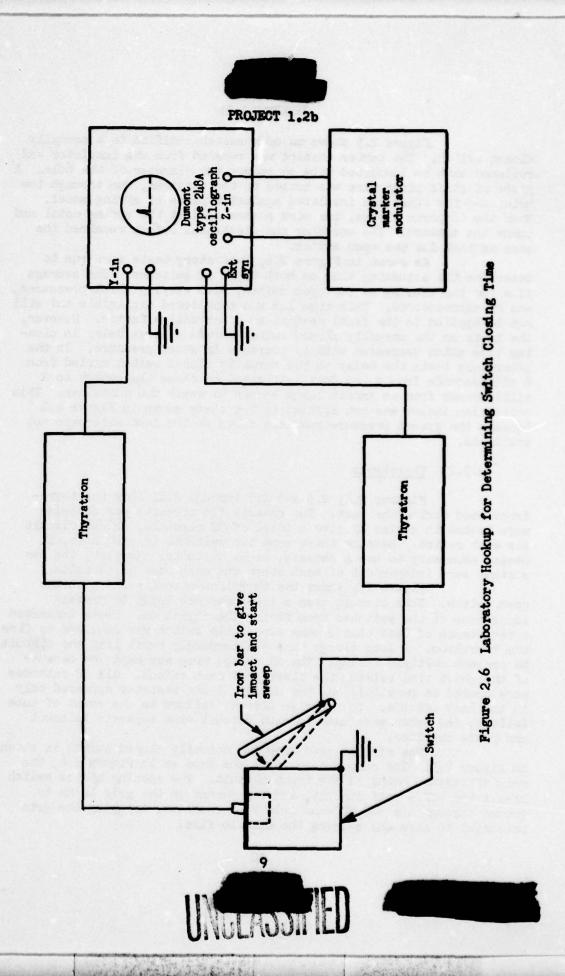


Figure 2.5 Closed-Switch Thyratron Circuit



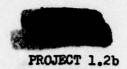


Figure 2.5 shows an open switch modified to a normally closed switch. The center contact was removed from the insulator and replaced with an insulated tube to reduce the diameter of the hole. A piece of stiff piano wire was brazed to the diaphram, run through the hole, and the other end insulated against a piece of spring metal. When the diaphram closes, the wire pushes against the spring metal and opens the contact. The mounting and electrical output remained the

same as that for the open switch.

As shown in Figure 2.6, laboratory tests were run to determine the actuating time on both types of switches. The average time for the closing of the open switch, with varying shock pressures, was 25 microseconds. This time lag was considered negligible and will not be applied to the final results as a corrective factor. However, the tests on the normally closed switch showed a large delay in closing time which decreased with an increase in shock pressure. In the laboratory tests the delay on the normally closed switch varied from 6 milliseconds from a tap just sufficient to close the switch to 2 milliseconds from an impact large enough to wreck the container. This correction factor was not applied to the curve shown in Figure 4.1 because the ground pressure readings taken at the test site were not available.

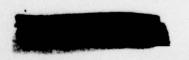
2.3.2 Thyratrons

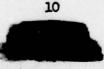
Figures 2.4, 2.5 and 2.7 through 2.11 show the thyratrons used during the test. Two chassis (16 circuits per chassis) were hooked in series to give a total of 32 circuits, or one circuit for each switch. Because there were two switches in each hole, it became necessary to use 4 chassis, or 64 circuits. However, the two systems were independent of each other and each used 32 circuits.

Figure 2.4 shows the thyratron circuit used with the open switch. This circuit uses a low-impedance input to prevent ionization at the switches from firing the thyratron. Tests indicated a resistance of less than 2 ohms across the switch was required to fire the thyratron. A long charge time was purposely built into the circuit to prevent multiple firing. The discharge time was kept low because of the short time between the closing of each switch. All 32 cathodes were hooked in parallel, and the output 51-ohm resistor appeared only in the last cathode. To minimize circuit failure in the event of tube failure, two tubes were used in each circuit with separate filament and plate supplies.

The circuit used with the normally closed switch is shown in Figure 2.5. The output circuit is the same as in Figure 2.4, the only difference being in the input circuit. The opening of the switch breaks the -22.5 volt circuit, and the charge on the grid leaks to ground through the 500,000-ohm grid leak resistor, bringing the grid

potential to zero and causing the tube to fire.







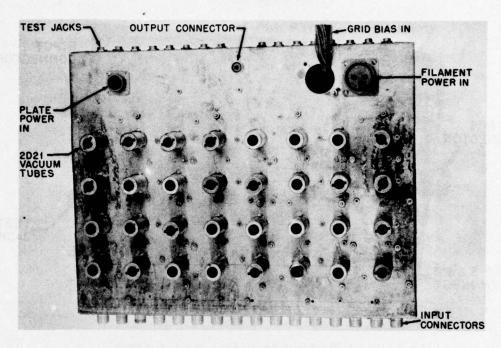


Figure 2.7 Thyratron Chassis (Top)

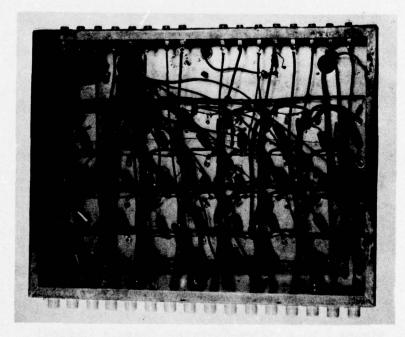
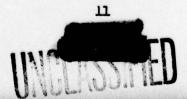
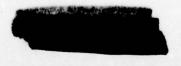
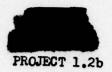


Figure 2.8 Thyratron Chassis (Bottom)







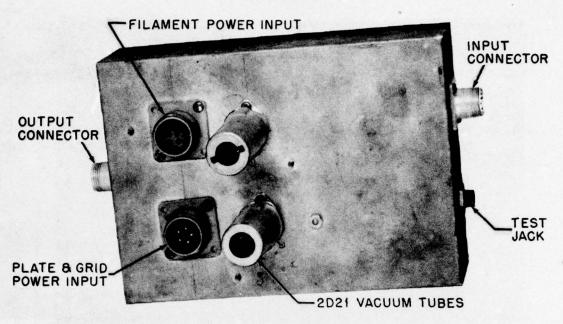


Figure 2.9 Synchro-Thyratron Chassis (Top)

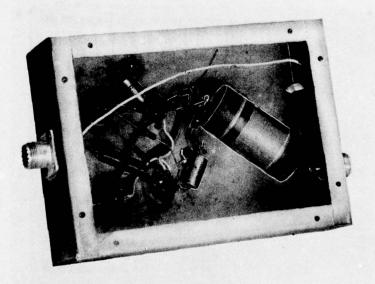
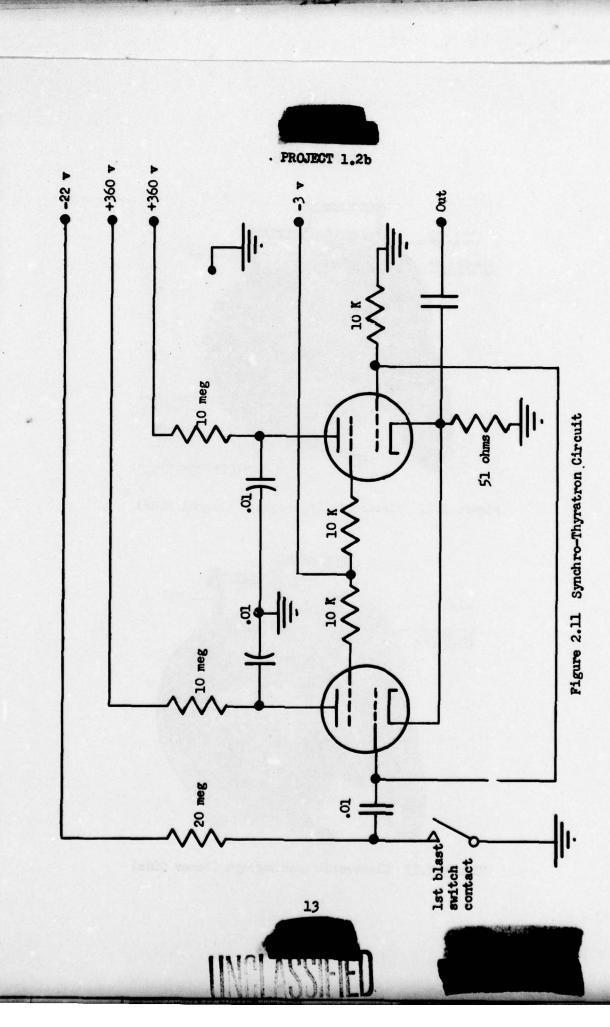


Figure 2.10 Synchro-Thyratron Chassis (Bottom)





PROJECT 1.2b

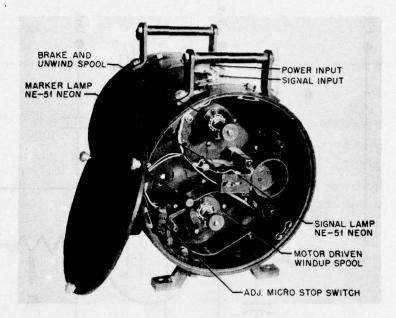


Figure 2.12 Electronic Chronograph (Signal Side)

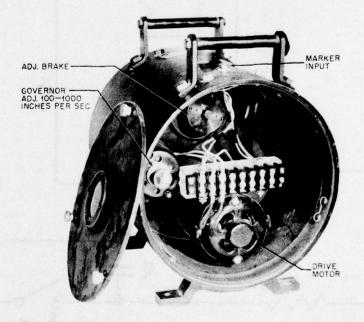
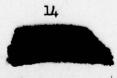
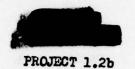


Figure 2.13 Electronic Unronograph (Power Side)







Reports from Oak Ridge National Laboratories state that thyratron tubes are highly sensitive to ionization; therefore these circuits were designed, built, and placed with extreme care.

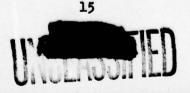
2.3.3 Electronic Chronograph and Associated Circuits

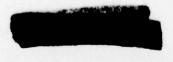
As shown in Figure 2.1, the output of the 32 thyratron circuits terminates into an 8000-foot run of RG-8/U coaxial cable and then into a signal amplifier. The output of this amplifier is used to furnish sharp pulses of short duration to light a neon lamp placed in a recording device which was built up from parts of a Sandia Corporation interferometer gauge and an obsolete Fastax 35-mm recording camera. Because this device records impulses furnished by electronic circuits as against time, it was called an electronic chronograph. Figures 2.12 and 2.13 show the signal and power sides of this device. The film on this chronograph moves continuously. Its operation is as follows (Figure 2.14).

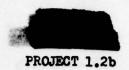
A 100-foot spool of 35-mm film is placed on the unwind spool, and the brake is adjusted for proper unreeling, then run over the holding spool, around the focusing wheel, over the other holding spool, and then into the motor-operated takeup spool. The speed of this 120-volt d-c operated motor is controlled by the governor for various film recording speeds of 100-1000 inches per second. The NE51 neon lamps are placed so that the firing of the marker lamp causes markers to appear on one side of the film and the signal lamp to show a line across the entire width of the film. All electrical connections are through the top of the device.

The signal amplifier is shown in Figures 2.14, 2.15, and 2.16. This amplifier was designed to give a power gain sufficient to light the neon lamp in the chronograph. One-half of the first 5670 vacuum tube is used as an isolation circuit connected as a cathode follower. The other half of the tube is used as a standard resistance-coupled amplifier. The second 5670 tube is used as an amplifier and a cathode follower to isolate the 6AQ5 tube from the amplifiers. This isolation is necessary because of the large amount of grid current drawn by the 6AQ5 tube.

The marker amplifier and shaper shown in Figures 2.14, 2.15, and 2.16 use the output of an electronic tuning fork and amplify it with a 6AQ5 tube. This output is put through a transformer which overdrives the grid of the first half of a 5670 vacuum tube, clipping off the top and bottom of the waveform. A resistance-capacitive circuit in the plate circuit differentiates the waveform. The other half of the tube is used as a cathode follower. Only the positive half of the differentiated waveform is used to fire the 6AQ5 tube and neon lamp. By overdriving the grid of the 5670 tube it is possible to use this circuit as a doubler, or at 2000 cycles per second.







This overall method (Figure 2.1) gave excellent results during the test. However, it is now apparent that several improvements can be made to the normally closed switch so that a comprehensible time delay curve can be run.

Figure 2.17 shows the remote control circuit of the chronograph and amplifier. This circuit used the -15 minute and -1 second time signals for battery and camera operation.

2.3.4 Drum Camera

To minimize the hazard of project failure, a second system was used in addition to the chronograph method. This system used open switches, the 2D21 thyratrons, and the 8000-foot run of RG-8/U coaxial cable (Figure 2.18). The drum camera used was borrowed from the Naval Proving Ground, Dahlgren, Virginia, and consists of a rotating drum 60 inches in circumference and 4 inches wide. The speed of the drum is variable from 50 to 1,800 rpm by varying the speed of the driving motor. The drum is so designed that by closing a switch, either locally or remotely, a spiral gear causes it to move axially across the lens at a rate of one-quarter inch per revolution. This gives a total film recording distance of 960 inches.

The exposure is by means of a solenoid-controlled shutter, and its operation is from the same switch that operates the spiral gear mechanism. The camera lens is a standard f/1.5, with the focus adjustable from 10 to 14 inches, which is the distance the dual beam oscillograph is placed from the camera.

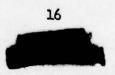
This camera gave excellent results up to 800 inches per second with the oscillograph intensity at normal settings and up to 1200 inches per second with intensity setting 'high'. Recording results were poor beyond 1200 inches per second.

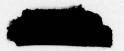
The overall results of this system are considered to be only fair. The camera was operated at 1000 inches per second during the test, and upon and after the closing of the first switch the intensity of the signal beam on the dual beam oscillograph increased tremendously. This increase is believed to be caused by a large voltage introduced into the signal line. Seventy per cent of the closing times of the switches were recorded, but the expected amplitude and shape of the record is not present in the film.

2.3.5 Type 250AH Dumont Oscillograph

The original recording method called for the use of an externally driven Z (intensity) modulated oscillograph having a sweep time of 300 milliseconds. The only high-voltage fast-recording oscillograph having these requirements is made by the Dumont Corporation.







PROJECT 1.2b

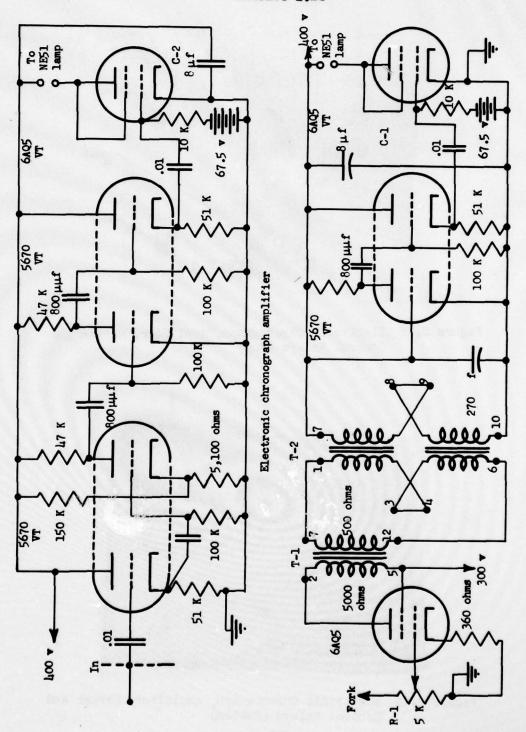
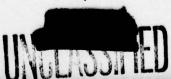
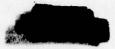


Figure 2.14 Electronic Chronograph Signal Amplifier and Marker Circuit







PROJECT 1.2b

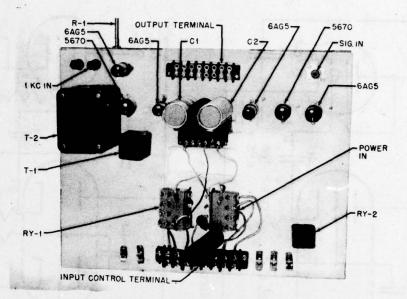


Figure 2.15 Electronic Chronograph, Amplifier, Marker and Control Relays (Top)

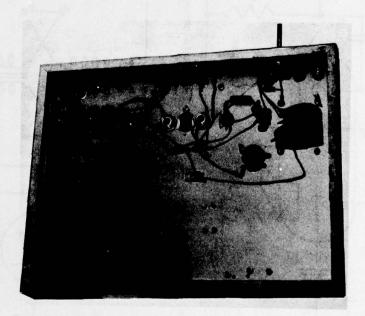
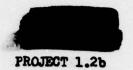


Figure 2.16 Electronic Chronograph, Amplifier, Marker and Control Relays (Bottom)







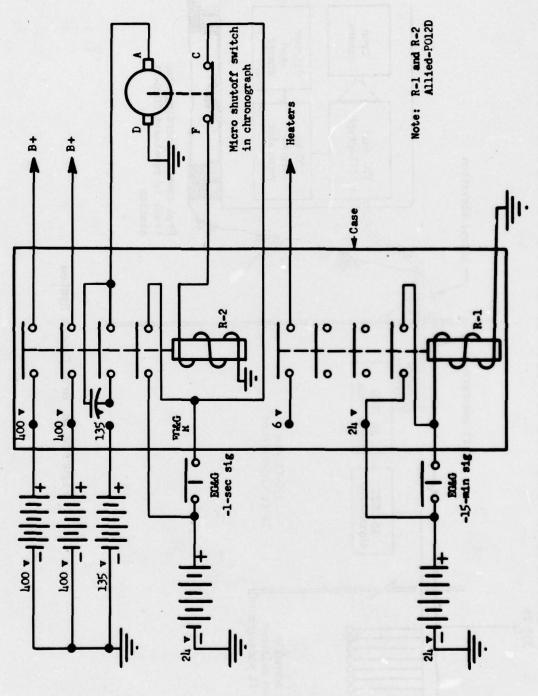


Figure 2.17 Remote Control Circuit for Electronic Chronograph and Amplifiers

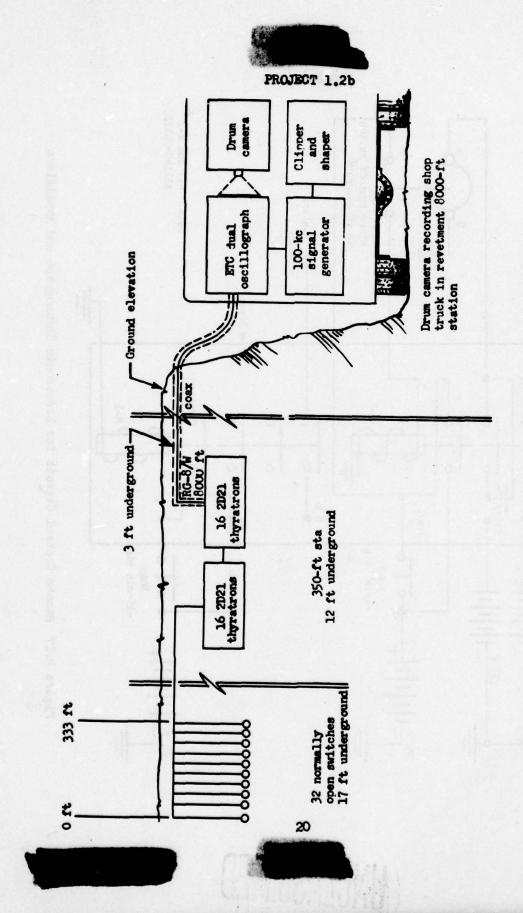
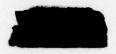


Figure 2.18 Drum Camera System

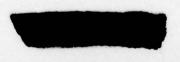


PROJECT 1.2b

In view of the unexpected arrival of the Dumont oscillographs it was decided to use them as a backup method and to obtain additional data on the first few switches. One of these instruments was used as originally planned, and the other was used on the 10millisecond sweep to give an expanded record of the closing of the first ten switches.

To drive the sweep externally, a separate thyratron circuit was built, an additional switch installed at point zero, and 8000 feet of W110b field wire used between the thyratron and oscillograph. This layout is shown in Figure 2.1. The signal input was taken off the same signal line as that to the chronograph. The cameras to record the results were solenoid-operated by the -1 second signal.

Even though considerable pretesting proved the system to be practicable, no records of the blast appeared on the film of either camera when the film was developed. This failure was believed to be caused by synchronizing failure either at the 350-foot station or in the field wire between the 350-foot and the 8000-foot stations.





SECTION 3

RESULTS

3.1 GENERAL

The times of arrival of the first earth motion as a function of distance, are given in tabular form in Table 1 and shown as a curve in Figure 4.1. It will be seen that for the first few feet, there is a terrific expansion with a velocity of the order of 10° feet per second. As the underground gas globe breaks through the ground surface, relief is given to lateral expansion and the lateral velocity drops markedly. From 25 to 100 feet the velocity is roughly 2700 feet per second. During the second hundred feet there is a slight decrease in average velocity to 2500 feet per second. Beyond 200 feet the velocity increases to more than 4000 feet per second.

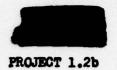
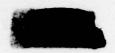


TABLE 3.1

Data on First Arrival in Ground at 17 Foot Depth on Underground Shot

STATION	DISTANCE	DISTANCE ARRIVAL BETWEEN STATIONS				
	feet	TIME Sec x 10	Distance 3 feet	Time Sec x 10 ⁻³	Velocity ft/sec x 10	VELOCITY
1	5.0	0.05	5.0	0.05	100.0	
2	7.8	0.1	2.8	0.05	56.0	
1 2 3 . 4 5 6 7 8 9 10	9.6	0.2	1.8	0.1	18.0	
. 4	11.8	0.3	2.2	0.1	22.0	
5	14.6	0.4	2.8	0.1	28.0	
6	17.5	0.6	2.9	0.2	14.0	
7	21.5	1.6	4.0	1.0	4.0	5-1-600
8	26.0	3.1	4.5	1.5	3.0	
9	31.5	4.2	5.5	1.1	5.0	*
10	39.0	7.5	7.5	3.3	2.3	
11	50.0	11.4	11.0	3.9	2.8	feet/sec
12 13	53.0	13.5	3.0	2.1	1.4	. •
13	57.0	15.6	4.0	2.1	1.9	*
14	62.0	18.6	5.0	3.0	1.9	2
15	68.0	21.2	6.0	2.6	2.3	0
16	75.0	24.0	7.0	2.8	2.5	2700
17	83.0	27.0	8.0	3.0	2.7	· · · · · · · · · · · · · · · · · · ·
18	93.0	29.4	10.0	2.4	4.2	
19	102.0	30.0	9.0	0.6	1.5	
20	112.0	32.5	10.0	2.5	4.0	
21	123.0	36.5	11.0	4.0	2.7	9
22	135.0	40.0	12.0	3.5	3.4	-
23	148.0	44.3	13.0	4.3 5.1	3.0	*
24	162.0	49.4	14.0	5.1	2.7	4
25	177.0	51.2	15.0	1.8	0.8	2
26	193.0	60.0	16.0	8.8	0.8	2500 feet/sec
27	213.0	68.8	20.0	8.8	2.3	
28	237.0	71.2	24.0	3.4	7.0	
29	265.0	78.7	28.0	7.5	3.7	2
30	297.0	89.0	32.0	10.3	3.1 7	8 5
31	333.0	96.5	36.0	7.5	4.8)	4200 feet/sec



SECTION 4

CONCLUSIONS AND RECOMMENDATIONS

4.1 GENERAL CONCLUSIONS

Tests have shown that the velocity of a shock wave traveling through the earth can be measured by using a closed diaphram switch in conjunction with a thyratron-pulsing circuit, provided extreme care is taken in the design of both. The readings obtained from tests using this method are subject to correction because of the delay in the opening of the switch contacts after the diaphram was actuated by the shock wave. Because adequate test equipment was not available and because there was not sufficient time applied to the correction factors, test results had to be obtained from crude laboratory tests (Figure 2.6) and incomplete readings taken with the drum camera. Time of arrival data, based on the work of this project are given in Figure 4.1.

If more accurate definition is required than that given in the corrected time-of-arrival curve in this report, a program should be set up to test the normally closed switch and obtain definite delay times for various operating pressures.

The use of a fast-moving 35-mm film, which recorded a flashing neon lamp, gave excellent results. Like all prototype models, this chronograph is subject to improvement.

Results obtained from the normally open switch method were not satisfactory because of the probable introduction of ionization and/or transient voltages of sufficient strength to cause intermittent failure of the readings.

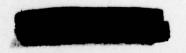
A distance of 8000 feet from 'blast zero' for the underground recording station is considered excessive. Any reduction in distance would not only tend to aid the logistic problem of cable but would help maintain the shape of the pulse and reduce attenuation.

4.2 RECOMMENDATIONS FOR FUTURE INSTRUMENTATION

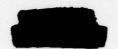
If the requirements for future operations of this kind are the same, it is recommended that the following equipment be further developed and used for the indicated distances.

4.2.1 From Blast Zero to 30 Feet

A closed resistance method, the sequence of operation to be recorded on an oscillograph using a 'raster' method. This recording method has been developed and gives excellent results. The procurement of the equipment should be no problem.







PROJECT 1.2b

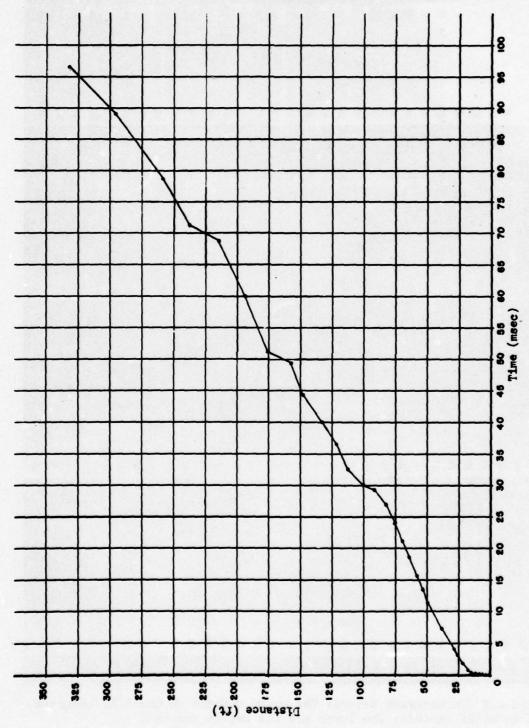


Figure 4.1 Project 1.2b Time of Arrival

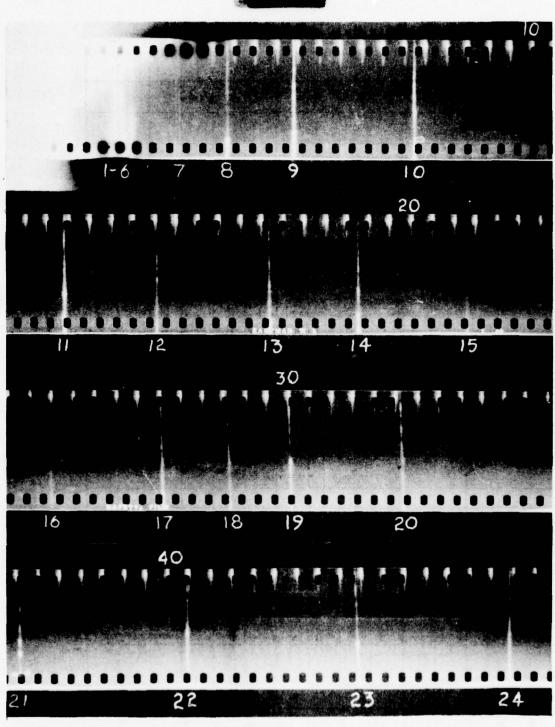
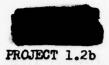


Figure 4.2 Chronograph Record: The upper numbers on the film indicate time in milli seconds; the lower are the switch numbers.



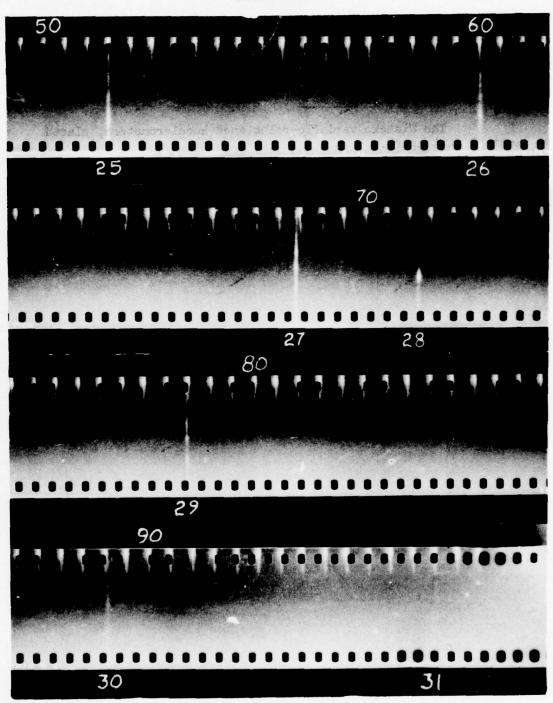
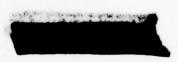
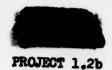


Figure 4.2 (Cont.)

27







4.2.2 From 30 to 150 Feet

An improved, normally closed diaphram-operated switch, using the same chronograph recording method discussed in this report.

4.2.3 From 150 to 350 Feet

The Wiancko variable-reluctance accelerometers, placed at least 50 feet apart.



OPERATION JANGLE

Project 1.3a

FREE AIR SHOCK ARRIVAL TIMES

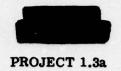
by

S. Rankowitz R.L. Chase J.B.H. Kuper

May 23, 1952

Brookhaven National Laboratory
Upton, N.Y.





ACKNOWLEDGEMENTS

It is a pleasure to acknowledge the assistance of Professor W. Bleakney of Princeton University on problems connected with shock measurements. Numerous members of the Brookhaven Laboratory staff contributed to the project, especially W.A. Higinbotham, H. McChesney, Jr., Martin Graham, John Garfield, E.H. Foster, F. Heemsoth, S.G. MacCormack and R. Rakenius.

The U.S. Weather Bureau is to be thanked for the loan of a theodolite and the Air Force for the loan of a Fairchild oscilloscope camera.





CONTENTS

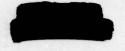
ABSTRA	ACT
СНАРТ	ER 1 INTRODUCTION
1.1	Objective
1.2	Historical and Theoretical
CHAPT	ER 2 OPERATION OF SYSTEM
2.1	Instrumentation
	Surface Shot
2.3	Underground Shot 8
CHAPTI	ER 3 ANALYSIS 20
3.1	Operations
3.2	Summary of Results
	3.2.1 Arrival time
	3.2.2 Pressure Gage
3.3	Conclusions





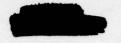
ILLUSTRATIONS

Fig. 2.1 Airborne Unit Showing Pie Plate and Power Supply Assemblies	11
Fig. 2.2 Block Diagram of Airborne Unit	12
Fig. 2.3 Airborne Vibrator Power Supply Schematic	12
Fig. 2.4 Airborne Unit Assembled	13
Fig. 2.5 Kytoons	13
Fig. 2.6 Airborne Unit Supported by Kytoons and Meteorological Balloons	14
Fig. 2.7 Block Diagram of Ground Station Recording Equipment	15
Fig. 2.8 Timing Circuit and Mixer for Blast Switch Data	15
Fig. 2.9 Band Pass Filter	16
Fig. 2.10 1000 Cycle Timing Circuit	17
Fig. 2.11 Block Diagram for Analyzing Magnetic Tape Recordings .	17
Fig. 2.12 Frequency Discriminator Schematic	18
Fig. 2.13 Timing Circuit Used in Analyzing Tape Recordings	18
Fig. 2.14 Location of Airborne Units	19
Fig. 3.1 Surface Shot: Blast Switches Subcarrier - Assembly 1	24
Fig. 3.2 Surface Shot: Assembly 1 - 40 psi Gage Record After Frequency Discrimination of Subcarrier and 1 kc Timing Wave	24
Fig. 3.3 Underground Shot: Upper Trace - Blast Switch Subcarrier Assembly 2 Lower Trace - Blast Switch Subcarrier Assembly 1	25
Fig. 3.4 Underground Shot: Assembly 2 - 5 psi Gage Record After Frequency Discriminations of Subcarrier and 1 kc Timing Wave	26



TABLES

Table 2.1.	Weights of Equipment and Lines	5
Table 2.2.	Location of Assembly 1, Surface Shot	8
Table 2.3.	Location of Assembly 1, Underground Shot	9
Table 2.4.	Location of Assembly 2, Underground Shot	9
Table 3.1.	Arrival Time Data	21
Table 3.2.	Comparison With Project 1.2a and Project 1.3b Data .	21



ABSTRACT

In order to provide data for correlation with results of other test shots, it was decided to measure the time of arrival of the shock wave at two points in free air along a line making an angle of 30° with the horizontal. An attempt was also made to measure the peak overpressure at the same two points. The points selected were at approximate ranges of 800 and 1200 feet from zero, at altitudes of 400 and 600 feet respectively. A combination of blast switches and pressure pickups was used. Information was telemetered to a manned recording station, using an FM/FM system. A combination of oscilloscope photography and tape recording was worked out to provide accurate time measurements and pressure indication. Balloons were used to suspend the equipment at the desired locations, and Program 4 undertook to determine photographically the exact location of the pickups as near as possible to the time of arrival of the wave.

Balloon failure limited the data obtained on the surface shot to the 800 ft. point. On the underground shot failure of an antenna resulted in a weak signal from the 800 ft. point so that only the blast switch information is available for that location. Arrival time information was obtained from both types of pickups at the 1200 ft. location. In neither case were the instrument locations determined, so they were estimated from the balloon positions.

The corrected arrival times are significantly (12 to 16 percent) shorter than those reported by Project 1.2a using gages near the ground.





CHAPTER 1

INTRODUCTION

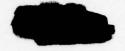
1.1 OBJECTIVE

In order to provide information on the energy partition between the ground and air for surface and subsurface explosions, and to permit correlating the effects of those explosions on structures with those observed in air bursts, it was planned to make measurements of the time of arrival of the shock wave at points sufficiently removed from the perturbing influences of the ground or test structures to yield a "free air" measurement. To minimize uncertainties with regard to the shape of the pressure wave it seemed advisable to use a combination of the direct and indirect methods.

1.2 HISTORICAL AND THEORETICAL

The whole philosophy of this project has been profoundly affected by the change in location and date from the original WINDSTORM plan. In particular, since it appeared likely that no other free air pressure measurements were to be attempted in WINDSTORM, in the early thinking reliability was stressed at the expense of detailed information, and the choice of equipment was dictated primarily by consideration of availability on a tight delivery schedule. This project did not provide for time-of-arrival data from a sufficient number of closely spaced positions to permit calculation of peak overpressures by the method employed in the GREENHOUSE Project 1.6. The subsequent addition of Project 1.3b employing rocket smoke trails was expected to provide time-of-arrival information at a large enough number of points in space to permit conclusions to be drawn concerning the symmetry of the shock wave. The original proposal called for two pairs of pickups to be located vertically one above the other so that in the event of failure of one of the telemetering transmitters time-of-arrival information would still be obtained at two points, which would not, however, be on a radial line from the explosion. Later it was felt more important to attempt to correlate the direct and indirect pressure measurements. Cutting the pickup locations from four to two effected an appreciable saving in weight and also eliminated the problem of failure of the signal





cable due to the thermal radiation. The kite balloons originally selected for WINDSTORM have rather little static lift but perform very well in winds of 15 to 20 miles an hour. The change to the Nevada site entailed a loss of approximately 50 percent of the static lift because of the altitude. To insure sufficient lift when the wind fell below perhaps ten miles per hour, additional round rubber balloons of the type used in meteorological work were employed.

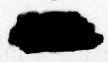
In previous weapons tests various methods have been used to obtain information on the blast pressures produced in free air. Because of obvious instrumental difficulties, in many cases the peak pressure has been inferred by calculation from the time of arrival of the shock. This method was used, for example, in Project 1.6 of the GREENHOUSE operation.

An inherent weakness of this method is that it may lead to incorrect estimates of the peak overpressure in any case where a multiple shock is encountered. For this reason it was decided to attempt to make pressure measurements directly, in addition to time-of-arrival observations, in the hope of obtaining an internal check on the data. Measurements of diffraction of shock waves by Bleakney, White and Griffith² indicate that if pressure pickups are located in baffles placed parallel to the direction of propagation of the shock, reasonable accuracy can be attained, provided the distance to the edge of the baffle is at least three to five times the baffle thickness.

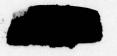
Somewhat arbitrarily it was decided to make the measurements along a radial line, making an angle of 30° with the horizontal, at distances of 800 ft. and 1200 ft. In contrast to air bursts or tower shots, in the JANGLE shots the reflected wave was practically coincident with the primary one, and so there was no question of locating the equipment above the triple point. Thus it was possible to choose convenient altitudes sufficient to be clear of ground disturbances.

The GREENHOUSE Project 1.6 report cited above contains an excellent discussion of the errors involved in time-of-arrival measurements and of the factors peculiar to atomic explosions which might

^{2.} Bleakney, White and Griffith, Journal Applied Mechanics, Page 439, Dec. 1950.



Frolick, Lt. Col. A.J., C.E., USA and personnel from AFSWP, "The Measurement of Free Air Peak Pressures by Telemetering from Moored Balloons", June, 1951.



affect the performance of the measuring and telemetering equipment. Because of the small yield, the effects of the JANGLE surface shot attributable to gamma and thermal radiation were considerably less than those encountered at GREENHOUSE. Calculations of the radio attenuation by the equations derived by Foner predicted a loss of only 2 db for a transmitter located 800 ft. from zero at 0.1 sec. after the explosion. The expected temperature rise with the equipment housed in an aluminum container was quite negligible. Radiation effects were, of course, markedly less for the underground shot. It was expected that the balloons used for suspending the equipment would not survive the thermal radiation and also that the nylon cords used for anchoring the equipment would melt. Therefore, no provision for a quick-acting cable release was believed necessary.

Program Four undertook to determine the exact locations of the pickups by photographic methods just prior to the shots.





CHAPTER 2

OPERATION OF SYSTEM

2.1 INSTRUMENTATION

The basic instrumentation is made up of components of the AN/DKT-3 subminiature telemetering system as supplied by the Pacific Division of Bendix Aviation Corp., North Hollywood, Calif. TTP-9 pressure gages in various ranges were used with TOL-5 subcarrier oscillators modulating TXV-4A frequency modulated transmitters. These have rated power outputs of 2 watts in the 230 megacycle telemetering band. In addition to the pressure pickups, blast switches as designed by Higgins of Johns Hopkins University Applied Physics Laboratory were used. Subcarrier frequencies of 5.8, 9.5 and 15.5 kc were used for the pressure gages and a frequency of 50 kc for the blast switches. The airborne transmitter fed a half wave antenna of the "skinback" type suspended vertically below the transmitter casing. The pressure pickups and telemetering gear, with the exception of power supply and antenna, were housed in shallow cylindrical containers formed by a pair of spun aluminum pie plates (Figure 2.1) each 15 in. in diameter and one in. deep, sealed around the edges. The openings for the pressure pickups are located near the centers of the pie plates and the suspension from the balloons was so arranged that the flat faces were parallel to the direction of propagation of the shock. If, because of yawing action in the wind, this orientation was not maintained exactly, the pressure readings on the two sides of the case would differ and it was expected that the true pressure could be estimated. At each location two pressure ranges were employed to minimize the possibility of obtaining off-scale readings or readings too small to be useful. No detailed information is available concerning the speed of response of the TTP-9 pressure gages under shock conditions, but it was felt that this might be undesirably slow, particularly in the low pressure ranges. The blast switches were designed to operate at pressures of the order of two pounds and give a clean indication of arrival time. A block diagram of the airborne unit is shown in Figure 2.2.

Because of the rather heavy current drain of the transmitter (6.3 volts at 0.6 amp. and 180 volts at 60 ma) it was difficult to select batteries that would operate the equipment for two to three hours and not contribute excessive weight. In the past special dry battery packs have



been made up, but the procurement situation made this inadvisable. Yardney "Silvercel" storage batteries, Type 20-HR-15, were finally selected as the primary source with a home-made vibrator high voltage supply (Figure 2.3). The complete power supply capable of running the airborne equipment for 5 hours weighs 8 pounds. It is housed in a cylinder (4 in. dia., 20 in. long) made of 1/32 in. aluminum (Figure 2.4). This type of power supply has the great advantage that the output voltage (which, of course, affects transmitter power and frequency) remains substantially constant until the batteries are nearly discharged. Also, the provision of a simple charger eliminated worries about shelf life under adverse storage conditions.

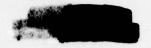
The airborne equipment was suspended below a pair of kite balloons (Jalbert Aerological Laboratory JX-6) which have a capacity of 400 cubic ft. (Figure 2.5). At sea level and 20°C temperature one of these balloons will give a net lift of 9 lbs. when filled with helium. At the altitude of the test site, about 4200 ft. above mean sea level, this static lift decreased to 4.5 lbs. The balloons, flown side by side in pairs, were anchored with three nylon lines in a pyramidal arrangement, with the equipment suspended from the apex of the pyramid by short tie wires to maintain the orientation or the baffle containers. The upwind nylon line was tested at 500 lbs. and weighs 1 lb. per 210 ft. The other two lines were tested at 160 lbs. and weigh considerably less. The total weight to be lifted to altitudes of 400 and 600 ft. respectively is shown in Table 2.1.

TABLE 2.1
Weights of Equipment and Lines

	400 ft.	600 ft.
Telemetering equipment and case	4 lbs.	4 lbs.
Power supply	8 lbs.	8 lbs.
Flying Lines	4 lbs.	6 lbs.
Total	16 lbs.	18 lbs.

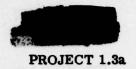
With a moderate wind the two kite balloons are easily capable of lifting this load, but to guard against the possibility of the rig sagging and the lines fouling objects on the ground if the wind should drop, even





momentarily, additional lift was furnished with two rubber meteorological balloons, holding approximately 200 cu. ft. of helium each. These balloons were attached to the flying line between the kite balloons and the apex of the pyramid (Figure 2.6).

Signals from the airborne transmitters were received on Clarke Model 167E telemetering receivers fed by simple Yagi antennas. The composite signals, together with a 1000 cycle timing wave were recorded on Ampex Model 302 telemetering tape recorders. A block diagram of the receiving equipment is shown in Figure 2.7. It was found necessary to use specially selected tape to minimize "nodule noise." In addition, the signal from the blast switches was separated off with a high pass filter (Figure 2.8) and displayed on an oscilloscope which was photographed with a moving film camera. A dual-beam oscilloscope was employed for this purpose so that a single oscilloscope and camera was capable of recording signals from both locations. In order to lose as little as possible of the speed of response of the entire system, the telemetering subcarrier frequencies were chosen with somewhat greater separations than are conventionally used. Specially designed filters (Figure 2.9) with a bandwidth of 10 percent attenuate the adjacent carrier by 26 db. The original composite magnetic tape record was rerecorded with the appropriate filter combinations to produce individual records for each of the pickups with a timing wave. This timing wave was modulated with the zero time signal (Figure 2.10). Special circuitry was devised for measuring the time between successive cycles of the subcarrier frequencies (see Figures 2.11 and 2.12). This is accomplished by triggering a one-shot multivibrator at a definite point in each cycle. The multivibrator is proportioned so as to flip back before the end of the cycle. When the multivibrator flips back it starts a sawtooth which is cut off when the multivibrator is retriggered at the start of the next cycle. Thus, the voltage developed by the sawtooth is a measure of the difference between the length of the signal cycle and duration of the first phase of the multivibrator cycle. A condenser is charged by the sawtooth and is "clamped" at the end of each cycle. Thus, the voltage on the condenser is a measure of the incoming subcarrier frequency. This voltage is displayed on the oscilloscope along with the timing wave (Figure 2.13) and the received signal. The oscilloscope is photographed with a moving film camera so that it is easy to locate the time of arrival of the blast and to measure the peak pressure as indicated by the change in frequency.



2.2 SURFACE SHOT

The two telemetering assemblies were supported as shown in Figure 2.14. Because the static lift of the kite balloons at the altitude of the site was insufficient, two round meteorological balloons with approximately 200 cu. ft. of helium each were tied to the line between the kite balloons and the pickup equipment.

At about one hour before shot time one of the kite balloons at the Assembly 2 position burst, releasing the helium. The weight of the torn balloon which remained tied to the assembly dragged it to the ground. No results were obtained from this position.

Because of photographic difficulties Program 4 was unable to locate the instruments. The only measurements which could be obtained were the positions of the meteorological balloons, and an attempt was made to estimate the location of the instruments, as follows: These balloons were tied to the main flying line between the pie plate and the kite balloons from lines approximately 8 ft.long. The length of line from the pie plate to the tie point of the lower balloon was approximately equal to the length of the line between the tie points of the two meteorological balloons. From the positions of the round balloons the line length between them was determined. This distance was assumed to be the distance between the pie plate and the tie point for the lower balloon. The angle of line holding the balloon to the main line was estimated and a correction added to the line length between the pie plate and the lower balloon tie point. In this manner the position of the pie plate was estimated. The positions of the balloons from ground zero with their limits of error as obtained from Program 4, and the estimated positions of the pickup equipment are indicated in Table 2.2.

Zero time was obtained from a "blue box" supplied by EG and G.

The uncorrected time of arrival of the shock wave at the Assembly 1 point obtained from the blast switches was 4.5 percent less than the time recorded from the pressure gages, all of which agreed with each other.

The two 40 psi gages located on opposite faces of the "pie plate" at the Assembly 1 position gave very different readings, indicating that the



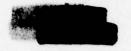


TABLE 2.2

Location of Assembly 1, Surface Shot

Assembly 1	Vertical (feet)	South (feet)	West (feet)	Radial dis- tance from zero (feet)
Bottom of upper balloon	461 ± 5	242 ± 5	674 ± 5	850 ± 10
Bottom of lower balloon	446 ± 5	259 ± 5	674 [±] 5	850 ± 10
Estimated position of pickups	427 ± 15	280 ± 10	674 [±] 5	845 [±] 20

assembly did not remain in the desired orientation with the axis perpendicular to the radial line to zero. One subcarrier (that indicating the higher pressure) disappeared 6 milliseconds after arrival of the shock; the other continued in operation. It is believed that the disappearance of the subcarrier resulted from the shorting out of the subcarrier oscillator due to partial collapse of the "pie plate" housing under the pressure. No evidence of radio attenuation by the ionized gases was observed. As expected, the balloons caught fire and were consumed; whether the nylon lines melted or were parted by the wind was not determined. The signals were observed for nearly 30 sec. after the shot, indicating that the burning balloons still acted as parachutes.

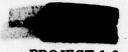
The failure of the kite balloon could probably have been prevented by a suitable relief valve, which was omitted to save weight.

2.3 UNDERGROUND SHOT

The assemblies of the telemetering equipment and balloons were flown in the same manner and at the same positions with respect to ground zero as in the surface shot, except that more sensitive gages were used, as shown in Figure 2.14.

Again Program 4 was unsuccessful in locating the instruments, but





did furnish the positions of the balloons. The positions of the pie plates were estimated in the same manner as in the surface shot. The positions of the balloons from ground zero, with their limits of error as obtained from Program 4, and the estimated positions of the pickup equipment are indicated in the tables below.

TABLE 2.3

Location of Assembly 1, Underground Shot

Assembly 1	Vertical (feet)	South (feet)	West (feet)	Radial dis- tance from zero (feet)
Bottom of upper balloon	350 ± 5	580 ± 5	257 ± 5	723 [±] 10
Bottom of lower balloon	337 ± 5	584 [±] 5	256 ± 5	720 [±] 10
Estimated position of pickups	317 ⁺ 15	586 [±] 10	256 ⁺ 5	713 [±] 20

TABLE 2.4

Location of Assembly 2, Underground Shot

Assembly 2	Vertical (feet)	South (feet)	West (feet)	Radial dis- tance from zero (feet)
Bottom of upper balloon	615 - 10	868 ± 10	530 ± 10	1190 ± 20
Bottom of lower balloon	594 ± 10	873 ± 10	527 ⁺ 10	1183 [±] 20
Estimated position of pickups	565 ± 20	880 [±] 15	523 [‡] 15	1170 ± 30





Due to an error in transmitting the requirements of this project to EG and G, they made no provision for a zero time signal with sufficient accuracy, so it was necessary to improvise a method for producing this signal. This was accomplished simply by running a cable from the telemetering station to ground zero. The voltage induced in the cable at zero time provided a good signal.

The transmitting antenna at the Assembly I position became disconnected or was broken aloft, and as a result the signal at the telemetering receiver station from this point was not sufficient to produce complete limiting in the FM receiver. Nevertheless, the time of arrival recorded from the blast switches was easily detected to within one millisecond. It was impossible to determine any timing information from the pressure gages because the noise prevented proper discriminations of the FM subcarriers associated with the gages.

As in the surface shot, the uncorrected time of arrival of the shock wave at the Assembly 2 position obtained from the blast switches was 4.5 percent less than the time recorded from the pressure gages, all of which agreed with each other.

Because of the repeated postponements of this shot the telemetering transmitters were on the air for a much longer time than anticipated. The batteries, however, held up for the full time with no indication of failing signal strength.





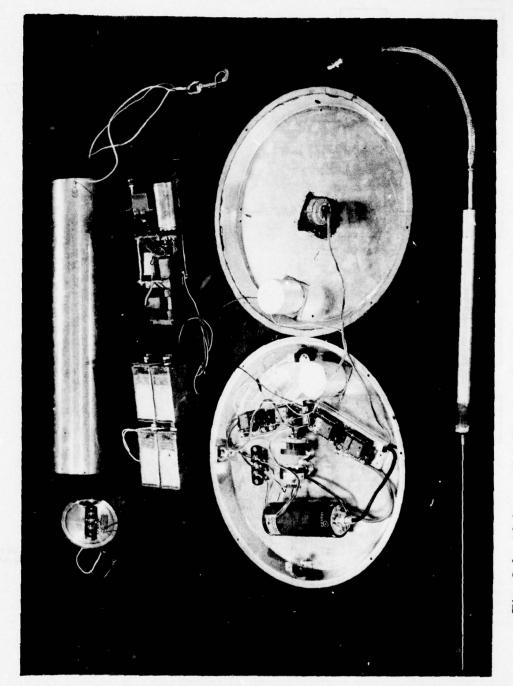
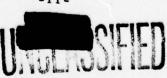


Fig. 2.1 Airborne Unit Showing Pie Plate and Power Supply Assemblies









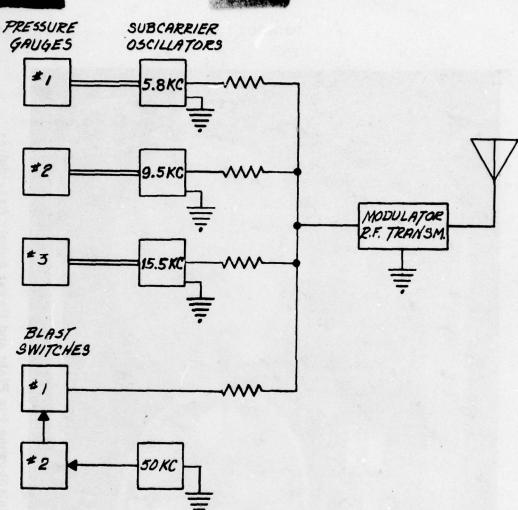


Fig. 2.2 Block Diagram of Airborne Unit

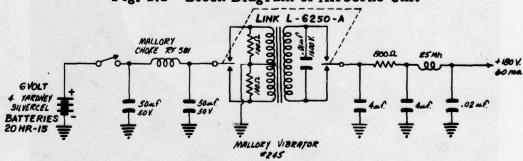


Fig. 2.3 Airborne Vibrator Power Supply Schematic '





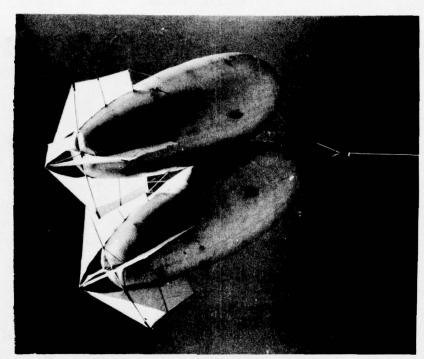


Fig. 2.5 Kytoons

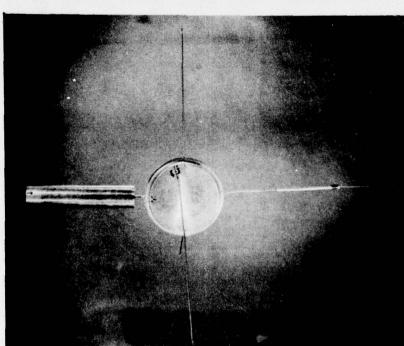


Fig. 2.4 Airborne Unit Assembled

-13-

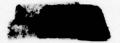




Fig. 2.6 Airborne Unit Supported by Kytoons and Meteorological Balloons





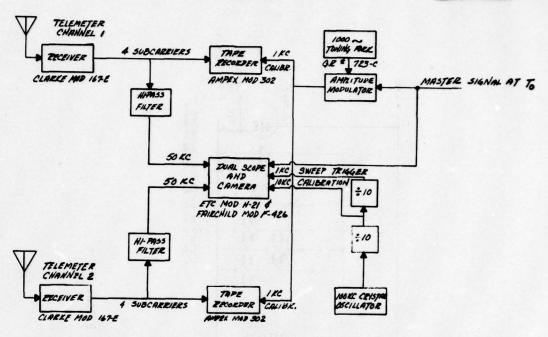


Fig. 2.7 Block Diagram of Ground Station Recording Equipment

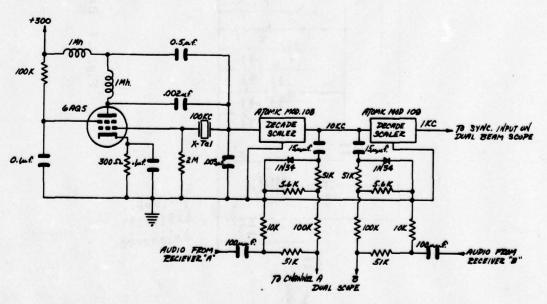
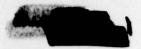


Fig. 2.8 Timing Circuit and Mixer for Blast Switch Data



PROJECT 1.3a

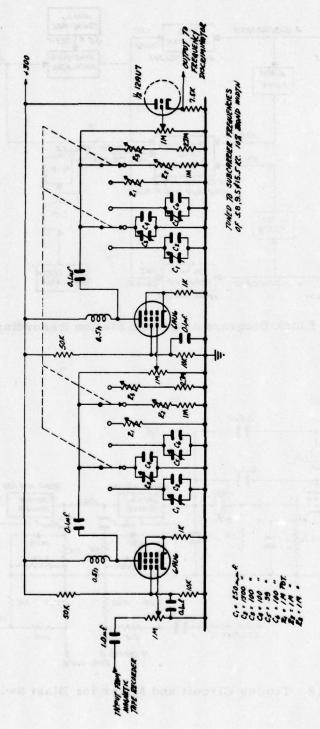


Fig. 2.9 Band Pass Filter







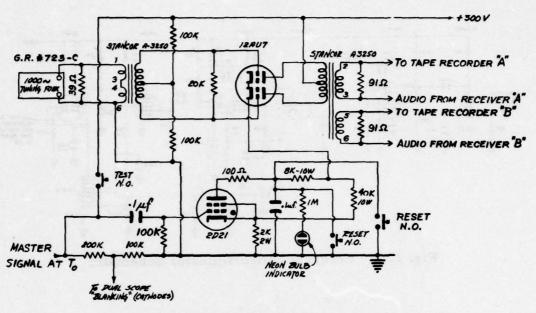


Fig. 2.10 1000 Cycle Timing Circuit

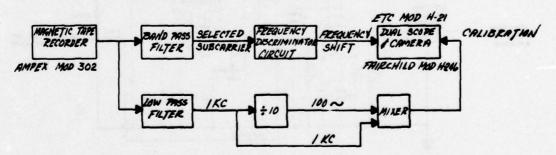


Fig. 2.11 Block Diagram for Analyzing Magnetic Tape Recordings







PROJECT 1.3a

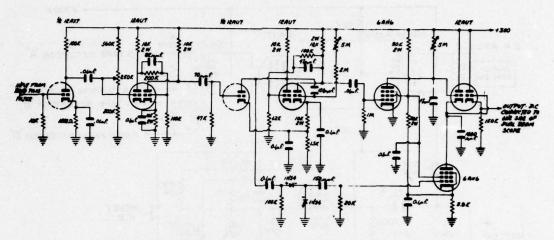


Fig. 2.12 Frequency Discriminator Schematic

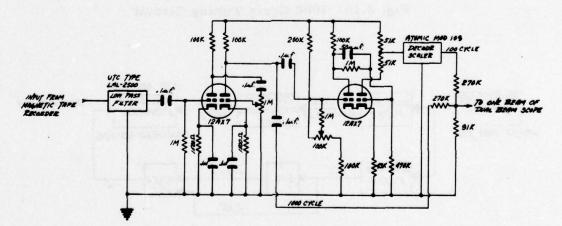
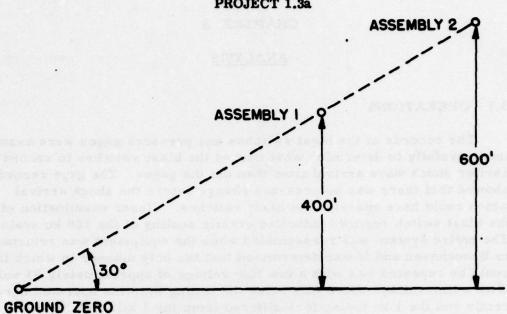


Fig. 2.13 Timing Circuit Used in Analyzing Tape Recordings









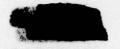
Two blast switches are used in series in each assembly for each shot. The switches are set to interrupt a 50 kc carrier at 1 lb. over-pressure.

Three blast gages are used in each assembly. Arrangement of gages is shown in the following table. Figures in table are maximum pressure reading for each gage.

TEST	7		SUR	FACE	UNDER	RGROUND
Assembly l	Gage	1	40	lbs.	15	lbs.
	.11	2	40		15	11
SI YEMARAGA S		3	15	,	5	
Assembly 2	Gage	1	15	lbs.	5	lbs.
chane than to a	11	2	15		5	
	"	3	5	11	15	•

Fig. 2.14 Location of Airborne Units





CHAPTER 3

ANALYSIS

3.1 OPERATIONS

The records of the blast switches and pressure gages were examined carefully to determine what caused the blast switches to record an earlier shock wave arrival time than did the gages. The gage records showed that there was no pressure change before the shock arrival which could have operated the blast switches. Closer examination of the blast switch records indicated erratic scaling of the 100 kc scaler. The entire system was reassembled when the equipment was returned to Brookhaven and it was determined that the only manner in which this could be repeated was with a low line voltage of approximately 95 volts. With a line voltage above this value the timing systems operated correctly and the 1 kc tuning fork differed from the 1 kilocycle obtained from the 100 kc scaled down by the two decade scalers by approximately l cycle per second. At the low line voltage the plate supply regulator was inoperative and the plate supply voltage was lower than normal. The most likely contributing factors to the timing failure were: 1) failure of scaler because of low B+; 2) reduced amplitude of 100 kc out of oscillator.

As judged by the behavior of the oscilloscope sweep circuit, the scalers functioned correctly up until the time the tape recorders were switched on, at which time all the other equipment in the shack and in the other projects using the same generator was operating, so the voltage may have dropped as low as 95 due to line losses, etc. The decade scalers used were of the type in which a binary scale of 16 is fed back internally such that it goes through its cycle with only 10 input pulses. At low line voltage the scaler may scale by 12, 14 or possibly 16. Inspection of the record shows that failure of the first scaler occurred once every nine or ten times, which accounts satisfactorily for the timing error. There is no evidence of failure in the second scaler.

The blast switch times of arrival were, therefore, discarded in favor of the 1 kc tuning fork calibration which is known to be correct. However, there was no arrival time at the Assembly 1 position on the underground shot from the tuning fork method. For this case the blast switch record was measured to determine the number and distribution



PROJECT 1.3a

of scaling errors, and the apparent arrival time was corrected accordingly, making allowance for the fact that failures occurring during the flyback of the oscilloscope sweep could not be seen. The result agreed within one millisecond with the time obtained by simple interpolation from the Assembly 2 data.

3.2 SUMMARY OF RESULTS

3.2.1 Arrival Time Data

Table 3.1 presents the times of arrival of the shock wave at each position.

TABLE 3.1
Arrival Time Data

Shot	Assembly	Radial Distance from zero (feet)	Time of Arrival (sec.)
Surface	1	845 ± 20	0.266 + .0005
Underground	1	723 ± 20	0.301 ± .0005 0.605 ± .0005
a contestion airco	2	1170 ± 30	0.605 ± .0005

TABLE 3.2

Comparison with Project 1.2a and Project 1.3b Data

Shot	Distance	Arrival Time "Free Air" (Proj. 1.3a)	Arrival Time "Free Air" (Proj. 1.3b)	Arrival Time near ground (Proj. 1.2a)
Surface	845 ⁺ 20 ft.	0.266 sec.		0.310 sec.
Underground	723 ⁺ 20 ft. 1170 ⁺ 30 ft.	0.301 sec. 0.605 sec.	0.295 sec. 0.628 sec.	0.370 sec. 0.705 sec.



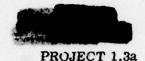


Table 3.2 presents a comparison of the "free air" arrival time data as determined by BNL Project 1.3a and NOL Project 1.3b with the arrival time data near the ground as read from Figures 3.5 and 3.9 of the Final Report of BRL Project 1.2a-1. The data furnished by Project 1.3b checks the measurements of Project 1.3a within the errors in estimated positions.

3.2.2 Pressure Gage Data

Surface shot - The 40 psi and 15 psi gages on one surface of the "pie plate" at the Assembly 1 position read off scale, whereas the 40 psi gage on the other face indicated a very low pressure. Therefore, it was concluded that the high readings are in error because of reflection effects.

Underground shot - The peak pressures indicated by the 5 psi and 15 psi gages on one surface of the "pie plate" at the Assembly 2 position were approximately 5 psi and 4 psi respectively. The 5 psi gage on the other surface indicated approximately 5 psi peak pressure.

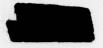
The behavior of the gages appears to be sufficiently variable so that little confidence can be placed in these readings.

The records were examined for indications of multiple shocks or long rise times, with negative results. The only cases in which a rise time was clearly measurable were those of a 40 psi gage at 845 ft. from the surface shot and a 15 psi gage at 1170 ft. from the underground shot. In both of these cases the apparent rise time (10 to 90 percent) was about 2 milliseconds. There is a possibility that this is an instrumental effect since both of these gages were on the lowest subcarrier frequency, 5.8 kc.

Figures 3.1 and 3.3 are records of the blast switch performance for the surface and underground shots respectively. Figures 3.2 and 3.4 are pressure gage records after frequency discrimination presented with their respective 1 kc timing waves on a dual beam oscilloscope.

3.3 CONCLUSIONS

Lacking accurate data on the positions of the pickups, there is little hope of calculating the free air pressure using meteorological data for the sound and wind velocities. In any event, the locations were





poorly chosen, so that the pressure calculations would not be very accurate even if the missing data were available.

Better gages and better orientation of the baffles might have resulted in useful data, but in general it is felt that the complexities and expense of this system make it inherently less practical than other methods, such as the smoke rockets. This is especially important when it is desired to obtain enough points to get a good curve of peak pressures as a function of distance.

The discrepancy between the "free air" arrival times as measured by Projects 1.3a and 1.3b (Table 3.2) and the arrival times near the ground as determined by Project 1.2a-1 is much too large to be accounted for by differences in wind velocity. It is concluded that the free air pressures were markedly higher than those measured near the ground.



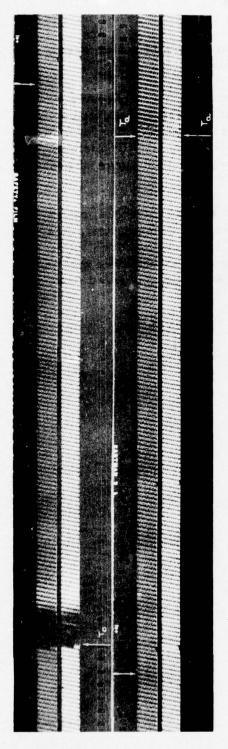


Fig. 3.1 Surface Shot: Blast Switches Subcarrier - Assembly 1

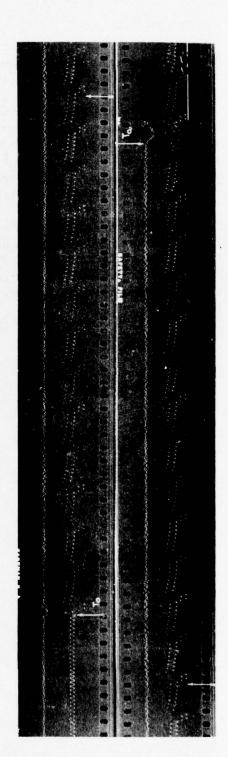


Fig. 3.2 Surface Shot: Assembly 1 - 40 psi Gage Record After Frequency Discrimination of Subcarrier and 1 kc Timing Wave



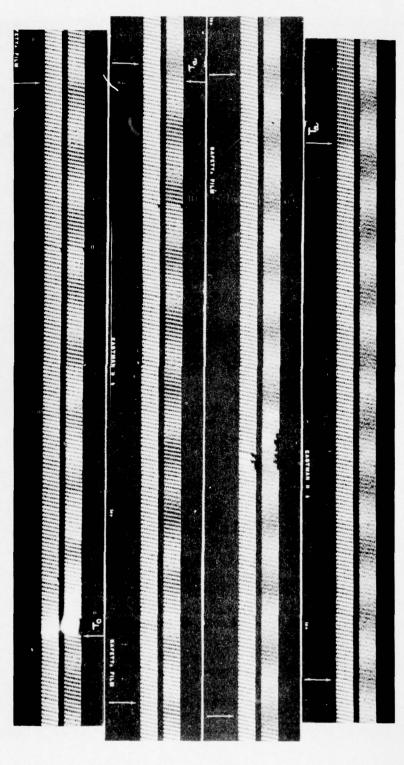


Fig. 3.3 Underground Shot:

Upper Trace - Blast Switch Subcarrier Assembly 2

Lower Trace - Blast Switch Subcarrier Assembly 1

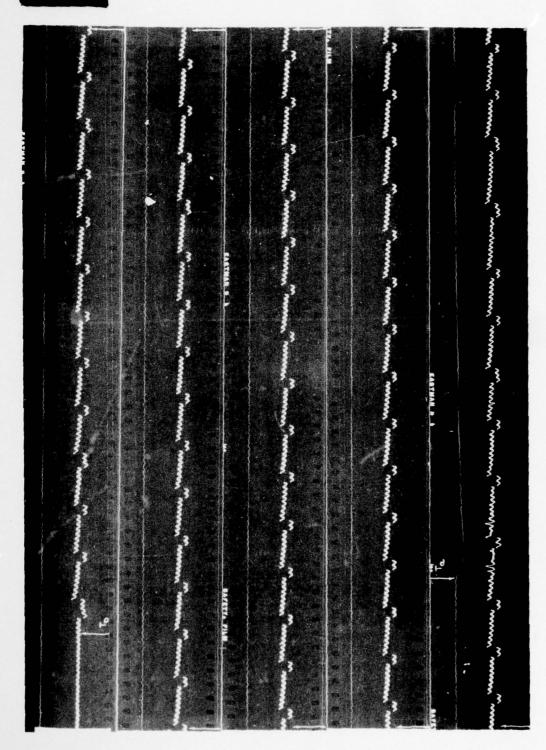


Fig. 3.4 Underground Shot: Assembly 2 - 5 psi Gage Record After Frequency Discriminations of Subcarrier and 1 kc Timing Wave

OPERATION JANGLE

Project 1.3b

PEAK PRESSURE VS DISTANCE

IN FREE AIR

USING SMOKE-ROCKET PHOTOGRAPHY

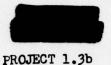
By

J. F. Moulton, Jr. E. R. Walthall P. Hanlon

June 1952

U. S. Naval Ordnance Laboratory White Oak Silver Spring 19, Maryland





ACKNOWLEDGMENTS

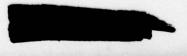
This work was done under the supervision of W. E. Morris.

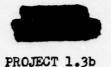
The photographic records and associated timing data were obtained by the Photographic Division, Sandia Corporation under the direction of H. C. Barr. They were submitted to the Naval Ordnance Laboratory for analysis through CDR E. Hoffman, Director, Programs 4 and 6.

C. L. Karmel of the U. S. Naval Ordnance Laboratory assisted the authors in the numerous measurements and calculations required to produce the results. R. Q. Macleay, formerly of this Laboratory, rendered valuable asssistance in setting up the field installations.

The Naval Ordnance Laboratory Shops are to be commended for producing the rockets in their modified form and the associated lawnchers, power boxes, etc., in the short amount of time given them before the tests.







ABSTRACT

The primary objective of the experiment was to obtain accurate information leading to the evaluation of the peak overpressure in the shock wave as a function of distance radially along the ground and vertically above the event.

The method employed was that of establishing a smoke rocket trail grid, high speed photographs of which showed the time of arrival of the shock front at a measurable distance in the desired directions. Knowledge of the shock velocity thus obtained was used to calculate peak overpressure by substitution in the Rankine-Hugoniot relation stating the dependence of shock velocity on peak pressure in the shock.

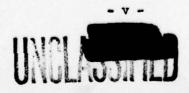
Despite the total loss of timing records for the surface shot a time base was established using the time of arrival results of Project 1.2a-1. As a result, peak overpressures were obtained only in the vertical direction for this event, since pressures along the ground would be identical to those of Project 1.2a-1. Peak overpressures, both along the ground and vertically, were determined for the underground shot.

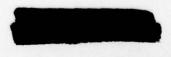
Based on existing high explosives (HE) data, the following TMT kilotonnage equivalents were determined for the 10 psi pressure level:

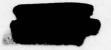
Event	Along the Ground	Vertically Above Zero
Surface	-	1.08 KT
Underground	1.01 KT	0.81 10

It is pointed out in the report that these values, being critically dependent on scaled HE data, are considered by the authors to be poor for accurate comparisons. They are based on data having wide scatter and caution should be exercised in making judgments based on them.

Suggestions and recommendations are made where necessary throughout the report in the event that similar tests are conducted in the future.

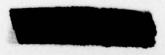


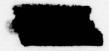




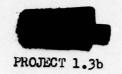
CONTENTS

ACKNOWLEDO	MENT	3		. 111
ABSTRACT				. 1
CHAPTER 1	INI	RODUCTIO	<u>or</u>	. 1
	1.1	Object	tive	. 1
	1.2	Histor	cical	. 1
		1.2.1	Refraction of Light	. 1
			Smoke Rocket Grid	
		1.2.3		
			Trails	. 2
	1.3	Basic	Theory	
			The Rocket Smoke Trail Method	
CHAPTER 2	EXP	RIMENTA	AL PROCEDURE	
	2.1	Detect	tion Grid	. 4
			Purpose	
			The Smoke Rocket	
			Firing Positions	
			Firing Method	
		215	Precautionary Measures	
	00		ption of Photographic Facilities	
	2.2			
		2.2.1	General Equipment Details	
		2.2.2	Camera Positions	
	2.3		alibration Procedure and Basic Measurement	
			otogrammetric Analysis	
			Fiducial Marker Locations	
		2.3.2	Scaling	. 11
		2.3.3	Film Measuring Instruments	. 11
		2.3.4	Timing	. 11
	2.4	Instru	mentation Performance	. 11
		2.4.1	Rocket Trail Grid	. 11
		2.4.2	Cameras and Timing	. 12
		2.4.3	Film Exposures	. 12
CHAPTER 3	RESU	LTS		
	3.1		e Shot	. 13
			Establishment of Time Base	. 13
		3.1.2	Meteorological Data	. 16
		3.1.3	Peak Overpressure in Free Air Vertically	
			Above Zero	
		3.1.4	TMT Kilotonnage Equivalent	
		3.2.7	THE THE COMMON PARTY ATTENDED	. 4





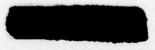
	3.2 Underground Shot	. 22
	3.2.1 Shock Wave Measurements	. 22
	3.2.2 Meteorological Data	. 22
	3.2.3 Peak Overpressure in Free Air Along	
	the Ground	. 22
	3.2.4 Peak Overpressure in Free Air	
	Vertically Above Zero	. 28
	3.2.5 TMT Kilotonnage Equivalent	. 28
GEAFTER 4	DISCUSSION AND CONCLUSIONS	
	.1 General Evaluation of Method and Results	. 33
	4.1.1 Validity of Assumptions	. 19
	4.1.2 Suitability of Smoke Rocket Trail Grid	. 33
	4.1.3 Suitability of Cameras, Film, and Photographic Techniques	
	4.1.4 Free Air Peak Overpressure Vertically	. 31
	Above Zero, Surface Shot	. 37
	4.1.5 Free Air Peak Overpressure Along the Ground, Underground Shot	
	4.1.6 Free Air Peak Overpressure Vertically	. 30
	Above Zero, Underground Shot	. 39
	.2 Sources and Computed Magnitudes of Errors	. 10
	4.2.1 Wind Correction	. 30
	4.2.2 Distance Scale	. 10
	4.2.3 Timing Scale	. ho
	4.2.4 Estimated Errors in Calculated	
	Pressures	. 40
	.3 Conclusions and Recommendations	. 41
	4.3.1 General	. 41
	4.3.2 Peak Pressure Along the Ground	. 42
	4.3.3 Peak Pressure Vertically Above	
	Ground Zero	. 42
BIBLIOGRAPH		. 43

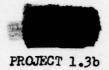


ILLUSTRATIONS

CHAPTER	2	EXPERIMENTAL PROCEDURE
		2.1 5.0 Spin Stablized Rocket Modified to
		Produce Smoke Trail
		2.2 Modified Single Tube Rocket Launcher
		and Battery Box 5
		2.3 Power and Timing Installation Showing
		Power Box, Safety Switch, and EGG Relay 5
		2.4 Loaded Launcher with Cover and Power and
		Timing Station 5
		2.5 Test Layout, Surface 6
		2.6 Test Layout Underground
		2.7 Firing Circuit for Rocket Line 9
CHAPTER	3	RESULTS
		SURFACE SHOT
		3.1 Time of Arrival of Shock Wave Vertically
		Above Ground Zero 14
		3.2 Sound Velocity, Co, and Atmospheric
		Pressure, Po, vs Altitude 17
		3.3 Free Air Overpressure vs Distance
		Vertically Above Zero 19
		3.4 Free Air Overpressure vs Distance Vertically
		Above Zero Corrected to Sea Level 20
		UNDERGROUND SHOT
		3.5 Time of Arrival of Shock Wave Along the
		Ground
		3.6 Time of Arrival of Shock Wave Vertically
		Above Ground Zero
		3.8 Free Air Overpressures Along the Ground
		and Vertically Above Zerc
		Vertically Above Zero Corrected to Sea Level . 32
CHAPTER	h	DISCUSSION
ODL 111.		<u> </u>
		4.1 Surface Event, 0.3557 Sec 34
		4.2 Surface Event, 0.4753 Sec
		4.3 Underground Event, 0.5790 Sec
		4.4 Underground Event, 0.0 Sec 35
		4.5 Underground Event, 0.1624 Sec
		4.6 Underground Event, 0.3248 Sec 36







TABLES

CHAPTER	2	EXPERIMENTAL PROCEDURE
		2.1 Photographic Equipment Details 10
CHAPTER	3	RESULTS
		SURFACE SHOT
		3.1 Shock Wave Arrival Times at Distances
		Vertically Above Zero
		3.2 Meteorological Data 16
		3.3 Free Air Peak Overpressures Vertically
		Above Zero
		3.4 Free Air Peak Overpressures Vertically
		Above Zero Corrected to Sea Level 18
		UNDERGROUND SHOT
		3.5 Shock Wave Arrival Times at Distances Along
		Ground and Vertically Above Zero 23
		3.6 Meteorological Data
		3.7 Free Air Peak Overpressures Along the
		Ground and Vertically Above Zero 29
		3.8 Free Air Peak Overpressures Along the
		Ground and Vertically Above Zero Corrected
		to Sea Level 31



CHAPTER 1 INTRODUCTION

1.1 OBJECTIVE

The objective of Project 1.3b was to determine the peak pressure of the shock wave in free air as a function of distance both vertically and along the ground from weapons detonated on and under the surface of the ground. Specifically, this objective was to be accomplished by the shock velocity method by measuring shock wave times-of-arrival at measured distances on high speed motion picture records of smoke rocket trail grid distortions caused by the shock wave.

1.2 HISTORICAL

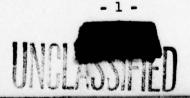
1.2.1 Refraction of Light

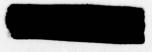
The phenomenon of refraction of light on passing through the region occupied by the shock front has been utilized in scientific laboratories for many years to obtain photo-shadowgrams and in conjunction with shock-wave detection techniques. On occasion, motionpicture photographs of large explosions produced by conventional military explosives have shown rather clearly the locus of the expanding shock front, the diffused background lighting being refracted on passing through the denser gas within the shock front and detected by the camera. The refraction of the light reflected from large objects, such as trees and telephone poles in the background, has also been observed, but the effect is small, being proportional to the strength of the shock and the rate of decay behind it. However, frame-by-frame examination of such photographs has shown that the location of the distortion is extremely difficult to detect against an irregularly shaped background such as trees. This indicated the necessity of some type of grid or regular background of considerable dimensions. Experiments were conducted to determine the feasibility of such a grid by J. F. Moulton, Jr. and LCDR B. T. Simonds of the Naval Ordnance Laboratory.

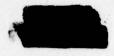
1.2.2 Smoke-Rocket Grid

During 1950 an FS smoke-rocket was developed by J. F. Moulton, Jr. and LCDR B. T. Simonds at NOL for use on Operation Greenhouse (see ref (a)).* The grid formed by a number of these

^{*}All references will be found in the Bibliography appearing at the end of the report.







smoke-rockets launched vertically before the burst in a plane perpendicular to the line of sight of the camera and behind the explosion center proved to be very successful in obtaining a photographic record of the arrival time of the shock at various distances. Refraction of the light reflected from the trails on passing through the shock front caused the trails to appear broken at the shock front and hooked just behind the shock front determining the locus of the shock front very accurately.

1.2.3 Effect of Relative Humidity on Rocket Trail

Since the smoke from the rockets is obtained by the combination of FS with the water vapor in the air (see Sec. 2.1.2), it was felt that the low humidity at the Nevada Test Site might reduce the density of the trails seriously. In the first two weeks of September, 1951 an experiment was conducted at the test site by J. F. Moulton, Jr. to determine the seriousness of this effect. One smoke-rocket was fired and photographed under approximately the same conditions expected for the actual tests. The density of the trail, though reduced somewhat, was observed to be sufficient for the necessary contrast with background lighting and the effect of the relative humidity on the trail was not considered serious.

1.3 BASIC THEORY

1.3.1 The Rocket Smoke Trail Method

To obtain peak overpressure as a function of distance the photo-optical technique described above is employed to record the time of arrival of the shock at measured distances from the explosion center. A third order polynominal of the form

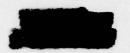
$$t = A_0 + A_1 R + A_2 R^2 + A_3 R^3$$
 (t = time, R = distance)

is fitted by the method of least squares to the data thus obtained. Differentiation of this equation gives

$$\frac{dt}{dR} = \frac{1}{U} = A_1 + 2A_2R + 3A_3R^2$$

correlating shock velocity, U, with distance. From it a set of instantaneous shock velocities is obtained for the chosen values of distance. In addition to these values, a knowledge of the absolute atmospheric pressure, P_0 , and the velocity of sound, C_0 , ahead of the shock is required to determine the peak overpressures, P_8 . The overpressure is calculated from the complete set of data by using the Rankine-Hugoniot relation for shock pressure as a function of shock velocity:





$$\frac{P_s}{P_o} = \frac{2 \gamma}{\gamma + 1} \left[\frac{v^2}{C_0} 2 - 1 \right]$$

where %, the ratio of specific heats for air, = 1.403.

A complete example of the rocket smoke trail analysis may be found in appendix B of ref (a).



CHAPTER 2

EXPERIMENTAL PROCEDURE

2.1 DETECTION GRID

2.1.1 Purpose

To follow the progress of the shock front in free air photographically a detection grid is required. This grid was formed by FS smoke rockets, whose smoke trails reflect the light produced by the explosion and sunlight. The light from the grid is refracted by the shock front and appears distorted, indicating the locus of the shock front.

2.1.2 The Smoke Rocket

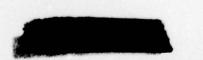
The smoke rocket consists of a standard inert 5.0 Rocket Head Mark 10 and 5.0 Spin Stabilized Rocket Motor Mark 4 combination (see Fig. 2.1). The head is filled about four-fifths full (10 lb) of FS (55 per cent sulfur trioxide and 45 per cent chlorosulfonic acid). Three small metal nibs, covering exit holes drilled 120° apart near the base of the rocket head, are knocked off by the lands in the launcher during the launching phase. Centrifugal force then dispenses the FS, directed by scoops, through the exit holes. Upon combination with the water vapor in the air, the FS forms a dense white trail of fuming sulfuric and hydrochloric acids which is fairly persistent, about 2 meters thick, and continues up to about 3,000 ft altitude. Details of the development and test of the rocket can be found in ref (a). The single-tube launcher is shown in Fig. 2.2.

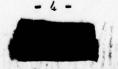
2.1.3 Firing Positions

The smoke trails forming the grid were aligned in azimuth such that they projected down the line of sight of the camera stations. This was done to present essentially vertical lines to the cameras. The trails were spaced at equal intervals as shown in Figs. 2.5 and 2.6.

2.1.4 Firing Method

Each rocket line received its firing impulse at -5 seconds through an EG&G timing relay which closed a circuit of 110v AC in the rocket line. The 110v power box and EG&G relay were appropriately mounted in the blast hut (see Fig. 2.3). The rocket line voltage closed a number of power relays (Potter and Brumfield type MR11A), each connected in parallel across the line, completing the individual firing









Modified Single Tube Rocket Launcher and Battery Box

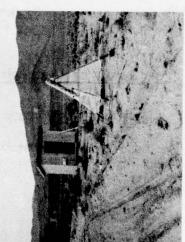
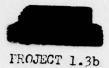


Fig. 2.4 Loaded Lemoner wave was and Power and Timing Station



Fig. 2.3 Power and Timing Installation Showing Power Box, Safety Switch, and NGG Relay



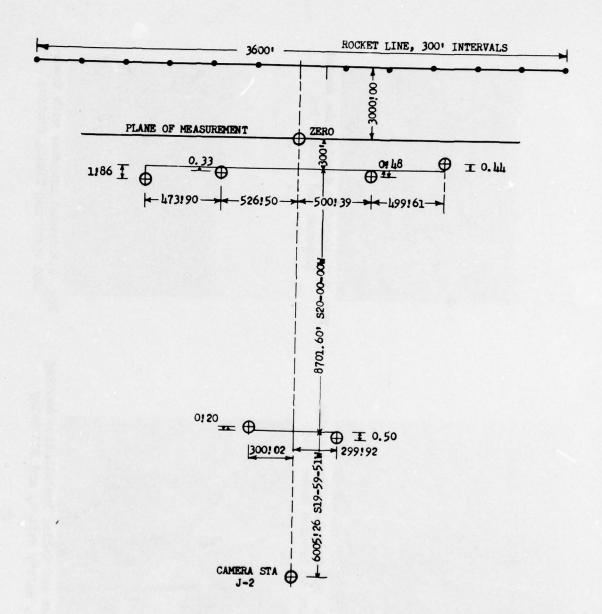
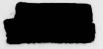


Fig. 2.5 Test Layout, Surface



PROJECT 1.3b

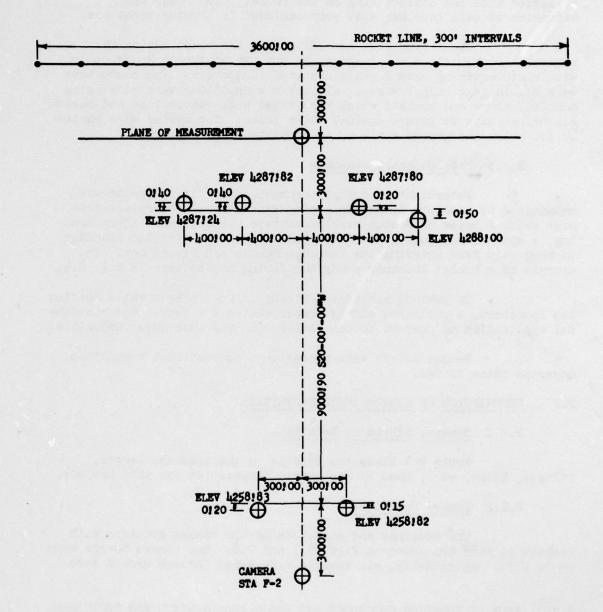
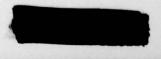
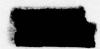


Fig. 2.6 Test Layout, Underground







circuits at each rocket station (see Fig. 2.7). Each individual rocket firing circuit consisted of one power relay and two 6v BA-222/u batteries in series with the contact ring on the rocket. The relay and batteries at each launcher site were enclosed in a water-tight box.

The firing line extending from the blast hut to the various launcher sites was composed of one two-conductor Romex cable with cloth covering around plastic-coated conductors. The conductors were No. 14 gage copper wires. All cable connections were made using amphenol plugs and sockets which were taped with rubber tape and Scotch electrical tape to insure against water leaks. The cables were buried 18 in. below the ground surface, no conduits being required.

2.1.5 Precautionary Measures

Watertight circuitry throughout the firing system was maintained by sealing all amphenol plug connections with rubber tape over which a layer of Scotch electrical tape was applied. After loading, a special raincoat made of Koroseal was placed over the launcher to keep rain from entering the launcher muzzle and firing box. An example of a rocket launcher ready for firing may be seen in Fig. 2.4.

To prevent accidental firing of the rockets while loading the launchers, a padlocked safety jumper switch was used. The accidental application of current to the firing line was thus made impossible.

Rocket motors were stored in a conventional ammunition magazine prior to use.

2.2 DESCRIPTION OF PHOTOGRAPHIC FACILITIES

2.2.1 General Equipment Details

Table 2.1 lists the details on the cameras, lenses, filters, films, etc., used by the Sandia Corporation for this project.

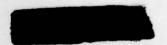
2.2.2 Camera Positions

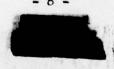
The bearings and distances of the camera stations with respect to zero are shown in Figs. 2.5 and 2.6. The camera towers were 25 ft high. Azimuthally, all cameras were aimed through ground zero.

2.3 FILM-CALIBRATION PROCEDURE AND BASIC MEASUREMENTS FOR PHOTOGRAM-METRIC ANALYSIS

2.3.1 Fiducial-marker Locations

The space fiducial markers, used to establish the horizontal scale and horizontal-vertical orientation of the film record,





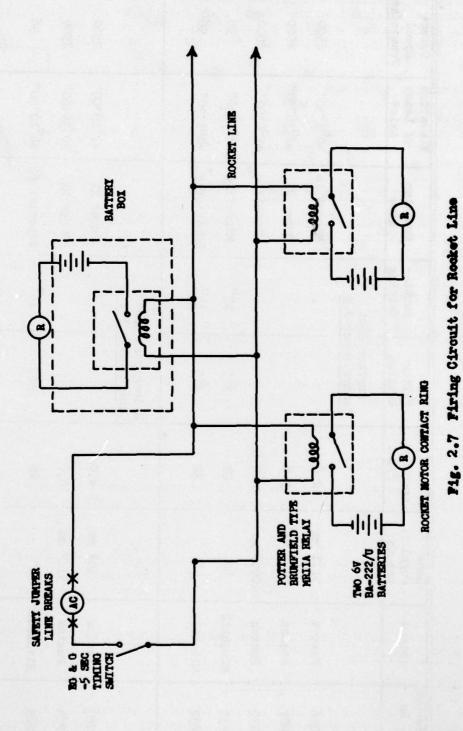




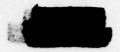
TABLE 2.1

Photographic Equipment Details

Record No.	Camera	Lens Focal Length	Aperture f/No.	Filter Wratten	Shutter Setting	Emulsion Type	Elevation of Lens Axis*	Camera Speed Frames/sec
				Surface Shot Camera Tower J-2	Shot er J-2			
526	Fastax	51.7 mm	2.8			Microfile	-09.30.	2500
227	Fastax	51.7 mm	5.6			Super XX	+2°38"30"	2500
230	Fastax	100.8 mm	0.4			Microfile	+100,00,1+	2500
231	Mitchell	†	83	#15	150	Microfile	+4°7'30"	%
232	Mitchell	" †1	8	#15	150	Superior #1	+001,30,	%
				Underground Shot Camera Tower F-2	Shot F-2			
283	Fastax	101	0.4			Super XX	+1°18'00"	2500
284	Fastax	51.7 mm	4.0			Super XX	+0034.00"	2500
285	Mitchell	., ,	83	#15	150	Superior #1	**************************************	%

+ = Camera Axis Elevated Above Horizontal Level

- = Camera Axis Depressed Below Horizontal Level



were provided by the Sandia Corporation. Details on the space-marker locations are shown in Figs. 2.5 and 2.6. The plywood markers nearest the camera station were 4 ft square and the farthest ones were 6 ft square. Four smaller alternating black and white squares were painted on each marker.

2.3.2 Scaling

The fiducial markers were placed at known positions with respect to the camera, thus establishing a horizontal distance scale in any desired plane of measurement. A vertical scale was established using the fiducial marker geometry together with a knowledge of the direction of the optical axis of the camera and engineering survey data.

2.3.3 Film-measuring Instruments

A direct-projecting Recordak (Model MPE) was used for the distance measurements given in this report. The shock front, made discernible by the refraction of light from the trails and the scattered background light, was traced frame-by-frame on special drafting vellum to reduce distortion effects caused by humidity. The enlarged images were measured to the nearest 0.005 in. representing approximately 1 ft in the plane of measurement.

2.3.4 Timing

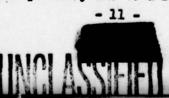
Timing scales furnished by the Sandia Corporation on the surface shot showed that just before zero time a power failure at the camera station occurred. The measurements recorded were useless during the period of interest.

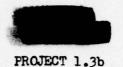
Timing for the underground shot was also furnished by the Sandia Corporation in the form of a string galvanometer record. A 100 cps signal was recorded on the same record showing a timing pip for each frame of the film as it was being exposed. The position of each frame with respect to zero time was measured and thus the speed of the camera and time of each frame during the period of interest was determined. The film used to obtain the results for the underground event presented in Chap. 3 was exposed at a constant rate within the error of measurement. The time per frame was found to be 0.0108475 sec. The accuracy of this figure is + 0.00005 sec. The maximum error over the entire period of measurement (65 frames) is 0.00325 sec (0.3 per cent) which is considered to be negligible.

2.4 INSTRUMENTATION PERFORMANCE

2.4.1 Rocket Trail Grid

All but one rocket fired on both shots at the proper time and the one failure was probably due to a faulty motor. This occurred





on the surface shot. Of the 23 rockets that fired, five failed to smoke (four on the underground shot and one on the surface shot). Although this was a large percentage of failures, the grid was sufficient to extract the necessary data. Failure of the rocket launcher lands to knock off the metal nibs covering the exist holes in the head has been determined as the cause for the rockets not smoking. The modified inert heads were actually at fault because the nibs were recessed too much with respect to the outer surface of the rocket.

2.4.2 Cameras and Timing

All cameras used for this project were running at zero time for both shots. The cameras and timing for the surface shot fluctuated due to an erratic fluctuation in the voltage supply and eventual power failure. No such difficulties were encountered on the underground test.

2.4.3 Film Exposures

In general, film exposures were poor. Only one usable film was obtained on each shot, film No. 232 on the surface shot and film No. 285 on the underground shot. All others lacked the necessary contrast or were overexposed. Even film No. 232 was overexposed during the first 0.25 sec, during which time the shock wave advanced some 750 ft radially.



CHAPTER 3

RESULTS

3.1 SURFACE SHOT

At the photographic station J-2 a power failure occurred on the surface test which all but ruined the experiment from the standpoint of this project. Although the cameras were in operation throughout the time of interest, their speed was erratic. This would have presented only minor difficulties in the analysis had not the local primary timing standard also failed. If the timing standard had been battery-operated there would have been far less chance of its failure.

Despite the timing failure an attempt was made to get some information from the films since the shock wave could be seen out to about 2,000 ft in film No. 232. The procedure given immediately below was used to obtain the time of arrival of the shock wave.

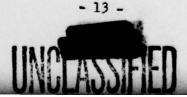
3.1.1 Establishment of the Time Base

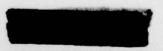
Timing of the individual frames of film No. 232 is based on the Ballistic Research Laboratories (BRL) shock wave arrival times along the ground, given in ref (b), and the assumption that the shock wave is symmetrical radially along the ground. By definition, then, it follows that the two sets of data, those of the Naval Ordnance Laboratory (NOL) and the Ballistic Research Laboratories, are identical and lead to the same pressure results along the ground.

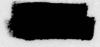
The BRL data were plotted and connected by a smooth curve drawn through the points. The NOL shock wave distances (radii) measured along the ground were matched frame-by-frame to the corresponding distances on the BRL curve and the time of each frame was thus obtained. Knowing the time of each frame, the arrival time of the shock along the vertical axis was established. These data are plotted in Fig. 3.1 as given in Table 3.1. The oscillations appearing in the time of arrival curve are the result of film speed variation due to voltage fluctuations prior to the power failure and vibrations set up by the film feed mechanism.

The empirical equation fitted to the arrival time data is:

 $t = -0.18653780 + 0.54415300R + 0.04845880R^2 + 0.01321468R^3$







PROJECT 1.3b

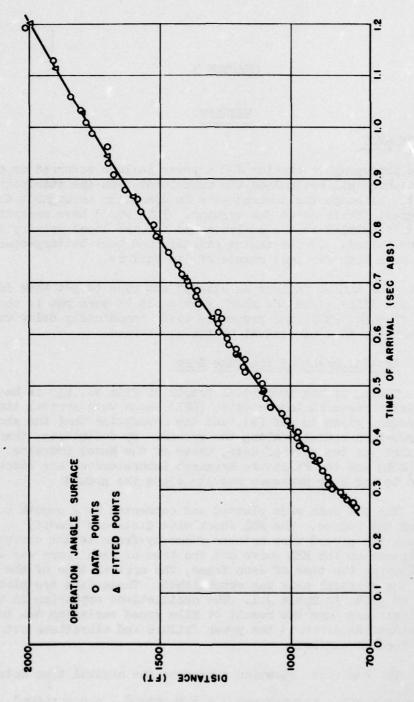


Fig. 3.1 Time of Arrival of Shock Wave Vertically Above Ground Zero

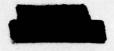
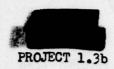


TABLE 3.1

Shock Wave Arrival Times at Distances Vertically Above Zero

Surface Shot

R (ft)	t (sec)	R (ft)	t (sec)	R (ft)	t (sec)	R (ft)	t (sec)
757-37	0.2663	1008.50	0.4205	1241.16	0.5790	1512.76	0.7888
762.33	0.2710	1012.47	0.4235	1245.99	0.5910	1522.46	0.8217
784.17	0.2790	1034.31	0.4475	1271.62	0.6030	1574.30	0.8360
809.98	0.2925	1076.00	0.4585	1273.59	0.6210	1588.20	0.8610
840.75	0.3000	1095.86	0.4753	1262.62	0.6288	1631.88	0.8800
857.63	0.3087	1099.83	0.4820	1282.47	0.6405	1673.56	0.9075
853.65	0.3237	1105.78	0.4920	1349.97	0.6575	1699.37	0.9300
873.51	0.3372	1107.77	0.5055	1363.87	0.6743	1701.36	0.9600
891.37	0.3557	1125.63	0.5200	1357.91	0.6825	1762.90	0.9885
919.17	0.3635	1175.26	0.5275	1389.68	0.6930	1782.75	1.0075
944.97	0.3782	1177.25	0.5350	1397.62	0.7045	1800.62	1.0335
966.82	0.3843	1177.25	0.5500	1417.47	0.7175	1840.33	1.0580
976.74	0.4000	1209.02	0.5610	1425.41	0.7345	1905.84	1.1288
972.77	0.4097	1211.00	0.5707	1469.08	0.7588	2017.01	1.1885



3.1.2 Meteorological Data

The meteorological data required to obtain the desired pressure results using the Rankine-Hugoniot relation were taken from ref (c). These data were originally reported by the Test Site Weather Station and were computed by the Experimental Weather Station of the Geophysics Research Division, AFCRC. Temperatures and pressures at the ground surface and at 1,334 ft above the surface were chosen as base points to establish an assumed linear variation of atmospheric pressure and sound velocity with altitude. These values are shown in Table 3.2. The resulting variations of these values are shown in Fig. 3.2.

TABLE 3.2
Meteorological Data, Surface Shot

Altitude (ft)	P _o (psi)	(°C)	Co (ft/sec)
0	12.69	10.3	1,108.39
1,334	12.04	6.2	1,100.29

3.1.3 Peak Overpressure in Free Air Vertically Above Zero

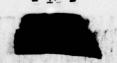
Using the data from Table 3.1 and Fig. 3.2, pressures were calculated by means of the Rankine-Hugoniot relation for distances measured vertically above zero. These pressures are listed in Table 3.3 and are plotted in Fig. 3.3.

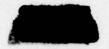
The pressures, P_s, given in Table 3.3 apply only at a ground elevation of 4,213 ft above mean sea level. These pressure and distance values have been corrected to sea level using the relations as found in ref (e):

R(sea level) = R(test site)
$$\left[\frac{P_0(\text{test site})}{P_0(\text{sea level})} \right]^{1/3}$$

$$P_s(\text{sea level}) = P_s(\text{test site}) \left[\frac{P_o(\text{sea level})}{P_o(\text{test site})} \right]$$

where R = distance and P_S = peak overpressure in shock wave.





PROJECT 1.3b

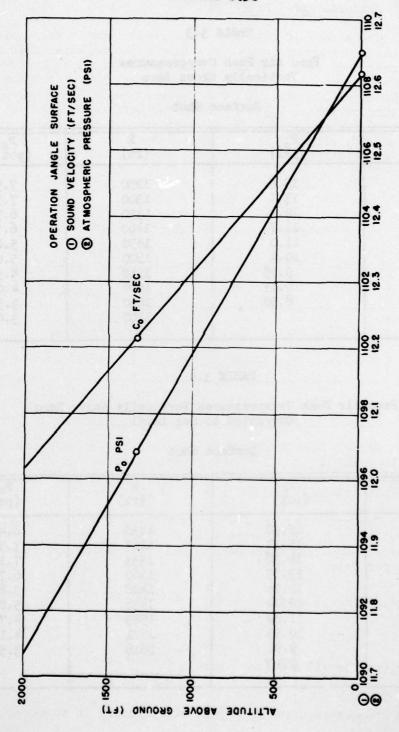


Fig. 3.2 Sound Velocity, Co, and Atmospheric Pressure, Po, vs Altitude

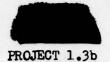


TABLE 3.3

Free Air Peak Overpressures Vertically Above Zero

Surface Shot

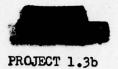
R (ft)	P (psi)	R (ft)	P _g (psi)
800 850 900 950	13.8	1250	7.90
850	13.8 13.1 12.4	1300	7.31
900	12.4	1300 1350 1400	6.51
950	11.7	1400	6.17
1000	11.0	1450	5.82
1050	10.4	1500	5.09
1100	9.75	1550	4.56
1100 1150	9.75 9.11 8.50	1550 1600 1650	7.90 7.31 6.51 6.17 5.82 5.09 4.56 4.06
1200	8.50	1650	3.57
		1700	3.57 3.09

TABLE 3.4

Free Air Peak Overpressures Vertically Above Zero Corrected to Sea Level

Surface Shot

R (ft)	P _B (psi)	R (ft)	P _s (psi)
762 809 857 904 952 1000	15.98 15.17	1238 1285	8.46 7.54
857	15.17 14.36	1285 1333 1380 1428	7.54 7.14 6.74 5.89 5.28 4.70 4.13
952	13.55 12.74	1428	5.89
1000	12.04	1476	5.28
1047 1095 1142	11.29	1523 1571	4.70
	9.8 4 9.15	1618	3.58
1190	9.15		



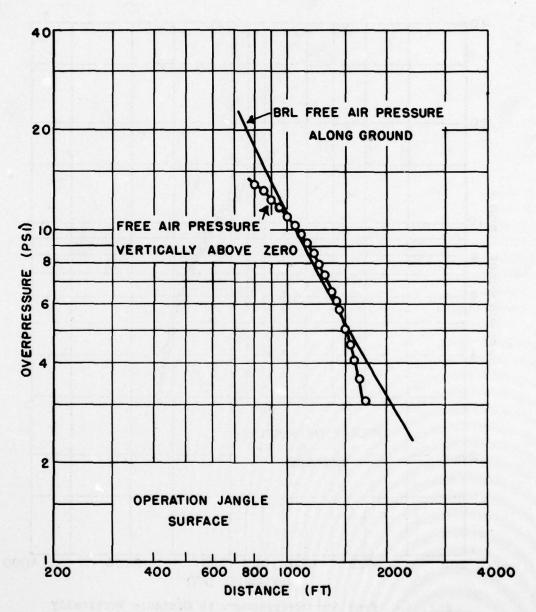
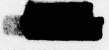


Fig. 3.3 Free Air Overpressure vs Distance Vertically Above Zero







PROJECT 1.3b

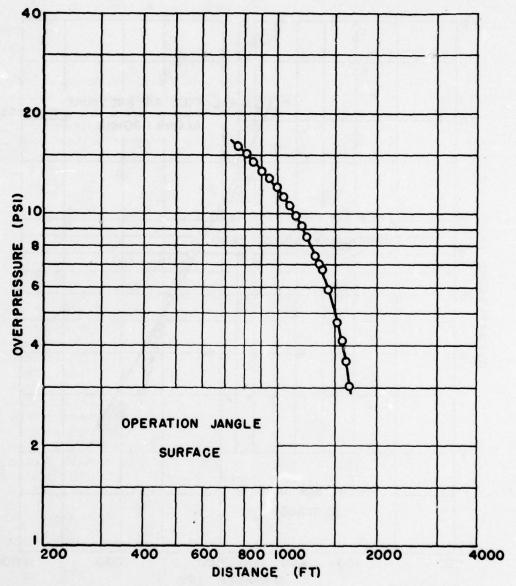
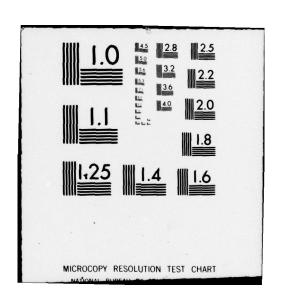
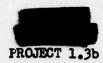


Fig. 3.4 Free Air Overpressure vs Distance Vertically
Above Zero Corrected to Sea Level

DEFENSE ATOMIC SUPPORT AGENCY WASHINGTON DC F/6 18/3
OPERATION JANGLE. NEVADA PROVING GROUNDS, OCTOBER - NOVEMBER 19--ETC(U)
MAR 52 AD-A078 577 UNCLASSIFIED AEC-WT-367 NL 2 of 3 AD A 078577





Assuming the atmospheric pressure, Po, to be 14.7 psi at sea level and taking 12.69 psi as measured at the test site the factors for reducing the data to sea level are 0.952 for distance and 1.158 for pressure. The corrected values appear in Table 3.4 and are plotted in Fig. 3.4.

3.1.4 TMT Kilotonnage Equivalent

Reference (d) describes some small scale high explosives tests conducted at the Naval Ordnance Laboratory late in 1950. Pressure measurements were made at reduced distances, λ , along the ground and vertically above spherical 1 lb Pentolite charges. The charges were placed at charge depths (or heights), λ_c , with respect to the ground surface level. By definition

$$\lambda = \frac{R}{W^{1/3}} \left(\frac{ft}{1b^{1/3}} \right),$$

$$\lambda_{c} = \frac{Depth \ of \ Burial}{W^{1/3}} \left(\frac{ft}{1b^{1/3}} \right)$$

where R = distance from ground zero
W = weight of charge.

Specifically, the report gives data for $\lambda_c=0$, corresponding to a charge center at the surface, and $\lambda_c=-0.125$, corresponding to a charge center almost 1 charge radius above the ground. The charge height of the surface test on Operation JANGLE was of the order of $\lambda_c=-0.024$, based on a radiochemical equivalent of 1.0 KT. Thus the data taken from the small scale tests should bracket those of the full scale test. For reduced distances (λ) vertically above zero at the 10 psi level the small scale tests yield values of $\lambda=8.4$ and $\lambda=9.2$ for $\lambda_c=-0.125$ and $\lambda_c=0$ respectively, after a correction factor of 1.19 is applied to convert from Pentolite to TNT. The full scale test yielded a corrected pressure of 10 psi at a distance of 1,135 ft above ground level. Hence

$$W^{1/3} = \frac{R}{\lambda} = \frac{1.135}{8.4} = 135 \text{ lb}^{1/3}$$
, if $\lambda_c = -0.125$ for the nuclear shot

and
$$W^{1/3} = \frac{1,135}{9.2} = 123 \text{ lb}^{1/3}$$
, if $\lambda_c = 0$ for the nuclear shot.

The values of W are therefore 1.23 KT and 0.93 KT, respectively. An exact high explosives comparison for $\lambda_c = -0.024$ does not exist but the value of 0.93 KT should be closer to the true value since the nuclear shot at $\lambda_c = -0.024$ more nearly approximates $\lambda_c = 0$.





3.2 UNDERGROUND SHOT

On the underground test all of the photographic and timing devices associated with this project fur tioned so that timing scales could be measured in the prescribed manner. During the time of interest, the camera in which film No. 285 was exposed functioned smoothly with the result that the time per frame was constant within the error of measurement.

3.2.1 Shock Wave Measurements

Measurements were made along the ground and vertically above ground zero. The shock-wave-arrival times in these directions are given in Table 3.5 and are plotted in Figs. 3.5 and 3.6.

The empirical equation fitted to the arrival-time data along the ground was:

 $t = -0.01167049 + 0.31622801R + 0.36429249R^2 - 0.09933107R^3$

In order to obtain a satisfactory fit, two empirical equations were derived for the arrival-time data vertically above zero. This was necessary because of the inflection point occurring at about 950 ft. Of these two equations, the first was fitted to the data from 600 ft to 1,000 ft; the second from 1,000 ft to approximately 2,000 ft. They were:

- (1) $t = -0.33554603 + 1.29906407R 1.19800814R^2 + 0.59248555R^3$
- (2) $t = -0.66074835 + 1.64960339R 0.88070709R^2 + 0.23719553R^3$

3.2.2 Meteorological Data

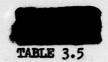
As on the surface test, the change of atmospheric pressure and sound velocity was assumed to be a linear function of altitude above ground level. The basic data were obtained, as before, from ref (c). They are given in Table 3.6 and plotted in Fig. 3.7.

3.2.3 Peak Overpressure in Free Air Along the Ground

The peak overpressures along the ground were calculated using the data in Tables 3.5 and 3.6 in the Rankine-Hugoniot relation. The results are given in Table 3.7 and are plotted in Fig. 3.8.

The pressures given in Table 3.7 have not been corrected to mean sea level. As they appear in this table, the data correspond to those from a charge in the ground at a ground level of 4,299 ft above sea level. Using the factors 1.150 to correct for pressure and 0.954 to correct for distance, as found by using the relations given in Sec. 3.1.3, the corrected data presented in Table 3.8 are those to be considered at sea level. These data are plotted in Fig. 3.9.



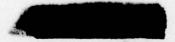


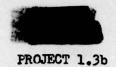
Shock Wave Arrival Times at Distances Along the Ground and Vertically Above Zero

Underground Shot

R (ft) Vertically Above Zero	R (ft) Along Ground	t (sec)
589.22	346.28	.13517
676.81	417.47	.17856
764.00	489.43	.22195
847.20	561.76	.26534
922.85	636.42	.30873
991.32	708.74	.35212
1082.89	761.42	•39551
1164.51	822.50	.43890
1246.12	883.10	.48229
1307.83	941.29	.52568
1392.23	993.91	.56907
1469.07	1049.24	.61246
1537.55	1110.49	.65585
1604.43	1174.03	.69924
1670.12	1235.95	.74263
1727.85	1297.00	.78602
1791.55	1345.40	.82941
1846.09	1405.13	.87280
1891.88	1458.15	.91619
1942.84	1516.99	.95958







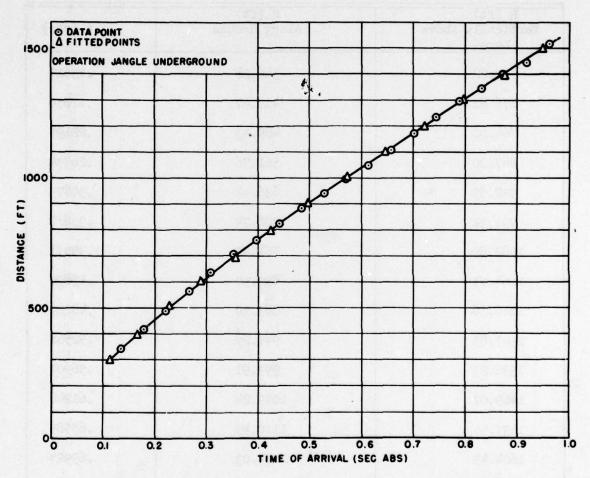
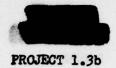


Fig. 3.5 Time of Arrival of Shock Wave Along the Ground



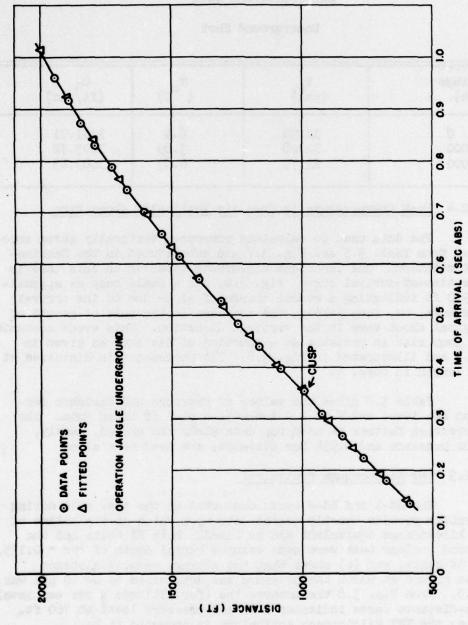


Fig. 3.6 Time of Arrival of Shock Mave Vertically Above Ground Zero

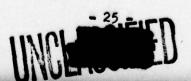




TABLE 3.6

Meteorological Data

Underground Shot

Utitude (ft)	(psi)	(^T oc)	Co (ft/sec)
0	12.78 12.28	6.9 3.89	1101.71
2000	11.79	0.83	1089.63

3.2.4 Peak Overpressure in Free Air Vertically Above Zero

The data used to calculate pressures vertically above zero are taken from Table 3.5 and Fig. 3.7 and substituted in the Rankine-Hugoniot relation. One important difference observed in this case is that the time-of-arrival curve, Fig. 3.6, has a small cusp at approximately 950 ft indicating a sudden change of slope due to the arrival of a new wave, or, less likely, the increase in the rate of growth of the original shock wave in the vertical direction. This event accounts for the jump rise in pressure as a function of distance as given in Table 3.7 and illustrated in Fig. 3.8. The phenomenon is discussed at greater length in Chap. 4.

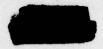
Table 3.8 gives the values of pressure and distance corrected to sea level and Fig. 3.9 includes a plot of these data. The same correction factors as used for data along the ground, namely, 1.150 for pressure and 0.954 for distance, are used here also.

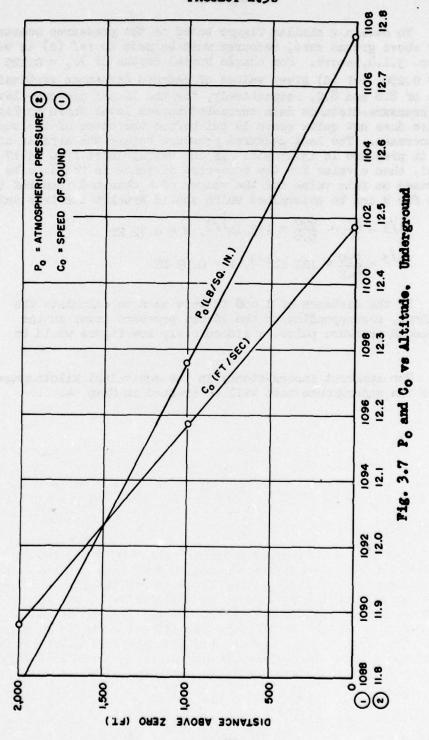
3.2.5 TMT Kilotonnage Equivalent

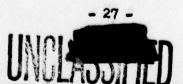
The HE-1 and HE-2 tests conducted at the test site during the operation provide exactly scaled data upon which an evaluation of the TMT kilotonnage equivalent can be based. Both HE tests and the underground nuclear test were made using a burial depth of $\lambda c = 0.135$. For the HE tests, ref (b) shows that the average reduced distance along the ground at which the pressure was determined to be 10 psi was $\lambda = 5.0$. From Fig. 3.8 the uncorrected (for altitude above sea level) pressure-distance curve indicates a 10 psi pressure level at 760 ft. Therefore, the TMT kilotonnage equivalent is computed to be

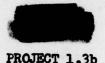
$$W^{1/3} = \frac{R}{\lambda} = \frac{760}{6.0} = 126.6 \text{ lb}^{1/3},$$

 $W = 1.01 \text{ KT}.$









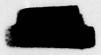
To obtain a similar figure based on the pressures measured vertically above ground zero, recourse must be made to ref (d) as was done in Sec. 3.1.4, above. For charge burial depths of $\lambda_c = 0.125$ and $\lambda_c = 0.250$, ref (d) gives values of reduced distances vertically above zero of 8.8 and 8.2, respectively, for the 10 psi pressure level. Using the pressure-distance data corrected to sea level shown in Fig. 3.9, the pressure does not quite reach 10 psi before the onset of the sudden pressure increase. The last measured pressure before the arrival of this rise in pressure is 13.17 psi. If one extrapolates from 13.17 psi to 10.0 psi, then a value for the corrected distance is found to be 990 ft. Based on this value and the values of λ obtained from ref (d), two values for W can be determined which should bracket the true value.

$$W^{1/3} = \frac{R}{\lambda} = \frac{990}{8.8} = 113 \text{ lb}^{1/3}, W = 0.72 \text{ KT}$$

 $W^{1/3} = \frac{990}{8.2} = 121 \text{ lb}^{1/3}, W = 0.89 \text{ KT}$

If the distance of 1,650 ft were used to calculate the TMT equivalent, corresponding to the 10 psi pressure level in the apparent second pressure pulse, a riduculously low figure would be obtained.

The apparent inconsistency in the equivalent kilotonnage weights for the underground test will be treated in Chap. 4.



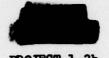
PROJECT 1.3b

TABLE 3.7

Free Air Peak Overpressures Along the Ground and Vertically Above Zero

Underground Shot

R (ft)	P _s (Vertical) (psi)	Ps (Along Ground) (psi)
300		32.80
400		24.00
500		18.64
600		14.76
650	35.00	
700		11.93
750	33.11	
800	30.03	9.54
850	25.49	The desired by 3
900	20.91	8.05
950	15.90	
1000	11.45	7.30
1100		6.56
1200	23.53	10 X00 TE 18 18 1
1250	23.45	
1300	23.26	
1400	21.17	
1500	17.66	
1600	13.51	
1650	11.28	
1700	9.15	C00 C08 OB
1750	7.02	
1800	5.06	118. 3.6 (a) P
1850	3.17	
1900	1.48	



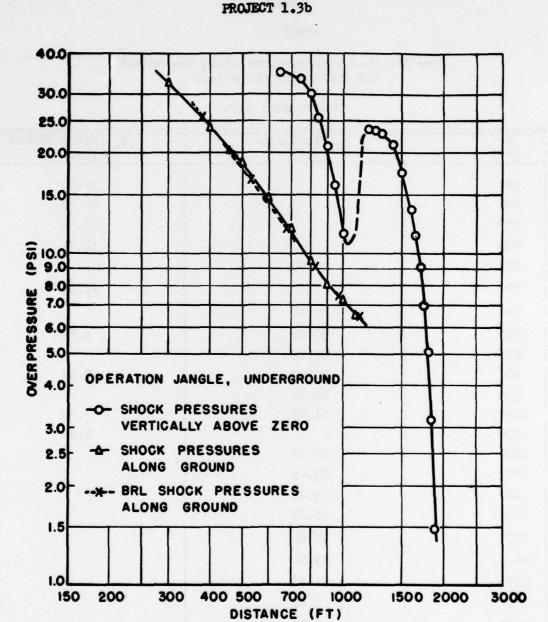


Fig. 3.8 Free Air Overpressures Along the Ground and Vertically Above Zero

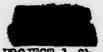
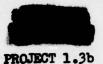


TABLE 3.8

Free Air Peak Overpressures Along the Ground and Vertically Above Zero Corrected to Sea Level

Underground Shot

R (ft)	P _s (Vertical) (psi)	P _s (Along Ground) (psi)
286.3		37.72
381.8		27.60
477.2		21.44
572.6		11.69
620.4	40.25	
668.1		13.72
715.8	38.07	
763.5	34.53	10.97
811.2	29.31	
859.0	24.05	9.26
906.7	18.28	Mary Mortan Maria
954.4	13.17	8.40
1049.8	4 38 62 6	7.54
1145.3	27.06	
1193.0	27.08	99 XADHE A -
1240.7	26.75	ALCOHOLA CONTRACTOR
1336.2	24.34	
1431.6	20.31	
1527.0	15.54	
1574.8	12.97	700 000 000
1622.5	10.52	9.54750
1670.2	8.07	
1717.9	5.82	44.4
1765.6	3.64	
1813.4	1.70	



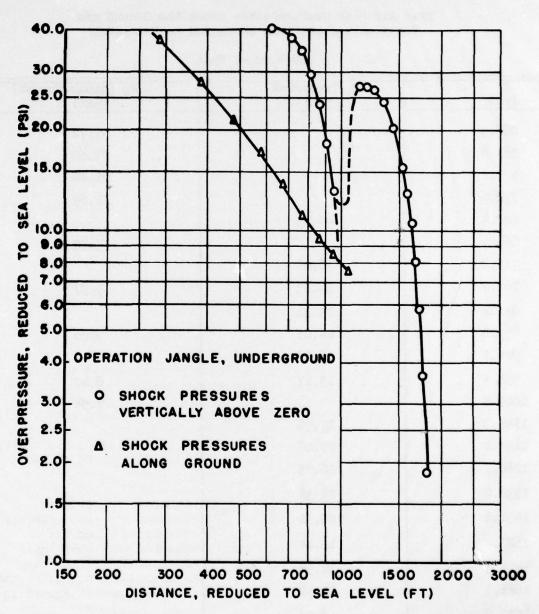
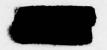


Fig. 3.9 Free Air Overpressures Along Ground and Vertically
Above Zero Corrected to Sea Level



CHAPTER 4

DISCUSSION AND CONCLUSIONS

4.1 GENERAL EVALUATION OF METHOD AND RESULTS

The shock velocity method of determining peak overpressure in free air as a function of distance rests on a firm foundation of successful results obtained by many laboratories in the past. The Rankine-Hugoniot relation, a theoretically derived equation indicating the relation between peak shock pressure and instantaneous shock velocity, is based on the reasonable primary assumptions of conservation of mass, momentum, and energy across the shock front. The utilization of the relation, however, can lead to serious erroneous conclusions if strict adherence to the rules governing its validity is neglected. The outstanding difficulty encountered when using the shock velocity method on tests such as are reported here stems from lack of information concerning the actual direction of propagation of the shock front. This is particularly true in the case of an underground event. Time-ofarrival measurements must be made only in the direction of shock propagation unless the angle between the line in which measurements are made and the direction of propagation is known.

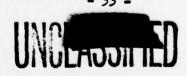
4.1.1 Validity of Assumptions

Before the tests were conducted it was assumed that the front of the shock wave for both tests would move in a radial direction parallel to the ground in the immediate vicinity of the ground surface and also parallel to a line extended vertically above ground zero. Only in these directions were time-of-arrival measurements made. Spherical symmetry of the shock, such as is observed on a high altitude air burst, could not be assumed on the basis of past experiences with HE charges mounted in similar positions.

As can be seen in Figs. 4.1 through 4.6, the original assumptions concerning the direction of shock propagation are perfectly valid except, possibly, for very short radial distances along the ground for the underground test. The photographs for this shot indicate that the shock was nearly spherical out to about 200 ft, and the shock front was definitely at an angle with the ground surface other than 90°. Any results in this region based on the velocity method should be treated cautiously.

4.1.2 Suitability of Smoke Rocket Trail Grid

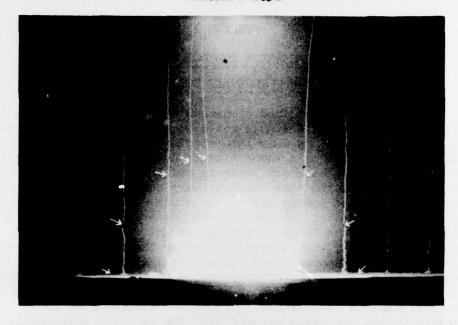
Aside from the fact that several of the rockets failed to smoke, it was apparent that two improvements would be desirable in any similar future test. In Figs. 4.1 through 4.6 it will be observed





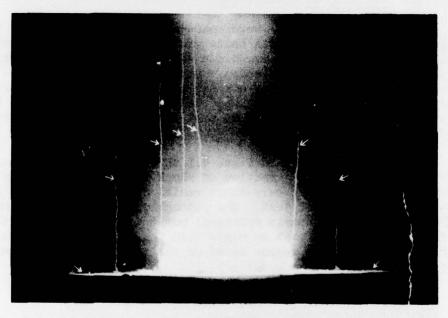


PROJECT 1.3b



500 FT

Fig. 4.1 Surface Event, 0.3557 Second



500 FT

Fig. 4.2 Surface Event, 0.4753 Second - 34 -



PROJECT 1.3b



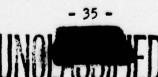
500 FT

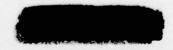
Fig. 4.3 Surface Event, 0.5790 Second

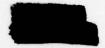


500 FT

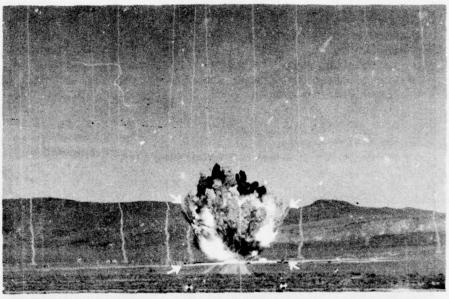
Fig. 4.4 Underground Event, 0.0 Second







PROJECT 1.3b



500 FT

Fig. 4.5 Underground Event, 0.1624 Second



500 FT

Fig. 4.6 Underground Event, 0.3248 Second



that directly behind the burst there are no rocket trails. They were purposely omitted in this region because the refraction effect is not discernible along a radial line from the explosion center. It would have helped substantially, however, if the gap in the smoke grid had been smaller in this region. The second suggested improvement is somewhat similar to the first. The spacing between all the grid lines should be smaller if measurements along the ground are to be made. In the present instance, the trails provided only a guide to the location of the shock wave at the point of ground intersection except where the line of sight from the camera to the shock included a trail directly beyond the shock. At other points along the ground the shock was barely strong enough to refract scattered background light. Ead the weapon been larger (the shock wave stronger) neither of the difficulties encountered would have been met.

Generally speaking, however, the rocket trail grid is considered suitable for tests similar to those herein reported.

4.1.3 Suitability of Cameras, Film, and Photographic Techniques

Camera equipment and films used were satisfactory but the results, in general, were poor. All films were overexposed during the first few tenths of a second after zero time on the surface event. The equipment used to obtain the pictures was similar to that used on Operation GREENHOUSE where decidedly better film records were obtained.

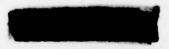
Timing records were a complete failure for the surface event but were successful for the underground event. As mentioned earlier, Sec. 3.1, there would have been less chance of a timing failure if the local primary timing standard had been battery-operated. Timing for each camera, rather than group timing for many cameras on a single record, is advocated by the authors. Otherwise, back-up installations lose half of their value before operation is begun.

Films and timing records were submitted to the Naval Ordnance Laboratory for analysis following an undue delay. In particular, the records for the underground event were evidently measured by some other group before being submitted, contrary to a specific request for the unscratched original films. This made the analysis very difficult. Figures 4.4 through 4.6 show numerous scratches which were found present in the film only in the region of interest.

4.1.4 Free Air Peak Overpressure Vertically Above Zero, Surface

The corrected free air peak overpressures are given for various distances vertically above zero in Table 3.4 and are shown graphically in Fig. 3.4. The most striking feature of the graph is its steep slope at the larger radial distances, indicating a more rapid







ressure decay with distance than that observed along the ground (see Fig. 3.3 for comparison). One reason for the more rapid rate of decay is the decline of atmospheric pressure (and air density) with increasing altitude above the surface. Even more rapid decay would be observed were it not for the bolstering effect introduced by the decrease in sound velocity with altitude.

Figures 4.1 through 4.3 show that the shock wave is not hemispherical, but has a greater radius from the explosion center along the ground than vertically upward. This is to be expected, especially en such a large scale explosion as compared with HE explosions where under similar conditions, the same effect has been observed.

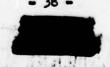
As was mentioned in Sec. 3.1.4, the TMT kilotonnage equivalent is of the order of 0.93 KV, based on the calculations described. The reader is cautioned against putting great faith in the THT kilotonnage equivalents reported by the various projects concerned with this operation. The figures quoted are critically dependent upon the value of Aused in the calculations. The authors are unaware of any extant HE vertical pressure data for which the scatter is not large, from which the values of & are taken. In addition, the error is cubed in reaching the final value in terms of kilotons of TMT.

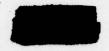
4.1.5 Free Air Peak Overpressure Along the Ground, Underground Shot

Very good agreement exists between the results reported by BRL Project 1.2a-1 (ref (b)), and those reported in Sec. 3.2.3. Both methods are fundamentally the same, yet completely different sets of records yielded nearly identical results.

The major difference between the two sets of data is that the EKL data yield a pressure-distance curve which is slightly concave downward, while in the same region the NOL results indicate the opposite trend, see Fig. 3.8. It is interesting to note that the HE-1 and HE-2 data, as reported in ref (b), have a slope which is concave upward similar to the NOL results. At greater distances, however, the NOL data assume a curvature similar to that of ERL.

The THT kilotonnage equivalent of 1.01 KT is comparable with that obtained by other projects. To illustrate how widely this figure can be made to vary, however, (see Sec. 4.1.4), consider the following argument: If instead of using an average value of Adetermined from both HE-1 and HE-2 one uses the individual values obtained, namely A equals 5.6 and 6.4 for the 10 psi pressure level, then one obtains kilotonnage equivalents of 1.23 and 0.84 MT, respectively. The percentage difference between the values for λ is approximately 15 per cent while the difference between ET equivalents is approximately 50 per cent.





4.1.6 Free Air Peak Overpressure Vertically Above Zero, Underground Shot

On this test a secondary wave overtook and passed the initial shock in the direction vertically above zero as indicated in Figs. 3.6 and 3.8. Along the ground this effect did not appear in the shock velocity results except possibly at the larger distances where the pressure-distance curve (Fig. 3.8) indicates a slower rate of pressure decay. However, the pressure-time results obtained by the Stanford Research Institute (Project 1(9)a), ref (f), showed a secondary pressure rise after arrival of the initial shock out to a radial distance along the ground of about 1,000 ft, beyond which it was not observed. It did not have a steep front like a shock but was undeniably a pressure wave.

If a sufficiently strong secondary pressure wave originated at or near the explosion center it would certainly grow faster in the vertical direction than along the ground because of the presence of the much hotter gases in the vertical direction. The apparent result would occur even for a wave of much lower strength than the primary shock wave since the pressure is a function of the Mach number (see Sec. 1.3.1). The cause of the secondary wave is unknown and deserves further study.

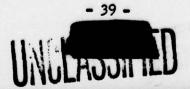
The TMT kilotonnage equivalents based on the 10 psi shock pressure vertically above zero and the results obtained in ref (d) are 0.72 and 0.89 KT. For distances along the ground the average kilotonnage equivalent was found to be 1.01 KT. The average of the three values is 0.87 KT. For reasons pointed out in Sec. 4.1.5 this figure should be used with caution.

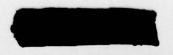
4.2 SOURCES AND COMPUTED MAGNITUDES OF ERRORS

With regard to errors due to resolution of the film and lens systems, foreshortening effect, curve fitting, etc., the reader is referred to ref (a) which deals with these usually negligible problems in complete detail. Pertaining to wind corrections, errors in using the incorrect values of atmospheric pressure and sound velocity, ref (b) provides complete information on how these errors affect the computed shock pressures.

4.2.1 Wind Correction

No corrections for wind were applied in obtaining the results presented in this report. On the surface shot where a time base was determined from BRL times-of-arrival along the ground any error due to wind along their line was automatically included in the results obtained here. For computing pressures vertically above ground zero







it is reasonable to assume that there were no vertical components of wind velocity large enough to warrant inclusion. A small error of unknown magnitude necessarily exists in these results.

On the underground test the wind was negligible and no corrections were warranted.

4.2.2 Distance Scale

The distances measured on the enlarged images of the film records were read to the nearest one-two hundredth (0.005) in., which corresponded to a distance in the plane of measurement of 1 ft. The error in locating fiducial markers was considerably less than this figure. Therefore, all measured distances are considered to be accurate to t 1.0 ft. Corrections for camera tilt and foreshortening were applied in obtaining the vertical and horizontal distance scales.

4.2.3 Timing Scale

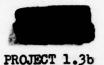
The timing scale for the surface shot, as taken from ERL time-of-arrival data, contains an uncertainty due to lack of knowledge of the asymmetry of the growth of the shock wave. Symmetry was assumed to exist along the ground in all radial directions in the establishment of the time scale. Because the camera speed was erratic it is impossible to state a value of the time per frame. The maximum error in time, however, probably does not exceed 5 millisec over the entire period of interest.

For the underground shot the timing information is more precise. The time per frame was constant and, as mentioned in Sec. 2.3.4, was found to be 0.0108475 ± 0.00005 sec. The maximum error in time over the entire period of interest is 0.00325 sec or 0.3 per cent. The error is negligible.

4.2.4 Estimated Errors in Calculated Pressures

The error in the peak overpressures determined for the surface shot cannot be calculated because of the uncertainty in the timing measurements and wind correction factor. All things considered, the pressures are estimated to be accurate to within 10 per cent.

A figure of accuracy of 3 per cent can be justified for the underground test in which the magnitudes of the numerous small uncertainties can be tallied.



4.3 CONCLUSIONS AND RECOMMENDATIONS

4.3.1 General

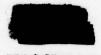
The method of detecting the instantaneous location of the shock front using a grid formed by smoke rocket trails is good for tests of these types to obtain peak pressures at various distances in free air in the directions specified. In films for each test the trails served well as guides indicating the contour of the shock front. In the majority of cases, however, the locus of the shock front in the directions along the ground and vertically above zero was observed directly, i.e. by observing the scattered background light refracted by the shock wave. The weakness and short duration of the shock wave made this observation and measurement a matter of special skill acquired by the authors over a period of years. Without the much more apparent refraction of light from the smoke trails it is quite conceivable that the shock would have passed undetected.

If similar tests are conducted in the future, two simple improvements could be made to advantage. The smoke trails should be moved closer together and, instead of establishing vertical grid lines, establish a grid of lines making an angle of about 60° with the surface, in a plane normal to the camera line of sight, thus aiding in the detection of the shock vertically above zero.

The contrast exhibited in the films of the underground test used for these measurements was low. The sky was cloudy and presented a steaky background which caused much difficulty in obtaining the measurements. The low contrast could have been improved considerably if a better figure for the exposure had been chosen.

An experimental film developed by Eastman Kodak, Inc. by direction of EGAG resembling commercial Microfile film should have been used but was not available to the Sandia Corporation. The film has very wide latitude covering a wide range of exposure and has, before this operation and since, proved to be superior in obtaining desirable records of this type. It is strongly recommended.

Failure of the timing system during the crucial period on the surface shot almost proved to be disastrous to this project. Once again it is repeated that timing records of the type used are not considered practical because of the large chance for failure. Each camera should have its own timing device built into it and should be operated from a separate timing signal generator. The additional cost for such installation is negligible with respect to that of the operation as a whole and may mean the difference between success and failure of a large number of the highly desired measurements.



4.3.2 Peak Pressure Along the Ground

As explained in Sec. 3.1.1, due to the timing failure on the surface test and the method used to establish a time base, the pressures along the ground must agree precisely with those obtained by ERL, Project 1.2a-1, by definition. The TMT kilotonnage equivalent was found to be 1 ± .05 KT at a pressure level of 10 psi.

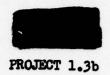
For the underground test the pressures along the ground agreed well with the results of Project 1.2a-1, the only difference being in the rate of decay (see Sec. 4.1.2). The pressures determined from NOL measurements are considered accurate to 3 per cent. The calculation of the TMT kilotonnage equivalent was shown in Sec. 3.2.5 to be 1.01 II.

4.3.3 Peak Pressure Vertically Above Ground Zero

Results were obtained for both events. The figure of accuracy of the peak pressures are different, however, largely due to the uncertainty involved in establishing the time base for the surface shot. For this shot a figure of 10 per cent is considered reliable. On the underground shot the figure of accuracy is 3 per cent.

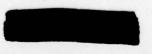
The occurrence of the sudden change of slope in the time-of-arrival curve for the underground shot led to the peculiar shape of the pressure-distance curves of Figs. 3.8 and 3.9 for pressures determined in the vertical direction. This phenomenon did not appear in the results obtained along the ground where the shock velocity method was used to determine peak pressures. A second pressure wave was recorded along the ground by pressure-time gages of SRI, Project 1(9)a. Further study of the cause of this phenomenon is warranted.

For the surface and underground tests, the TMT kilotonnage equivalents were found to be 0.93 - 1.23 KT and 0.72 - 0.89 KT, respectively, based on data at a pressure level of 10 psi vertically above zero. These values have been shown to depend critically on the value of λ employed. The only corresponding HE data found by the authors were those given in ref (d). Although in each case one of the values should be weighted more than the other, it is felt that the values are sufficiently flexible that their mean values are as good an indication of the TMT equivalents as any. The mean values are 1.08 KT for the surface test and 0.81 KT for the underground test as based on the 10 psi pressure level vertically above ground zero.



BIBLIOGRAPHY

- (a) Moulton and Simonds, Annex 1.6, Part II, Sec. 1, Greenhouse Report, 14 July 1951, Secret Restricted Data.
- (b) Molesky, Eberhard, and Kingery, "Peak Air Blast Pressures from Shock Velocity Measurements Along the Ground", ERL Report No. 805 RD, Project 1.2a-1, Operation JANGLE, 1952.
- (c) Haskell and Vann, "The Measurement of Free Air Atomic Blast Pressures", Air Force Cambridge Research Center, Preliminary Report Project 1.3c, Operation JAMGLE, 10 April 1952.
- (d) Stevens, "The Behavior of the Shock Wave in Air from Small Underground Explosions", NavOrd Report 1863, 26 April 1951.
- (e) Army, Mavy, Air Force (JCS) TM 23-200/OFRAV-P-36-00100/AFQAT 385.2: Supplement No. 1 dtd 8 Feb 1952 (Secret).
- (f) Doll and Salmon, "Ground Acceleration, Ground and Air Pressures for Underground Test", Operation JANGLE Preliminary Report, April 1952.



OPERATION JANGLE

PROJECT 1.3C

THE MEASUREMENT OF FREE AIR ATOMIC BLAST PRESSURES

ру

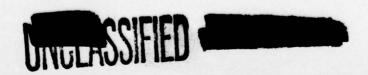
NORMAN A. HASKELL

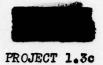
and

JAMES O. VANN MAJOR, USAF

10 APRIL 1952

GEOPHYSICS RESEARCH DIVISION
TERRESTRIAL SCIENCES LABORATORY
AIR FORCE CAMBRIDGE RESEARCH CENTER
230 ALBANY STREET
CAMBRIDGE, MASSACHUSETTS

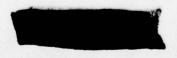


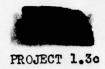


CONTENTS

ABSTRACT .				•	•	•	•	•	•	•	•	•	•	•	•	•	vii
CHAPTER 1	INTR	ODUCTION	. I	•	•	•			•	•	•	•	•			•	1
		OBJECT:					•		•							•	3
	1.3	HISTORY THEORE	PICAL		•	•	•	•	•	•	•						1
CHAPTER 2	EXPE	RIMENTAL	L PRO	CED	URE	•	•	•	•	•		•	•			•	5
	2.1	INSTRU	ENTA	TIO	N	•				•	•						5
	2.3	CALIBRA	CONS	·		·	•	:	:	:	:	:	:	:	:	:	8
CHAPTER 3	TEST	RESULTS	· ·														11
	3.1	DISCUS	SION	OF I	PRES	SSUE	CE I	REC	ORD	S							14
	3.2	DEPEND INTERP	ITAN TATES	MOI	OF (ANI	STI	er i	Posi	ITI.	OM	:	•	:	:	•	25
CHAPTER 4		LUSIONS	AND	REC	OMMI	NDA	TIC	INS									37
	4.1	CONCLUS	SIONS														37
	4.2	RECOMME	ENDAT	ION	S	•	•	•	•	•	•	•	•	•	•	•	37
APPENDIX A	RADIO	TELEM	TRY	INS	PRUM	TWE	'AT'	ON	ANI	D C	ALI	BRA	TIO	N	•	•	39
		INSTRU					•		•	•	•	•	•	•	•	•	39
	A-3		DUOT	ION	PR	CEI	URI	·	:	:	:	:	:	:	:	:	46
APPENDIX B		PLE OB				IG I	NSI	RU	VEN!	TAT	ION	AN	D C	ALI	BRA	-	
		• • •				•	•	•	•	•	•	•	•	•	•	•	48
	B.1 B.2					:	:	•	:	:	:	:	:	:	:	:	52
APPENDIX C	MATH	MATICAL	SYM	BOL	S												53
BIBLIOGRAPHY						•	•			•					•	•	51

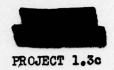






ILLUSTRATIONS

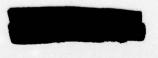
CHAPTER 2	EXPERIMENTAL PROCEDURE
4	2.1 Location of Ground Stations
CHAPTER 3	TEST RESULTS
	3.1 Peak Pressure Oscilloscope Trace
	3.8 Overpressure vs. Time, Canister No. 3
APPENDIX A	RADIO TELEMETRY INSTRUMENTATION AND CALIBRATION
	A.1 Parachute-Borne Cenister Photograph
APPENDIX B	MULTIPLE OBJECT TRACKING INSTRUMENTATION AND CALI- BRATION
	B.1 Airborne Beacon Photograph

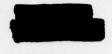


TABLES

CHAPTER 3	TEST RESULTS
	3.1 Observed Peak Pressure and Travel Times
	ters 3.7 Altitude Correction Scale Factors
APPENDIX A	RADIO TELEMBERY INSTRUMENTATION AND CALIBRATION
	A.1 Canister Equipment 47







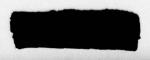
ABSTRACT

The object of the project was to measure the free air peak pressure of an atomic detonation as a function of time and space. The operational procedure consisted of deploying, from two aircraft, eight instrumented parachute-borne canisters positioned from 2000 feet to 29,000 feet vertically above ground zero. Each canister contained an altimeter transducer, two differential pressure transducers, a radio telemetry transmitter and a radio tracking beacon. The ground equipment consisted of a radio telemetry receiving station for recording pressure data, four multiple object tracking stations for recording the positions of the canisters by triangulation method, and two SCR 584 radar stations for positioning the aircraft over a drop point.

The operation was a preliminary test of equipment and techniques in anticipation of future tests involving a more extensive array of parachute-borne canisters. Any conclusions may be considered tentative since the positions actually attained by the parachute-borne canisters were inconsistent with the intended vertical array and did not provide a clear cut test of the Fuchs altitude correction. For the lowest four canisters this correction is of the same order as the estimated error of the peak pressure measurements. Two canisters were at such great horizontal distances and low shock pressure levels that erratic results are to be expected, due both to errors of measurement and the effects of shock wave refraction. Data from one canister were questionable because the canister was in the aircraft bomb bay at the arrival time of the shock wave. No data was received from one canister because the pressure transducers were off scale due to a restricted pressure line. There is justification for concluding that the data obtained in the project supported the Fuchs theory within the probable accuracy of the observations out to overpressures of about 0.1 psi.

It is recommended that further tests be made using up to 20 parachute-borne canisters in an extensive array to cover the range of peak overpressures from about 0.15 to 4.0 psi.







1.1 OBJECTIVE

The primary objective of the project was to measure the free air peak blast pressure of an atomic detonation as a function of time and space. Secondary objectives were to test operational procedures and instrumentation to improve techniques and increase accuracy of measurements in a later operation involving a larger detonation.

Although approximate theoretical treatments of the effect of ambient pressure and temperature gradients on blast wave peak pressures have been developed, there has been no reliable experimental test of the theoretical conclusions. Because of the importance of these effects in relation to the optimum height of bomb burst, particularly for bombs of much larger yield than present types, and the determination of the minimum range and altitude for aircraft safety, a direct experimental test is an urgent requirement.

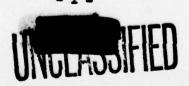
1.2 HISTORICAL

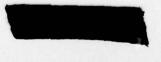
The military requirement for an experimental test of the Fuchs theory was brought to the attention of the Terrestrial Sciences Laboratory, Air Force Cambridge Research Center, early in 1950. At that time the basic techniques described in this report were devised and a proposal was prepared for participation in Operation GREENHOUSE. However, the time for preparation of such an extensive project was insufficient and no action was taken.

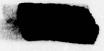
In December, 1950 the project was revived under Operation WINDSTORM and was officially included in February, 1951. Later the project was tentatively included in Operation BUSTER but due to unsuitable frequency requirements was included in Operation JANGER on a reduced operational scale.

1.3 THEORETICAL

In discussing the propagation of shock waves from chemical explosives the range of distances over which military significant effects occur is ordinarily so small that the atmosphere may be treated as a homogeneous body of gas, initially at the same pressure and temperature everywhere. (This is not, of course, the case with the occasional minor damage that may be done at comparatively long ranges due to focusing







effects caused by temperature variations and winds.) However, in the case of a nuclear explosion it is necessary to consider propagation over a range of altitudes so great that the variation of atmospheric temperature, pressure, and density with altitude is not insignificant. The effects of the inhomogenity of the actual atmosphere are particularly important in connection with (a) the height of burst of atomic bombs of very large yield, (b) the determination of the zone of danger to aircraft in the neighborhood of an atomic bomb, and (c) the use of blast pressure measurements on aircraft in connection with bomb damage assessment systems.

The variation of atmospheric properties with altitude affects the prediction of peak overpressure in two ways (a) the effect of the ambient pressure at the altitude at which the bomb is detonated, and (b) the effect of variation in atmospheric properties between the altitude of detonation and the point at which the peak pressure is to be determined. The first effect has been discussed theoretically by R. G. Sachs and the second by K. Fuchs². These two theories lead to scaling laws for peak overpressure which may be expressed in the following form.

Let f(r) be the peak overpressure vs. distance function for a bomb of 1 KT yield (radiochemically determined) in an unbounded homogeneous atmosphere at standard sea level pressure (14.70 psi). The free air peak overpressure at slant range, R, and altitude, z, due to a bomb of yield, W, fired at altitude, h is then?

$$\Delta P (R,z,h) = k \frac{3}{4} f(k R/S)$$
 (1.1)

where
$$S = W^{y_3}$$
 (1.2)

$$k = [P_0(h)/P_0(o)]^{1/3}$$
 (1.3)

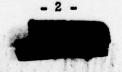
$$\lambda = \exp \int_{A}^{z} \left[\left\{ c(h)/c(z) \right\}^{2} \left\{ \rho(h)c(h)/\rho(z)c(z) \right\}^{2} -1 \right] dz/(z-h) \quad (1.4)$$

$$M = \lambda \left[P(z)c(z)/\rho(h)c(h) \right]^{\frac{1}{2}}$$
(1.5)

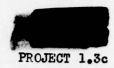
and $P_0(z)$, and c(z) are respectively the atmospheric pressure.

2 K. Fuchs. The Effect of Altitude, Vol VII, Pt II, Chap 9 of Los Alamos Technical Series, LA-1021.

3 See Appendix C for a consolidated list of mathematical symbols.



R. G. Sachs, The Dependence of Blast on Ambient Temperature and Presure. Ballistics Research Lab., Aberdeen, Report No. 466 (May 1944). The effect has also been treated by J. G. Kirkwood and S. R. Brinkley in OSRD Report No. 5271. The two treatments lead to similar results and Sachs' scaling law will be used here since it can be applied directly to empirical data.



density and sound velocity at altitude z. Since $c(h)/c(z) = [T(h)/T(z)]^{\frac{1}{2}}$ and $\rho(h)/\rho(z) = P_0(h)T(z)/P_0(z)T(h)$, where T(z) is the absolute temperature, equations (4) and (5) may also be written in the form.

$$\lambda = \exp \int_{h}^{z} \left[\left(T(h) / T(z) \right)^{24} \left\{ P_{o}(h) / P_{o}(z) \right\}^{2} - 1 \right] dz / (z-h)$$

$$M = \lambda \left\{ T(h) / T(z) \right\}^{24} \left\{ P_{o}(z) / P_{o}(h) \right\}^{2}$$
(1.6)
(1.7)

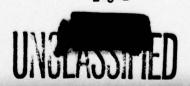
The quantity k is the Sachs scale factor expressing the effect of the ambient pressure at the altitude of detonation and λ and μ are the Fuchs scale factors.

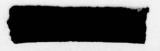
The Sachs scaling law has been at least roughly verified by measurements with TNT charges fired at altitudes up to 14,000 ft., but no experimental test of the Fuchs theory has been made. Actually a completely unambiguous test of the theory is not possible since the basic pressure vs. distance function, f(r), for an atomic bomb in an unbounded uniform atmosphere is not a directly observable quantity. An indirect test may be made, however, by measuring ΔP at various ranges and altitudes and plotting $\Delta P/k_M$ against k_L^2R/S . If the observed points define a reasonably smooth curve within the experimental error, with no systematic deviations correlatable with altitude, the theory may be accepted as adequate for practical applications.

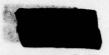
One of the basic assumptions of the Fuchs theory is that the flow is purely radial at all points, that is, no consideration is given to the effect of refraction of the shock wave. This is probably an adequate approximation within the region of overpressures of military significance, but it will certainly not be correct at very large distances and low overpressures. As a very rough estimate, we may expect to find observable departures from the Fuchs theory due to refraction effects at peak overpressures of about 0.1 psi or less.

In addition to the uncertainty in the correct form of the f(r) curve, there is the further complication of the effect of the ground surface. Ideally, it would be desirable to establish f(r) by using an air burst and measuring the peak pressure of the direct shock at airborne gauges located above the Mach stem. Practically, the difficulty of placing an array of parachute-borne gauges at the desired positions with respect to the bomb, and at the correct time, makes the use of a ground or tower burst preferable, at least for preliminary tests. It is then necessary to know how much the effective yield is increased by reflection from the ground. If the ground were perfectly rigid, all of the energy that would have been emitted in the lower hemisphere in the free air would be reflected into the above-ground hemisphere, and the

NDRC, Summary Technical Report of Division 2, Effects of Impact and Explosion, pp 106 & 107







effective yield would be twice the actual yield. To allow for the loss of energy to the ground due to cratering and other permanent deformation near the point of detonation and to the radiation of elastic wave energy a reflection factor of 1.5 or 1.6 instead of 2 has sometimes been used. This is, however, a questionable figure and for the purposes of the present discussion a reflection factor of 1.8 will be assumed. The radiochemically determined yield of the JANGE surface shot is taken as 1.2 KT, so that the yield scale factor is S = (2.2) = 1.301.



CHAPTER 2

EXPERIMENTAL PROCEDURE

2.1 INSTRUMENTATION

Instrumentation involved in the operation consisted of four objectives: radio telemetry instrumentation to obtain free air pressure data, canister tracking instrumentation to obtain time-space data of the parachute-borne canisters, radar instrumentation to position the aircraft for deployment of the eight canisters vertically above the atomic detonation, and the instrumentation of the parachute-borne canister.

2.1.1 Radio Telemetry Instrumentation

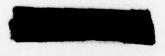
Reference is made to Appendix A for a more detailed description of the instrumentation employed in obtaining radio telemetry pressure data. Pressure measuring instrumentation and the parachute-borne canister were developed by the Pacific Division Development Laboratories, Bendix Aviation Corporation, Burbank, California, under Contract AF 19(122)-459.

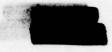
The airborne radio telemetry system installed in each canister consisted of a pressure altimeter transducer, two differential
pressure transducers one having a scale range of approximately twice
the other and the radio telemetry transmitter unit. Upon receiving a
pressure stimulus each transducer in the canister frequency modulated
a sub-carrier; the three sub-carriers were mixed and frequency modulated the radio frequency carrier, the data link between the parachuteborne canister and the recording ground station. The ground radio
telemetry recording station consisted of a separate FM receiver for
each parachute-borne canister. The output of each receiver, being a
mixture of the three original frequency modulated sub-carriers, was
separated by a filter network. Subsequently each sub-carrier was
channeled to a sub-carrier discriminator which produced a current proportional to the original pressure stimulus. These proportional currents were applied to galvanometers of the recording oscillograph.

2.1.2 Canister Tracking Instrumentation

Reference is made to Appendix B for a more detailed description of the instrumentation employed in obtaining the time-space positions of the parachute-borne canisters. The system employed to







track the multiple number of canisters was developed by The Glenn L. Martin Company, Baltimore, Maryland, under Contract AF 19(122)_460.

The Multiple Object Tracking System is based on the method of triangulation to obtain position data. Radio range measurements were determined from four ground interrogating stations to the canisters in space. The system is capable of tracking 32 objects in space at one second intervals with an accuracy of + 100 ft.

During each second of operation all ground stations shared time to alternately interrogate each parachute-borne canister. Interrogation by the ground station was accomplished by transmitting a binary code train of five digits and a range pulse which initiated the operation of the range counting circuit. Each airborne beacon was designed for a selected binary number which was established in the beacon decoder. The decoder differentiated between the selected number and all others so as to excite the modulator only when the selected number occurred. The modulator fired the transmitter which initiated the reply pulse. The reply pulse, received by the ground station, stopped the range counter. The range count, in increments of 0.1 micro-seconds, was recorded and established the range from the ground station to the parachute-borne canister.

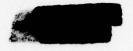
2.1.3 Aircraft Positioning Instrumentation

Two SCR 584 radar stations were used to guide two B-29 aircraft over a drop point, both in reference to time and position in space. Four parachute-borne canisters were deployed from each B-29 aircraft at a computed drop time and drop position, corrected for the integrated horizontal wind drift of the parachute-borne canisters through a vertical axis over ground zero.

2.1.4 Canister Instrumentation

Reference is made to Appendix A for a detailed description of the instrumentation used in the parachute-borne canisters.

The dual parachute system consisted of two parachutes, a 6-foot drag fist ribbon parachute and a 28-foot flat parachute. All canisters were deployed from the aircraft using the 6-foot ribbon parachute attached to the static line. Ballistic data and the particular position of a canister in the array determined the time of canister fall with the 6-foot ribbon parachute. At a predetermined time, different for each canister, an internal timer fired a squib cutter releasing the 6-foot fist ribbon parachute and deploying the 28-foot flat parachute. The canisters were internally preheated in the bomb bays of the aircraft three minutes prior to initiating deployment. Six



thermostats were installed in various compartments of the canister to regulate the internal temperature. The parachute-borne canister complete with dual parachutes weighed 275 pounds.

2.2 CALIBRATION PROCEDURE

Reference is made to Appendix A and B for a more detailed description of calibration procedures of the radio telemetry system and the Multiple Object Tracking System (MOTS).

2.2.1 Radio Telemetry Calibrating Procedure

The receiving radio telemetry ground stations were calibrated by measuring a series of standard audio frequency signals at the appropriate station discriminators. Records were made on the oscillograph for each standard frequency to the discriminators. Using these values, calibration curves were plotted of galvanometer deflection versus frequency.

Pressure transducers were calibrated by applying accurate pressure values to each pressure transducer, covering the entire range of each pickup. The frequency of the sub-carrier oscillator connected to the transducer was recorded and a curve of frequency versus transducer function was plotted from these data.

By use of the discriminator and transducer calibration curves, a correlation between the transducer function values and galvanometer deflection values was obtained.

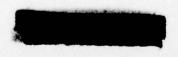
2.2.2 Canister Tracking Calibration Procedure

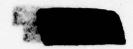
A ground sub-station containing a beacon similar to the airborne beacon was established northwest of ground zero. A survey was made to obtain the accurate slope range from each MOTS ground station to the ground sub-station. During Operation JANGE the sub-station was continuously interrogated by each MOTS station. A comparison of range readings from each MOTS station to the sub-station with the known range established the inherent delays or effective range error of each ground station. This range error was then applied as a correction factor to the range data obtained from the parachute-borne canisters.

2.2.3 SCR 584 Redar Calibration Procedure

Instructions contained in the applicable Technical Order's were employed.







2.3 OPERATIONS

The problems of the operation consisted of five phases: (1) the guidance of two B-29 aircraft over a drop point both in reference to position and time, employing two SCR 584 radar tracking stations; (2) the deployment of eight parachute-borne canisters from two B-29 aircraft, one aircraft flying at an altitude of 15,800 feet MSL and one aircraft flying at an altitude of 35,800 feet MSL; (3) the recording of blast pressure profiles from the positions of the parachute-borne canisters; (4) the continuous tracking of eight parachute-borne canisters employing the Multiple Object Tracking System; and (5) the calibration of the integrated horizontal wind drift of the parachute-borne canister through a vertical axis over ground zero to determine a corrected drop point and drop time for the aircraft.

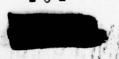
The locations of the radio telemetry station, the MOTS stations and the SCR 584 radar stations are indicated in Figure 2.1.

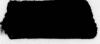
The operation consisted of the following sequence of events. Coordinated data between the aircraft navigator and the SCR 564 radar operators were used to position the aircraft for initiating the deployment of the parachute-borne canisters. The deployment position was
corrected for average wind drift of the parachute-borne canisters.
The low aircraft initiated deployment of canisters No. 1, No. 2, No. 3
and No. 4 at H-79 seconds required by timing factors of the arrival
time of the blast wave and the ballistic factors of positioning the
canisters in the array. The high aircraft initiated deployment of
canisters No. 5, No. 6 and No. 7 at H-100 seconds. Canister No. 5 was
deployed by the high aircraft at H+25 seconds to an intended position
of 33,000 feet horizontally from the vertical axis through ground zero.
The radio telemetry ground station monitored the canisters from aircraft deployment time to H+10 minutes. The MOTS ground stations monitored the canisters from aircraft deployment time to H+6 minutes.

2.3.1 Low Aircraft Operation

The low B-29 aircraft flying at 15,800 feet MSL completed five runs as follows:

- 0720 PST A calibration run was completed over ground zero to establish true ground speed.
- 0750 PST A simulated run was completed using the arbitrary time of 0750 PST as H-79 seconds. The aircraft was approximately 1800 feet short of the calibrated position at the simulated zero drop time. Some inconvenience and confusion was caused by a B-50 flying in formation with the B-29. This condition was undesirable since accurate guidance was required. It was fortunate that the





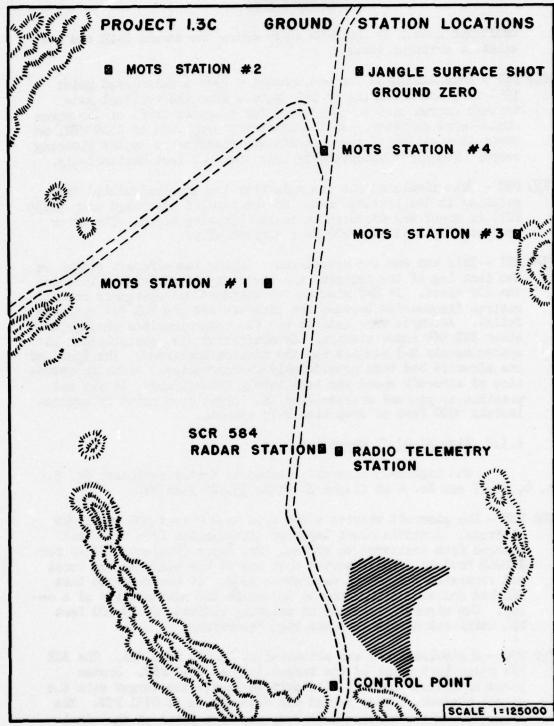
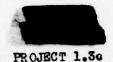


Fig. 2.1 Project 1.3c Ground Station Locations





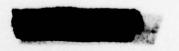
confusion caused by the B-50 in tracking the target B-29 did not exist at critical times.

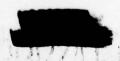
- 0810 PST This simulated run was completed over a calculated point 1950 feet and a bearing of 190 degrees from the vertical axis through ground zero to compensate for computed drift of the parachute-borne canister. At the arbitrary drop time of 0810 PST, no error in position of the aircraft was discernable on the plotting board. The error was probably less than 200 feet horizontally.
- OS35 PST This simulated run was made over the same calculated drop point as in the previous run. At the time of simulated drop (OS35 PST) no error was discernable on the plotting board. The error was probably less than 200 feet horizontally.
- O900 PST This run was the actual run. During the aircraft flight on the last leg of the pattern, the aircraft was advised to increase the air speed. At H-7 minutes the standard and emergency communications frequencies between the aircraft and the SCR 584 operator failed. Attempts were made to use the communications through the other SCR 584 radar station. Communication was reestablished at approximately H-3 minutes and the mission continued. The speed of the aircraft had been considerably overcorrected. Although reduction of aircraft speed was immediately accomplished, it was not possible to prevent overshotting the target drop point by approximately 6000 feet at drop time H-79 seconds.

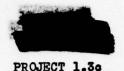
2.3.2 High Aircraft Operation

The high B-29 aircraft planned to deploy canisters No. 5. No. 7 and No. 8 at flight altitude 35,800 feet MSL.

- 9700 PST The aircraft started climb from 16,000 feet MSL to flight altitude. A middle cloud layer of alto-cumulus from the south changed from scattered to broken. Dr. Kuper (Project Officer for JANGLE Project 1.3a) reported that one of his balloons had burst and requested a delay in detonation time. It was reported that AEC had called a conference to determine the advisability of a delay. The aircraft remained at existing altitude of 29,000 feet MSL until detonation time had been determined.
- 0750 PST A simulated run was attempted at 29,000 feet MSL. The SCR 584 radar lost track of the target B-29 at 0742 PST. Broken cloud conditions made it difficult to locate the target with the visual tracker. Radar target was established at 0751 PST. The aircraft was two minutes late over the drop point at the simulated drop time of 0750 PST.







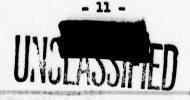
- 0755 PST Information was received that no delay in detonation time would be made. The aircraft pilot was informed to climb to operational altitude.
- 0810 PST This simulated run was made while the aircraft was climbing to altitude. The run was unsatisfactory because the time scale had not been established.
- 0835 PST This simulated run was attempted in conjunction with the other aircraft operation, using the same simulated drop time. The aircraft was late at the drop point by a minute. Overcast cloud conditions existed.
- O900 PST This rum was the actual rum. The aircraft pilot was informed by the SCR 584 operator to perform a 360-degree turn to lose time. The SCR 584 radar lost the target B-29 at H-12 minutes and did not locate the target B-29 until H-5 minutes. The aircraft position was considerably behind the time schedule. Every attempt was made to gain time. The aircraft reduced altitude from 35,800 feet to 32,800 feet MSL in an attempt to gain speed, however, the lost time could not be completely compensated. Parachute-borne canisters No. 5, No. 6 and No. 7 were deployed at H-100 seconds, about 45,000 feet short of the intended drop point. Canister No. 8 was deployed at H+26 seconds approximately over ground zero, however, the canister was in the bomb bay at the arrival time of the blast wave. The approximate positions of the canisters at arrival time of the shock wave compared to the intended positions are shown in Figure 2.2.

2.3.3 Canister Deployment Operation

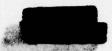
Deployment of both the 6-foot fist ribbon parachute and the 26-foot flat parachute was satisfactory for all canisters. All canisters and parachutes survived the shock wave. However, because of the comparative great ranges from ground zero to the canisters no conclusions can be formulated with respect to destructive blast and thermal effects on the parachute-borne canister.

2.3.4 Radio Telemetry Operation

Radio telemetry signals from all eight parachute-borne canisters were recorded by the radio telemetry ground station from deployment time until loss of radio signals resulting from the eventual low altitude of the parachute-borne canisters. Pressure profiles of the blast wave were recorded from seven of the eight canisters.







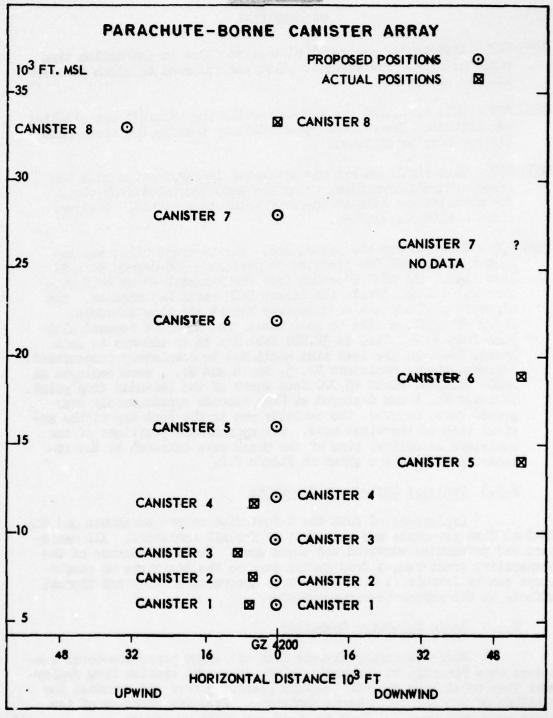


Fig. 2.2 Parachute-Borne Canister Array







2.3.5 Multiple Object Tracking System (MOTS) Operation

The Multiple Object Tracking System was originally conceived in February, 1951 and development was initiated in March, 1951. During Operation JANGLE the instrumentation was still in the stage of development, however, the results indicated that the system with minor modifications of instrumentation will be greatly improved for future operations.

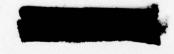
The range data obtained were intermittent and no positional information of parachute-borne canisters was obtained for the critical arrival time of the shock wave. The interrogated replies recorded at the four ground stations were as follows:

Ground Station	Canisters Which Responded
No. 1	No. 8 No. 4 and No. 8
No. 2	No. 4 and No. 8
No. 3	No. 3. No. 4 and No. 8
No. 4	No. 1, No. 3, No. 4 and No. 8

2.3.6 Wind Calibration Operation

Operational plans included the deployment of a parachuteborne canister at H-14 hours to determine the aircraft drop point. It was planned to track the position of the canister during descent with the MOTS to obtain wind drift data. However, at pre-test briefing of the aircraft crew the deployment of the calibration canister was cancelled by SWC. The pibal data available at the Control Point were used to compute the wind drift of the parachute-borne canisters.







TEST RESULTS

3.1 DISCUSSION OF PRESSURE RECORDS

The basic data obtained are summarized in Table 3.1. The oscillograph traces are reproduced as Figures 3.1, 3.2 and 3.3. The damped oscillations which appear on the differential pressure gauge traces immediately after the arrival of the shock wave are due to oscillation of the air column in the tube connecting the pressure probe to the gange and have no bearing on the structure of the shock wave itself. The peak pressures tabulated have been obtained by averaging these oscillations out and extrapolating the mean curve back to the arrival time of the shock front. The 0.7 psi gauge in canister No. 4 appears to be considerably over-damped, so that a longer extrapolation (over about 0.1 sec) was required in this case, but the peak overpressure obtained agrees well with that measured by the under-damped 1 psi gauge on the same canister. On canister No. 5 and No. 6 the pressure differential existing between the sealed reference chambers and the ambient atmospheric pressure put the low range differential pressure ganges off scale, so that no shock pressure readings could be obtained from these traces. On canister No. 7 both differential pressure games were off scale for the same reason.

Due to the large errors in the deployment of the canisters the observed peak pressures are in most cases only a small fraction of the total range of the differential pressure gauges used, and it is difficult to estimate the accuracy obtained. Anticipating that about 80% of the positive range of the lower range gauge would be used in each case, an overall accuracy of 3% of the total gauge range was considered acceptable. In the case of the + 10 psi gauge this would mean an allowable error of 0.6 psi, a value equal to the observed peak pressure at canister No. 1. However, it is quite obvious by inspection of the trace for this gauge, shown in Figure 3.1, that the error in reading the trace displacement is certainly not 100% of its maximum value, and is very likely less than 20%. Considering the excellence of the agreement between the high and low range gauge readings on canisters No. 1, No. 2 and No. 4, it is considered that the peak pressures at these positions are very unlikely to be in error by more than + 10%. In the case of the low-range gauge on canister No. 3 a gross error is suspected on the grounds of inconsistency with the other data. For canisters No. 5 and No. 6 the trace displacement is so small that the reading error is probably a major factor, but it seems unlikely that this





TABLE 3.1

Observed Peak Pressures and Travel Times

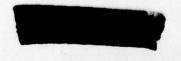
Cenister No.	Genge Range (psi)	Peak Over- pressure (psi)	Ambient Pressure (psi)	Arrival Time of Shock Wave (sec		
1	<u>+</u> 10	0.60	11.80	5.112		
1	± 5	0.60				
2	<u>+</u> 5	0.60	11.10	5.210		
2	<u>+</u> 2	0.59				
3	<u>+</u> 2	0.42	10.52	6.832		
3	<u>+</u> 1	0.25				
74	<u>+</u> 1	0.33	9.45	8.122		
4	± 0.7	0.34				
5	± 0.7	0.030	8.66	46.84		
6	± 0.4	0.030	7.14	148°0/1		
8	± 0.2	0.068	3.85	25.45		
8	+ 0.2	0.074				

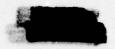
could be more than + 30% of the indicated peak pressure. Canister No. 8 was still in the bomb bay of the aircraft at the time of arrival of the shock wave. As a result, the noise level was quite high, amounting to about 50% of the peak shock pressure as shown by the traces for this canister in Figure 3.3. In spite of this, the difference between the two gauges in this canister is only 8% of the mean of the two and it will probably be conservative to assume that the mean peak pressure is reliable to at least 15%.

3.2 DETERMINATION OF CANISTER POSITION

In the absence of sufficient MOTS data for a complete determination of canister positions the altitudes and slant ranges have been determined as accurately as possible from the telemetered ambient pressures and shock wave arrival times. Radiosonds temperature, pressure,







and wind data for 0700 and 1000 PST on the day of the shot were supplied by the Nevada Test Site Weather Station and are given in Tables 3.2, 3.3, 3.4 and 3.5. From this data true altitude vs. pressure was computed by the Experimental Weather Station of the Geophysics Research Division, AFCRC, using standard meteorological procedures. The altitudes given in Table 3.6 were then obtained from the telemetered ambient pressure data by interpolating for the time of the shot (0900 PST). The ambient pressure values are considered to be accurate to about 0.1 psi, corresponding to an altitude accuracy of about + 200 ft. at 6000 ft. or + 500 ft. at 30,000 ft. At 30,000 ft. there may be an additional 500 ft. uncertainty in the pressure vs. altitude data used in the reduction.

To convert the observed travel times into slant ranges a provisional angle of elevation from ground zero for each canister was first assumed. Expected values of peak overpressure as a function of distance along the radial lines from the bomb to each canister were then computed and used in conjunction with the radiosonde temperature and pressure data to compute the shock propagation velocity from the Rankine-Hugoniot equation.

$$U = c\sqrt{1 + (6/7)(4P/P_0)}$$
 (3.1)

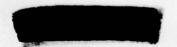
where U = shock front velocity

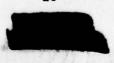
c = sound velocity at the ambient temperature

AP = peak overpressure

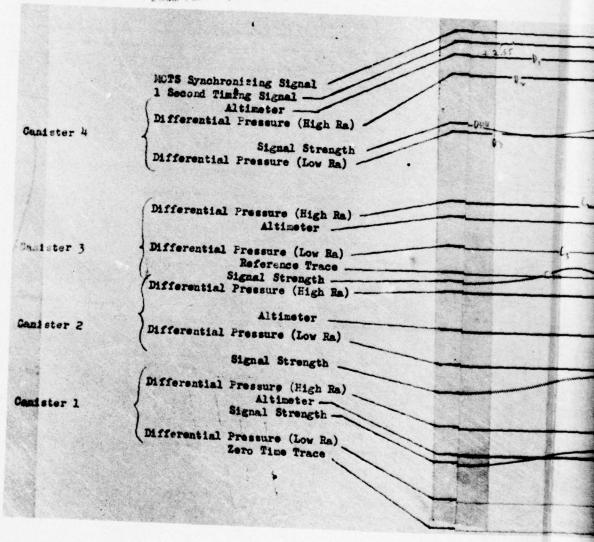
Po = ambient pressure

To this was added the component of the wind velocity, as determined from the radiosonde data, along the various radii to the canisters. (Since the azimuths of the canisters from ground zero were not accurately known, it was assumed that the whole array lay in a vertical plane along the flight path of the aircraft, which was 2100. Canisters No. 1 through No. 4 were known to have been dropped beyond ground zero and canisters No. 5, No. 6 and No. 7 were short of ground zero, hence it was assumed that the shot to canister azimuth was 210° for No. 1 through No. 4 and 30° for No. 5, No. 6 and No. 7. Canister No. 8 was sufficiently near to the vertical above ground zero so that the wind component in this case was negligible. From the resultant radial velocities the travel times along the radii to each canister were computed as functions of distance. These values were then converted into average velocities as functions of time. The average velocities and computed radial distances corresponding to the observed travel times for each canister are given in Table 3.6. Since the angles of elevation corresponding to the ranges and altitudes shown in the table do not differ greatly from those assumed initially, a second approximation was not justified by the accuracy of the data. At these ranges the computed average velocities are





THIS PAGE IS BEST QUALITY PRACTICABLE





PROJECT 1.3e

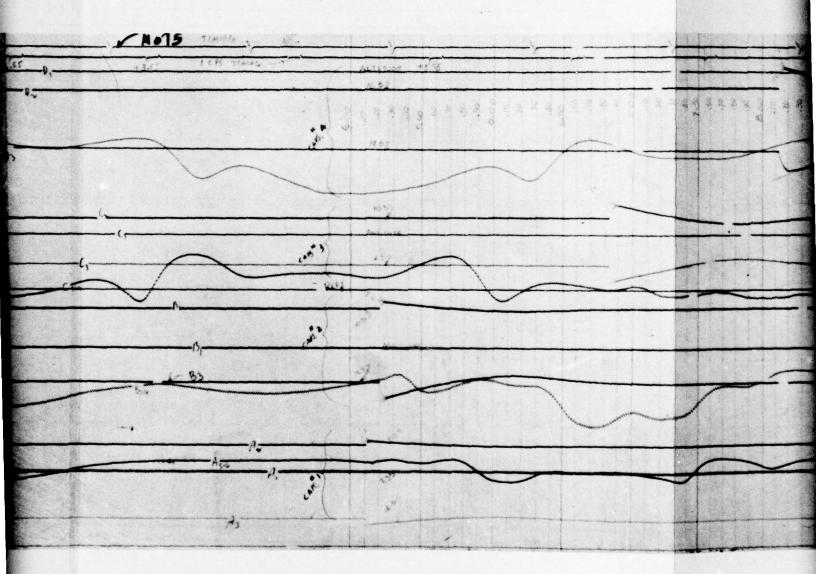


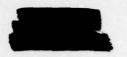
Figure 3.1 Peak Pressure Oscilloscope Trace

MOH COPY PURSISHED TO DOS

pe Trace

3UNCLASSIFIED

Note Synchronizing Pulse 1 Second Timing Pulse Altimeter -Differential Pressure (High RA) Canister 8 (Low RA) Sighal Strength . Altimeter -Differential Pressure (High RA) Canister 7 (Low RA) Signal Strength Reference Trace Altimeter -Differential Pressure (Righ Ra) Canister 6 (Low Ra) Signal Strength Altimeter -Differential Pressure (High Ra) Canister 5 (Low Ra) Signal Strength . Zero Time Trace .



PROJECT 1.30

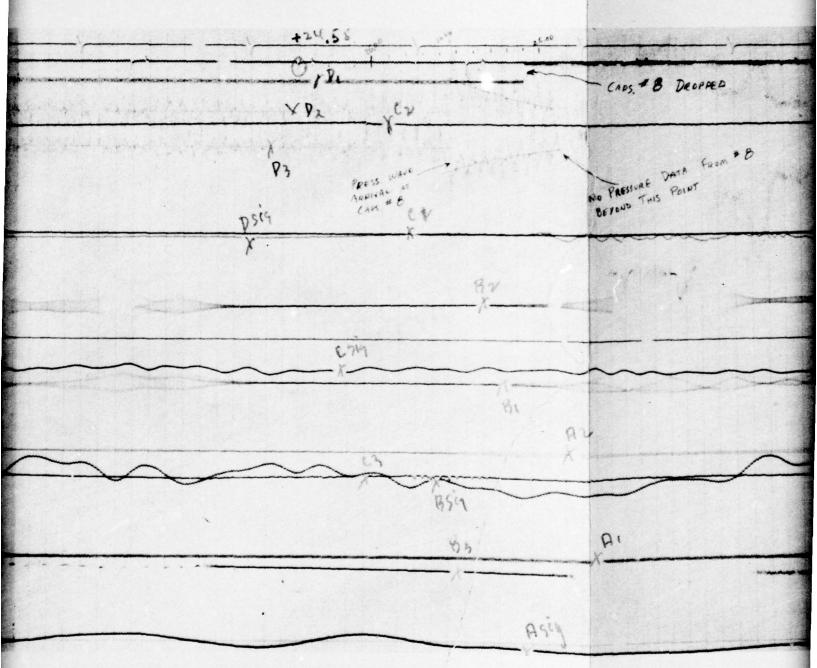
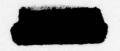


Figure 3.3 Peak Pressure Ossilloscope Trace

CADS # 8 DEOPPED X 73 NO PRESSURE DATA FROM & B BEYOUD THIS POINT x psiq Res 81 AU BSA AI Asia

Trace

3 UNCLASSIFIED



PROJECT 1.30

TABLE 3.2

Radiosonde Pressure-Temperature-Altitude Data for 0700 PST 19 November 1951

Pressure (millibars)	Temp. (°C)	Dew Point	Altitude (ft. MSL)
875	- 2.2	-15.6	4127
863	- 5.5	- 7.8	4467
850	- 4.5	- 8.5	4837
797	- 3.2	- 4.6	6587
708	- 3.2	- 5.2	9557
700	- 3.0	- 6.0	9847
687	- 2.2	- 8.6	10322
Ø53	- 4.8	-22.6	11632
585	- 4.5		14452
522	- 6.8		17372
500	-13.2		18454
700	-27.0	-39.2	23874
345	-34.0	740.2	27319
305	→10.0	-50.0	30089
300	-1 1.5		30449
257	-50.0		33849
200	-63.8		39049
150	-66.0		44789
142	-69.0		45865
100	-67.9		52765
70	-61.0		



PROJECT 1.30

TABLE 3.3

Wind Data for 0700 PST 19 November 1951

Altitude (ft. MSL)	Wind Velocity (knots)	Azimath
4127	calm	
5000	calm	
6000	13	160
7000	18	170
8000	22	190
9000	29	200
10000	33	200
12000	33	21.0
14000	46	200
15000	59	200
16000	37	200
18000	33	200
20000	75	200
21000	83	200

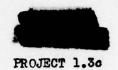


TABLE 3.4

Radiosonde Pressure-Temperature-Altitude Data for 1000 PST 19 November 1951

Pressure (millibars)	Temp. (°C)	Dew Point	Altitude (ft. MSL)
875	+10.5	- 9-5	4127
850	+ 6.5	- 8.5	4907
830	+ 6.2	- 4.2	55 ¹ +7
732	- 1.0	- 5.0	8887
700	- 2.0	- 8.1	10037
665	- 1.2	-20.1	11357
572	- 9.0		15237
561	- 8.2		15717
500	-15.0		18597
7000	-22.0		24047
370	-31.3	-43.2	25887
320	→40.2		29187
300	43.0		30627

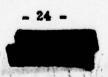


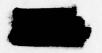
PROJECT 1.3e

TABLE 3.5

Wind Data for 1000 PST 19 November 1951

Altitude (ft. MSL)	Wind Velocity (knots)	Azimth
4127	calm	
5000	calm	
6000	13	170
7000	20	180
8000	26	180
9000	28	200
10000	32	200
12000	37	200
14000	140	21.0
15000	41	210
16000	7471	210
18000	63	200
20000	54	200
25000	57	200
30000	56	210
35000	60	210





PROJECT 1.3c

TABLE 3.6

Computed Slant Ranges and Altitudes of Canisters

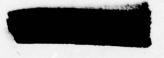
Canister No.	Computed Average Velocity to Canister (ft/sec.)	Slant Range, R (ft)	Altitude (ft above sea level)	Altitude (ft above ground zero)
1	1277	6530	5980	1780
2	1263	6580	7640	3440
3	1216	8310	9070	4870
4	1191	9670	11890	7690
5	1153	54010	14060	9860
6	1158	55630	18920	14720
8	1100	28000	33280	29080

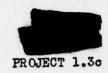
not particularly sensitive to the assumed variation of overpressure with distance since over most of the distance $\Delta P/P_0$ is a small quantity. An indication of the probable accuracy of the computed ranges may be obtained from canister No. 8. Since the calculated slant range comes out to be less than the altitude above ground as determined from the ambient pressure data, this canister must have been nearly directly above ground zero. The discrepancy of 1080 feet is 3.8% of the mean and this is at least as likely to be due to an error in the altimeter altitude as to an error in the range computed from the travel time. It is therefore considered that the computed ranges are accurate to at least 2%.

3.3 INTERPRETATION OF RESULTS

The atmospheric pressure at the altitude of the shot was 12.60 psi so that k3 = 12.60/14.70 = .857 and k = .950. The scale factors A and a have been computed as functions of altitude by numerical evaluation of the integrals appearing in eqs. (1.6) and (1.7), using the radiosonde meteorological data. The values for the altitudes of the various canisters are given in Table 3.7 together with the values of f(r) = AP/kA and r = kAR/S. For canister No. 8 the slant range used is the mean of those determined from the altimeter and from the shock wave







travel time. The values used for the peak overpressures are the means of the readings of the high and low range gauges when both were obtained, except in the case of canister No. 3, for which, as previously noted, the reading of the low range gauge is grossly inconsistent with the other data. The tabulated values of f(r) are plotted against r in Figure 3.4 (circled points). Similarly reduced values obtained from surface measurements are also plotted in the Figure (triangle points). The latter points have been computed from a tabulation of distances to given peak overpressures supplied by the Armed Forces Special Weapons Project and do not represent the original data. They are shown here for comparison purposes only.

To compare the present results with small charge measurements we use the data for pentolite spheres obtained by Stoner and Bleakney5. The analytic expression which the authors give to fit their data becomes for 1 lb. of pentolite

$$\Delta P = 1842/r^3 + 275.7/r^2 + 31.97/r \tag{3.2}$$

where ΔP is in psi and r is in feet. If we take 1 lb. of pentolite to be equivalent to 1.18 lb. of TNT this becomes

$$\Delta P = 1561/r^3 + 246.9/r^2 + 30.26/r \tag{3.3}$$

for 1 lb. of TNT. This expression is derived from experimental data covering the range of overpressures between 35 and 1.5 psi. According to an approximate theory for small blast pressures developed by Bethe and Fuchs, the peak pressure should diminish at long ranges like

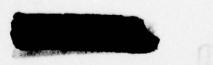
$$\Delta P = A/r\sqrt{\ln(r/B)}$$
 (3.4)

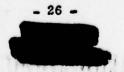
where A and B are constants. A numerical expression of this form which joins eq. 3.3 smoothly at about 1 psi is

$$\Delta P = 36.50/r \sqrt{\log_{10}(r/4.467)}$$
 (3.5)

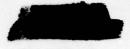
(The values of AP given by equations 3.3 and 3.5 agree to within 0.1% in the range between 0.86 and 1.29 psi, within 1% between 0.64 and 1.7 psi, and within 5% between 0.28 and 2.95 psi). From overpressure measure

⁶ H. A. Bethe and K. Fuchs, Asymptotic Theory for Small Blast Pressures, Los Alamos Technical Series LA 1021, Vol VII, Part II, Chapter 5.





R. C. Stoner and W. Bleakney, The Attenuation of Spherical Shock Waves in Air, Jour. App. Phys. 19, 670 (1948).



PROJECT 1.3c

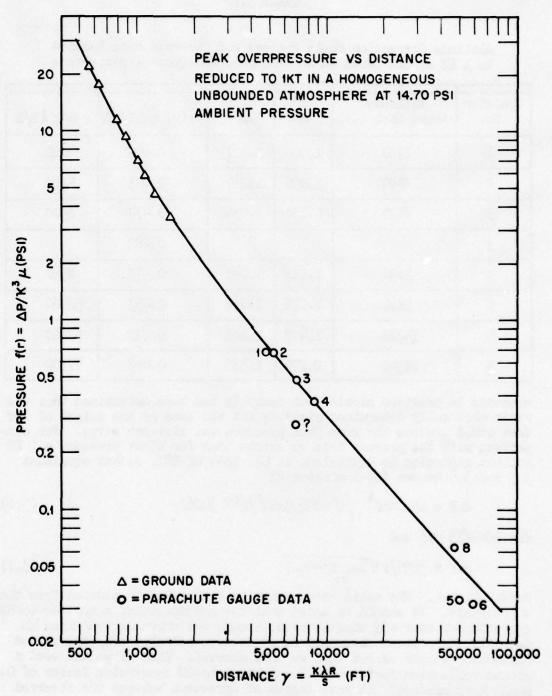
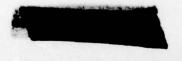
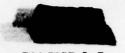


Fig. 3.4 Overpressure Function-Distance Curve







PROJECT 1.30 TABLE 3.7

Altitude Correction Scale Factors and Observed Data Reduced to 1 KT at Sea Level in an Unbounded Homogeneous Atmosphere

Canister No.	Altitude Above Shot (ft)	λ	м	f(r) = AP/k	r = k AR/S
1	1780	1.020	1.007	0.695	4860
2	3)1110	1.090	1.017	0.683	5240
3	4870	1.136	1.034	0.474	6900
3				0.282	
4	7690	1.212	1.047	0.373	8550
5	9860	1.278	1.068	0.033	50400
6	14720	1.447	1.101	0.032	58800
8	28540	2.270	1.335	0.062	47300

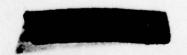
urements in previous atomic bomb tests it has been determined that the radio-chemically determined yield is not the same as the weight of TMT that would produce the same peak pressure vs. distance curve. For comparison with the present data we assume that for blast pressure a 1 KT nuclear explosion is equivalent to 500 tons of TMT, so that equations 3.3 and 3.5 become for 1 nuclear KT

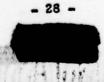
$$\Delta P = 1561 \times 10^6 / r^3 + 246.9 \times 10^7 / r^7 + 3026 / r$$
 (3.6)

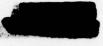
for 1(AP(35 psi and

$$\Delta P = 3650/r \sqrt{\log r} + 46.7$$
 (3.7)

for AP < 1 psi. The solid curve shown in Figure 3.5 is plotted from these expressions. It should be noted that the assumption of a nuclear-to-HE conversion factor of that we used to make the curve derived from HE data fit the present observations is no more reliable than the ground reflection factor of 1.8 that we have assumed. Thus if we had used a ground reflection factor of 1.5, a nuclear-to-HE conversion factor of 0.6 would have produced the same degree of agreement between the observed and computed pressures.







PROJECT 1.3e

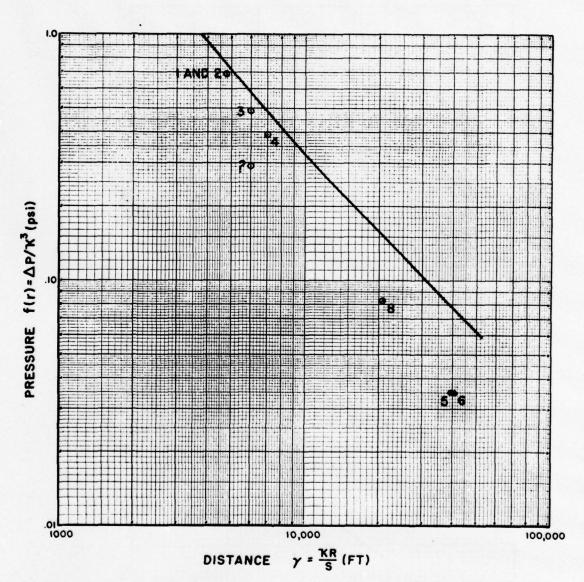
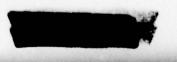


Fig. 3.5 Overpressure Function-Distance Curve Without Canister Altitude Correction





PROJECT 1.3e

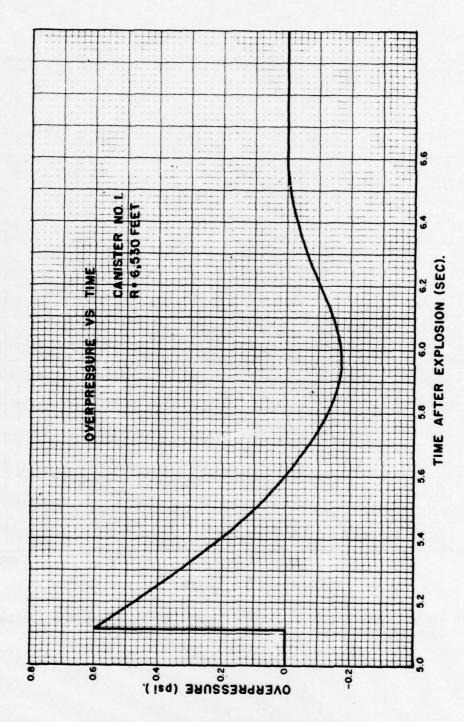
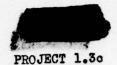


Fig. 3.6 Overpressure vs. Time, Canister No. 1

HURALINI



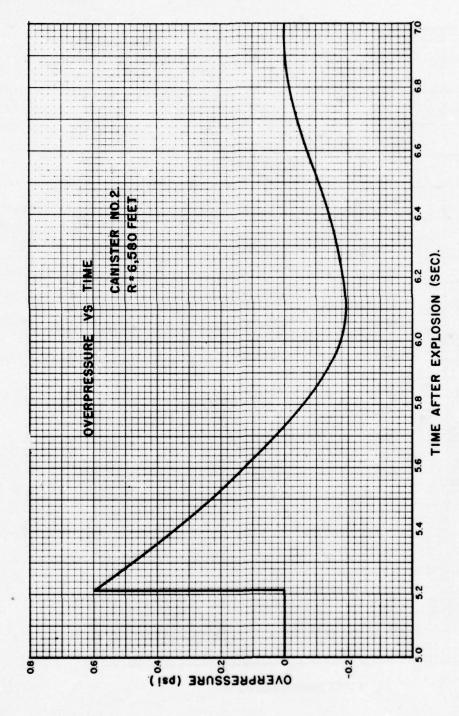


Fig. 3.7 Overpressure vs Time, Canister No.



PROJECT 1.30

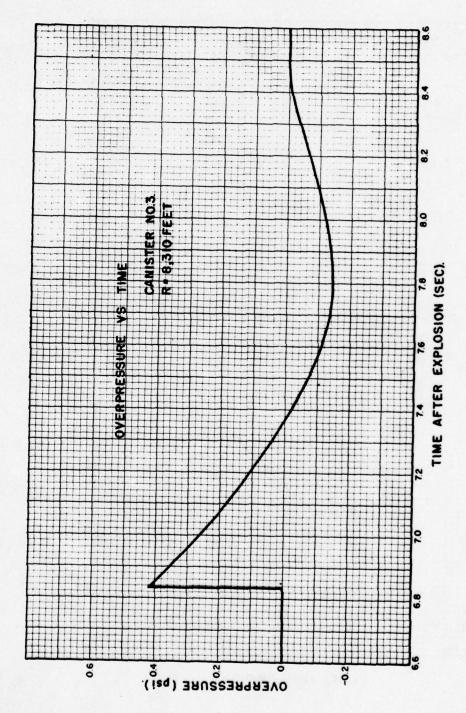
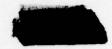


Fig. 3.8 Overpressure vs Time, Canister No. 3



PROJECT 1.3c

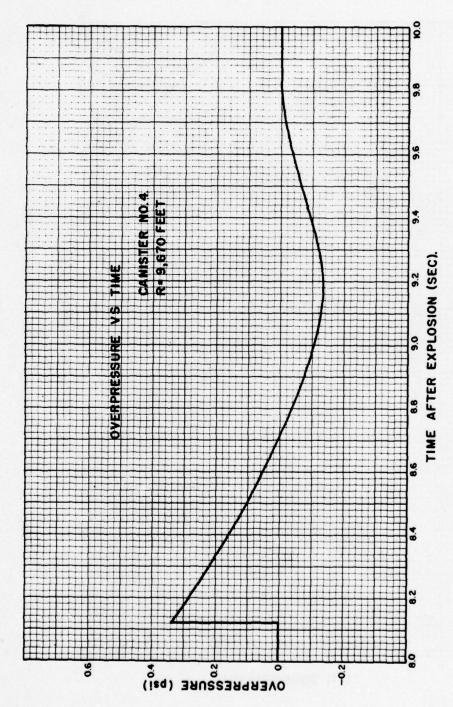


Fig. 3.9 Overpressure vs Time, Canister No. 4

UNULKOOFED



PROJECT 1.3c

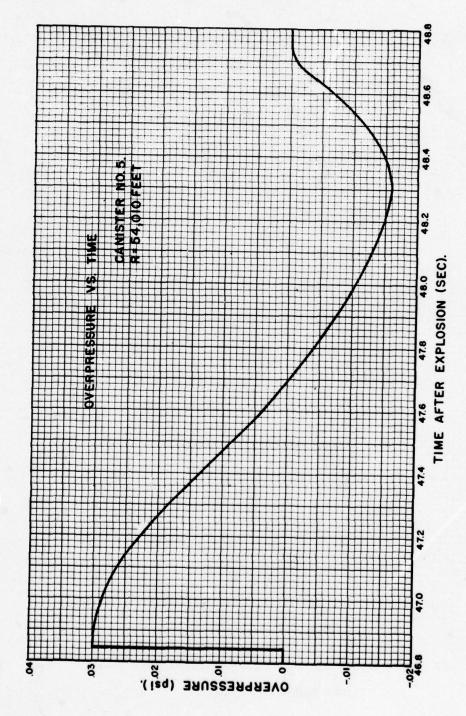
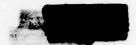


Fig. 3.10 Overpressure vs Time, Canister No. 5



PROJECT 1.3c

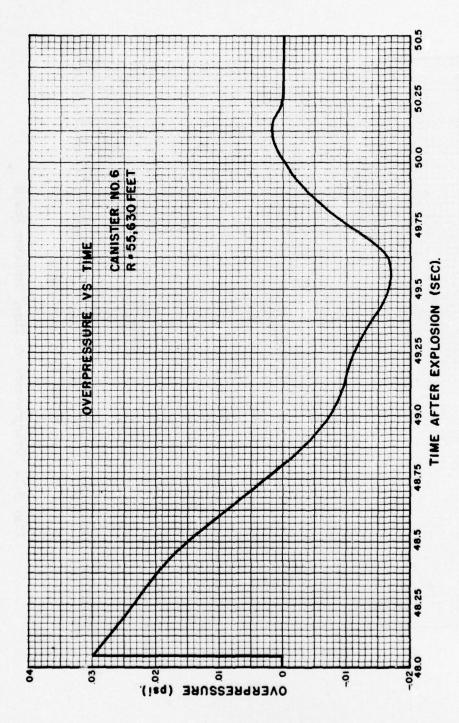
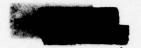


Fig. 3.11 Overpressure vs Time, Canister No.



PROJECT 1.3e

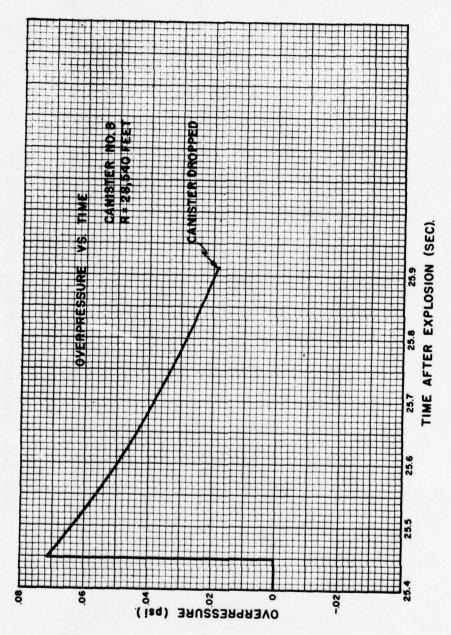


Fig. 3.12 Overpressure vs Time, Canister No. 8



CHAPTER 4

CONCLUSIONS AND RECOMMENDATIONS

4.1 CONCLUSIONS

The operation was intended primarily as a preliminary test of equipment and techniques in anticipation of future tests with a more extensive array of parachute-borne pressure gauges. Any conclusions that may be drawn from the present data must therefore be considered as tentative. In particular, the positions actually attained by the canisters were very far from the intended vertical array above ground zero and were not such as to provide a clear cut test of the Fuchs altitude correction. For canisters No. 1, No. 2, No. 3 and No. 4 this correction is of the same order as the estimated error of the peak pressure measurements, while canisters No. 5 and No. 6 were at such great distances and low shock pressure levels that erratic results are to be expected due both to errors of measurement and the effects of shock wave refraction. The data from canister No. 8 is questionable because of the relatively high noise level and the possibility of systematic error due to shock reflections within the bomb bay of the aircraft. With these cautions in mind it is, nevertheless, interesting to note the excellent agreement exhibited in Figure 3.4 between the reduced data from canisters No. 1, No. 2, No. 3 and No. 4 and the computed curve, which was derived from HE data as described above, and which forms a reasonable extrapolation of the ground pressure measurements. If the parachute gauge data is reduced without applying the Fuchs correction (i.e., if AP/k is plotted against kR/S) we obtain the points plotted in Figure 3.5, which fall systematically below the computed curve. It would, of course, be possible to draw a reasonably smooth curve through these points and the ground pressure points, but this would produce an f(r) curve that falls off at large distances at a rate considerably greater than 1/r, which cannot be reconciled with either experimental HE data or theory. There is therefore justification for concluding that the present data support the Fuchs Theory within the probable accuracy of the observations out to overpressures of about 0.1 psi.

4.2 RECOMMENDATIONS

Since the data obtained in the present test are insufficient for a definitive test of the altitude correction theory, it is recommended that further tests be carried out using up to 20 parachute-borne canisters in an array distributed symmetrically in the up and down wind directions from ground zero and positioned to cover the range of peak overpressures from about 0.15 to 4.0 psi. All possible effort should







PROJECT 1.3e

be made to perfect the MOTS system for position determination so that it will not be necessary to rely upon altimeter and travel time data for range determination in future tests.

After satisfactory data has been obtained from tower or surface bursts and canister positioning techniques have been perfected it would be very desirable to make air-borne blast pressure measurements with an air burst atomic bomb in order to separate the factors of equivalent HE blast yield and ground reflection.



APPENDIX A

RADIO TELEMETRY INSTRUMENTATION AND CALIBRATION

A.1 INSTRUMENTATION

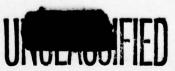
Pressure measuring instrumentation was accomplished by the Pacific Division Development Laboratories, Bendix Aviation Corporation, Burbank, California, under Contract AF 19(122)—159. Radio telemetry instrumentation included the design and fabrication of parachuteborne canisters and receiving-recording ground stations. Instrumentation required the simultaneous measurement of ambient pressure and differential pressure at eight locations vertically above an atomic detonation.

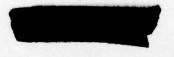
A.1.1 Canister Physical Data

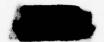
The parachute-borne canister in Figure A.1 has the following weight, and form factors:

Weight	275 pounds
Over-all length	86.25 inches
Air-frame length	50.75 inches
Antenna probe	25.50 inches
Air-frame diameter	14 inches
Nose section	450 cubic inches
Battery and power supply	680 cubic inches
Radio Telemetry equipment	570 cubic inches
MOTS equipment	1470 cubic inches
Parachute section	12,040 cubic inches

In addition, space was provided for antenna tuning and filter units, insulation, cable lines, circulation space around the equipment and mounting frames. The canisters were weighted with lead plates so that the CG fell approximately midway between the two bomb shackle lugs.







PROJECT 1.3c

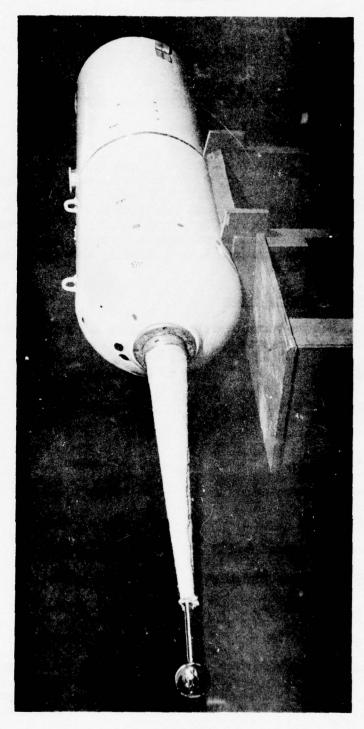


Fig. A.1 Parachute-Borne Canister



PROJECT 1.30

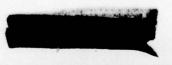
A.1.2 Canister Radio Telemetry Instrumentation

A block diagram of the radio telemetry instrumentation contained in the parachute-borne canister is shown in Figure A.2. The system operated on the principle of FM/FM and consisted of a pressure pick-up probe, two differential pressure transducers of different range, a pressure altimeter transducer, three sub-carrier oscillators of different frequency, a crystal controlled FM oscillator, a differential pressure reference chamber and associated parts.

Prior to deployment of the canister from the aircraft, the equipment was internally preheated by thermostatically controlled strip heaters strategically located in the air frame to maintain operating temperature of vital components during high altitude flight. The electronic equipment was powered by the aircraft's power system and controlled at a switch panel in the aircraft. During check-out procedure voltages and currents were monitored. At the instant of deployment the canister electronic equipment was automatically switched to the internal canister battery and the sequence timing motor was started. The canister was deployed on a six (6) foot fist ribbon parachute using the standard static line. The terminal rate of descent was equivalent to 135 feet per second at sea level. At a predetermined time after deployment a relay was actuated by the sequence timing motor which applied power to fire a squib cutter. The cutter released the 28-foot parachute which reduced the rate of descent to an equivalent 22 feet per second at sea level. During this time the pressure in the reference chamber increased and the altimeter data was telemetered to the ground receiving-recording station. The acoustic impedance No. 1 produced no appreciable lag in the pressure time characteristics of the system since the rate of change of pressure during the descent on the 28-foot parachute was extremely slow compared to the time constant of the impedance. Within ten seconds of the arrival time of the blast wave a second relay was actuated by the sequence timing motor. This relay circuit, in series with the power source, blast switch and solenoid valve, armed the blast switch.

On arrival of the blast wave, the blast switch was actuated and closed, completing the circuit to the solenoid valve thus sealing the pressure in the reference chamber. This pressure, as recorded by the altimeter, was the reference pressure value for the differential pressure gauges. The blast pressure was transmitted through the omnidirectional spherical pickup probe to the transducers. The differential pressure transducers were activated by the blast wave and produced the corresponding frequency shift in the sub-carrier oscillators. The output of the three sub-carrier oscillators were mixed and the composite wave then frequency modulated the high frequency carrier oscillator. The resultant FM/FM carrier was transmitted via radio link to the receiving-recording ground station.





PROJECT 1.36 .



RADIO TELEMETRY INSTRUMENTATION

PARACHUTE-BORNE CANISTER INSTRUMENTATION
DIFFERENTIAL

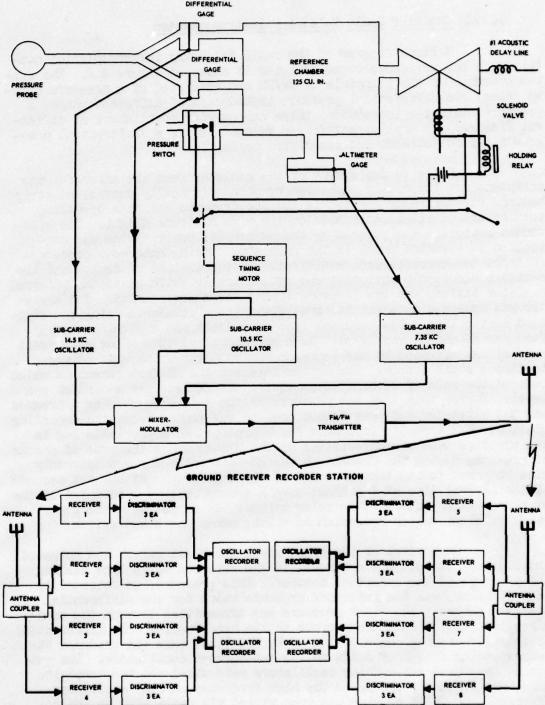


Fig. A.2 Radio Telemetry Instrumentation Block Diagram



Nominal frequency response capabilities of the three subcarrier channels used in each canister radio telemetry system were as follows:

Channel	Function	Freq. Response
7.35 KC	Altitude	110 cps
10.5 KC	Differential pressure, high range	160 cps
14.5 KC	Differential pressure, low range	220 cps

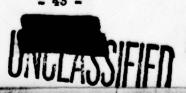
Table A.1 shows the specific types of equipment instrumented in the canister.

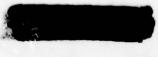
A.1.3 Ground Radio Telemetry Instrumentation

The ground receiving-recording radio telemetry station consisted of eight receiver-recorder sections, one section for each parachute-borne canister as shown in Figure A.3. Each section contained a IM receiver tuned to the carrier frequency of the particular canister. The output of the FM receiver, a mixture of the original three EM subcarrier frequencies, was channeled to filters adjusted to pass a frequency bend commensurate with and centered on the quiescent frequency of the particular sub-carrier. The output signals were separately connected to sub-carrier discriminators which produced a varying current proportioned to the original pressure stimulus. The output signals were then applied to appropriate deflecting galvanometers of the recording oscillograph. Two Consolidated Model 5-114-P4 recording oscillographs were connected in parallel to obtain a recording on Eastman Linograph type 809 paper at a recording speed of 1.8 inches per second and a recording speed of 21.6 inches per second. The galvanometers used in all oscillographs were Midwestern Geophysical Laboratory Model 107-400. These galvanometers had an undamped natural frequency of 400 cps but were magnetically damped to 60 per cent of critical damping.

Two antennas were mounted on 20-foot masts at opposite corners of the trailer. Each antenna consisted of two folded dipoles each with a reflector and director, spaced approximately one-half wave length apart. The antennas were mounted in a vertically polarized direction and were capable of being electrically trained through 180 degrees of azimuth and approximately 100 degrees of elevation, controlled from inside the trailer. A special coupler was employed which allowed each antenna to be connected to four receivers. The gain of the antenna and the loss of the coupler were such that an over-all gain was realized for each receiver over that which might be obtained with each receiver operated from a separate dipole antenna.

The operational trailer contained two sets of identical equipment located on opposite sides of the trailer interior. Each set







PROJECT 1.3e

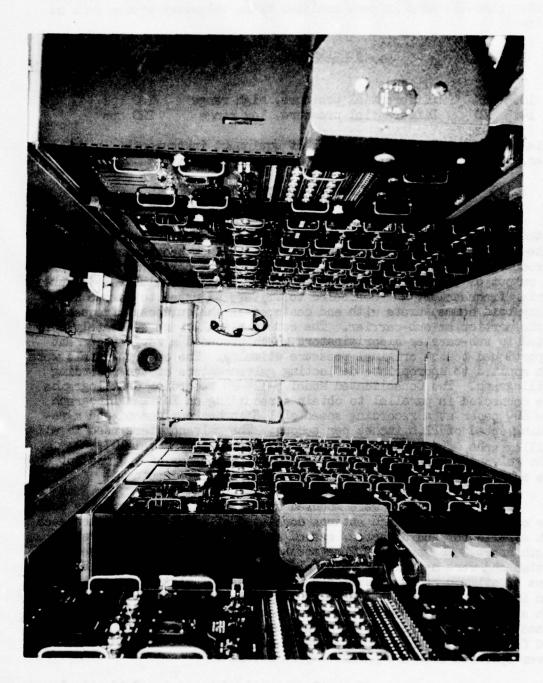


Fig. A.3 Radio Telemetry Station



PROJECT 1.30

of equipment consisted of four receivers, four filter-amplifier chassis, twelve discriminators, four low-pass filter chassis, one monitor panel, one oscillograph control panel and two consolidated recording oscillographs. The combined equipment of both sides of the trailer, the antennas and a common voltage regulator unit were sufficient to receive and record the radio telemetry data from the eight parachute-borne canisters.

A.2 CALIBRATION

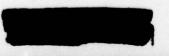
The receiving station instrumentation was calibrated by feeding a series of standard audio frequency signals to appropriate sectional discriminators. Nine standard frequencies were fed into a group of four discriminators having center frequencies of 7.350 KC. Another series of nine frequencies were fed into a group of 10.5 KC discriminators and likewise with the 14.5 KC discriminators. The frequency values were such that they covered the range of the discriminators, i.e. +750 of center frequency. The values of the calibrating frequencies used for each group were:

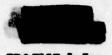
7.35 KC group	10.5 KC group	14.5 KC group
6800 cps 6900 7000 7150 7350 7550 7760 7800	9700 cps 9800 10000 10200 10500 10800 11000 11200	13400 cps 13600 13900 14200 14500 14800 15100
7900	11,500	1900

A short recording was made on the oscillograph for each calibrating frequency fed to the discriminators. Since the output of each discriminator was connected to a galvanometer of the oscillograph, every change in the frequency of the signal introduced to the discriminator, resulted in a corresponding change in the deflection of that particular galvanometer. The galvanometer deflection in each channel was measured and recorded for each input frequency to the discriminator. The values were used to plot curves of galvanometer deflection versus frequency.

The pressure transducers consisted of a small piece of mu-metal and an I-coil enclosed in a metal case. By varying the distances between the mu-metal and the I-coil the inductance of the I-coil is changed. The I-coil was the inductive section of an oscillator circuit, and by attaching the piece of mu-metal to a movable part of the diaphragm of the transducer the movement of the mu-metal caused a change in the frequency of the oscillator. Accurately standard pressure values were applied to







PROJECT 1.30

each transducer, covering the entire range of each pickup. The frequency of the sub-carrier oscillator connected to the transducer was recorded and a calibration curve of frequency versus transducer function was plotted.

A.3 DATA REDUCTION PROCEDURE

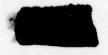
By use of the aforementioned discriminator and transducer calibration curves, a correlation between transducer function values and galvanometer deflection values was obtained. These data were tabulated for each common value of frequency. Curves were then plotted for transducer function versus galvanometer deflection for each telemetered channel of each canister. The curves were used to obtain scales which were calibrated in terms of the function to be measured.

PROJECT 1.30

TABLE A.1 Cenister Equipment

No. 1 2 3 4 5 6			Model	Cam.	Cen.	Equipme Can.	Equipment Serial Numbers Can. Can. Can.	Numbers	Can.	160
same rme-9A B-549 - <		Item	No.	1	2	3	†	5	9	1 80
sure rre-9A B-632 B-749 - - - - - sure rre-9A - B-548 B-547 - - - - sure r-11121-3 - - BX-27 BX-23 - - sure r-11121-3 - - BX-27 BX-23 - - sure r-11121-3 - - BX-27 BX-23 - - sure r-11121-3 - - - BX-24 - - sure r-11121-3 - - - BX-21 BX-3 sure r-11121-1 - - - BX-21 BX-3 so.* Bg r-11497 Bx-5 Bx-6 Bx-10 - - BX-10 so.* Bg r-11499 Bx-1 Bx-3 Bx-1 Bx-5 Bx-18 r-11439 Bx-1 Bx-3 Bx-1 Bx-5 Bx-6 Bx-	•	Differential Pressure Transducer, +10 psi	TTP-9A	B-549	1	ı	1	1	1	1
sure rm-9A - B-546 B-547 -		Differential Pressure Transducer, 15 psi	1712-9A	B-63 2	B-349	ı	1	1	1	1
sure r-11121-3 - - BK-27 BK-23 - - sure r-11121-3 - BK-25 BK-24 - - sure r-11121-3 - - BK-25 BK-21 BK-21 - sure r-11121-1 - - - BK-21 BK-3 soure r-11121-1 - - - BK-21 BK-3 sour r-111497 BK-5 BK-6 BK-9 BK-10 - - BK-18 sol* Bg r-11439 BK-1 - - BK-3 BK-18 BK-18 r-11439 BK-1 BK-2 BK-3 BK-1 BK-5 BK-6		Differential Pressure Transducer, +2 psi	м6-шп		B-548	140年	1	1		1
sure Y-11121-3 - BK-25 BK-24 -	47 -	Differential Pressure Transducer, 40.7 psi	¥-11121-3		1	1	BX-27	BX-23	,	
sure r-11121-2 - - - EX-21 EX-5 EX-5 EX-10 sure r-11121-1 - - - - EX-10 EX-10 5.0" Hg r-11497 EX-5 EX-6 EX-9 EX-10 - <		Differential Pressure Transducer, + psi	£-12111-1		1	H-25	BX-24	1	1	•
soure Y-11121-1 - - - - BX-10 5.0" Hg Y-11497 BX-5 BX-6 BX-9 BX-10 - - - .0" Hg Y-11497 - - - BX-26 BX-18 Y-11439 BX-1 BX-3 BX-3 BX-4 BX-5 BX-6		Differential Pressure Transducer, +0.4 psi	T- 11121-2		•		1	BX-21	BX-3	
5.0" Hg Y-11497 HX-5 HX-6 HX-9 HX-10 HX-26 HX-18 -0" Hg Y-11497 HX-26 HX-18 Y-11439 HX-1 HX-2 HX-3 HX-3 HX-5 HX-5 HX-6		Differential Pressure Transducer, 40.2 psi	r-11121-1				•	1	BX-10	BX-2 BX-17
.0" Hg T-11497 BX-26 BX-18 T-11479 BX-1 BX-2 BX-3 BX-4 BX-5 BX-6	—	Altimeter, 29.9/15.0" Eg	79/LL-Y	BK-5	BX-6	EX9	BX-10			
1-11376 A EX-1 EX-2 EX-3 EX-4 EX-5 EX-6		16.0ª	T-11497		•			BX-26	BX-18	BK-20
		Telemeter Package	r-11376 &		BK-2	E-3	†XX	展示	BX-6	H 25

University of FED



APPENDIX B

MILTIPLE OBJECT TRACKING INSTRUMENTATION AND CALIBRATION

B.1 INSTRUMENTATION

The instrumentation used to track the eight parachute-borne canisters was developed by the Glenn L. Martin Company, Baltimore, Maryland, under Contract AF 19(122)-460. The system is based on the triangulation of range measurements determined from each of three or more ground based interrogating stations to the airborne beacon responder unit. The system is capable of tracking thrity-two canisters, however, only eight parachute-borne canisters were deployed. A picture of the airborne beacon is shown in Figure B.1 and the ground station is shown in Figure B.2.

A block diagram of the airborne and ground station system is shown in Figure B.3. A one second timing signal initiated the operation of the synchronizer-coder through a station delay which proportioned the operating cycle of each ground station over a portion of the one second interval. The synchronizer-coder generated a code train consisting of a start pulse, a five digit binary code and a range pulse. This code train modulated the transmitter and also opened a range gate circuit in the range oscillator. When the range gate was opened the output of the range oscillator, 9.836 MC, was fed into a twelve digit binary counter.

The transmitted code train was received by all airborne beacon receivers and was passed to the decoder. Each decoder was designed for a selected binary number so that it differentiated between the selected number and all others so as to excite the modulator only when the selected number occurred. When the selected number was received the decoder excited the modulator which pulse modulated the beacon transmitter. beacon transmitter response pulse was then transmitted to the ground station receiver and then to the range timer which turned off the range gate. During the interval between the ground station transmission of the range pulse of the code train and the reception of the beacon pulse, the binary counter had counted the number of cycles of the 9.836 MC range oscillator. The number of counts being a function of the range from the airborne responder beacon to the ground interrogating station was recorded with the selected binary code number. A reset pulse resets the counters to zeros for the next code train.

When one ground interrogating station completed the cycle of thirty-two code trains and ranged on the airborne responder beacons, another ground station, delayed an appropriate time, initiated its cycle. Each ground station interrogated all beacons during the allocated time of



PROJECT 1.30

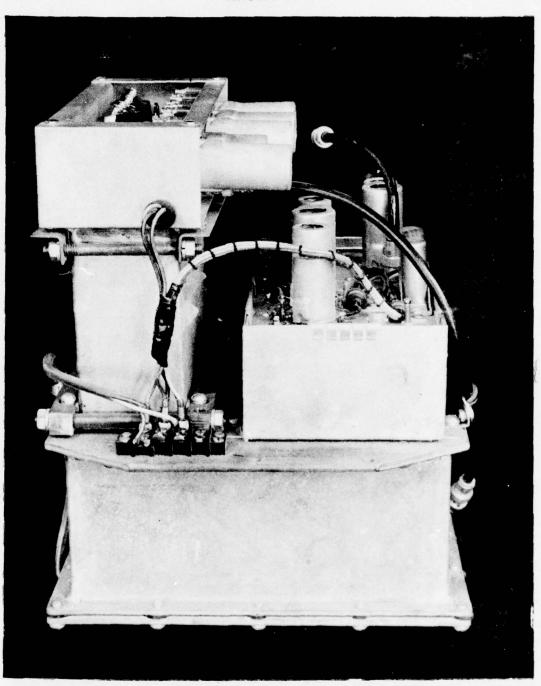


Fig. B.l Airborne Beacon





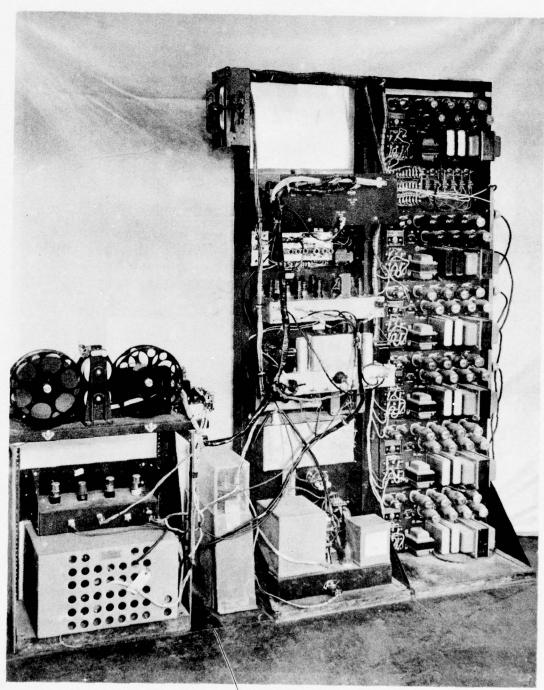


Fig. B.2 MOTS Station



MULTIPLE OBJECT TRACKING SYSTEM INSTRUMENTATION

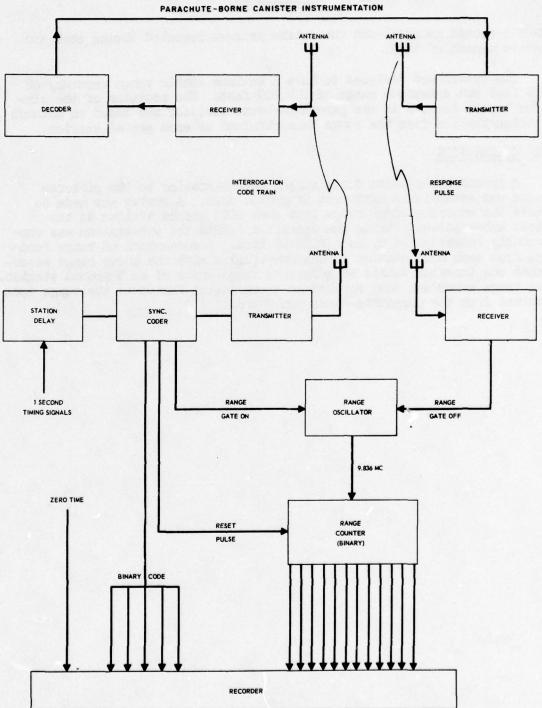
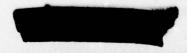


Fig. B.3 MOTS Block Diagram

- 51 -





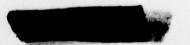


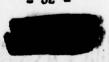
the one second interval and the entire process repeated during each successive second of time.

The system was designed to have a maximum static range accuracy of + 50 feet and a maximum range of 204,800 feet. The position of the air-borne beacon located in the parachute-borne canister was based on methods of triangulation from the range data obtained at each ground station.

B.2 CALIBRATION

A ground sub-station containing a beacon similar to the airborne beacon was established northwest of ground zero. A survey was made to obtain the accurate slope range from each MOTS ground station to the ground sub-station. During the Operation JANGLE the sub-station was continuously interrogated by each MOTS station. A comparison of range readings from each MOTS station to the sub-station with the known range established the inherent delays or effective range error of each ground station. This range error was then applied as a correction factor to the range data obtained from the parachute-borne canisters.



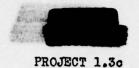




APPENDIX C

MATHEMATICAL SYMBOLS

f(r)	peak overpressure vs. distance function for 1 KT yield
R	slant range
z	altitude
V	yield of bomb
h	altitude of bomb detonation
AP	free air peak overpressures
S	scaling factor = W3
k	Sach's scale factor
P ₀ (z)	atmospheric pressure at altitude z
P(z)	atmospheric density at altitude z
c(z)	sound velocity at altitude z
Po(h)	atmospheric pressure at altitude h
(h)	atmospheric density at altitude h
c(h)	sound velocity at altitude h
T(z)	absolute temperature at altitude z
T(h)	absolute temperature at altitude h
1,1	Fuchs scale factors
U	shock front velocity
	⊾ ÅR/S



BIBLIOGRAPHY

- H. A. Bethe and K. Fuchs, Asymptotic Theory for Small Blast Pressures, Los Alamos Technical Series, LA-1021, Vol VII, Part II, Chapter 8
- K. Fuchs, The Effect of Altitude, Los Alamos Technical Series, LA-1021, Vol VII, Fart II, Chapter 9
- N. A. Haskell and J. A. Peoples, Jr., Final Report on Free Air Blast Pressure Pattern Studies, T. I. 2187-5 (W.D. CFS 119), October 1950 (Secret)
- N. A. Haskell, The Effect of Altitude of Blast Wave Peak Pressures, Air Force Cambridge Research Center, September 1950 (Secret)
- N. A. Haskell, Application of Velocity Measurements to the Free Air Blast Pressure Project, Air Force Cambridge Research Center, 7 March 1951 (Secret)
- NDRC, Effects of Impact and Explosion, Summary Technical Report of Division 2, pp 106 and 107
- R. G. Sachs, The Dependence of Blast on Ambient Temperature and Pressure, Ballistics Research Lab., Aberdeen, Report No. 466, May 1944.
- R. C. Stoner and W. Bleakney, The Attenuation of Spherical Shock Waves in Air, Journal of Applied Physics 19,670 (1948)
- Bendix Aviation Corporation, Burbank, California, Telemetering of Project 1.3C Operation Nevada Test Site, 19 November 1951, dated 21 January 1952 (Secret)

OPERATION JANGLE

PROJECT 1.4

FREE AIR PRESSURE MEASUREMENTS

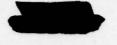
By

W. J. HOWARD R. D. JOHAS

19 February 1952

SANDIA CORPORATION





CONTENTS

ABSTRACT .	••••••••	1
SECTION 1	INTRODUCTION	1
		1
	1.2 Method of Obtaining Data	1
SECTION 2	DISCUSSION OF INSTRUMENTATION	4
	2.1 Wieneko Gauges	4
	2.2 Pipe Probe	8
	2.3 Interferemeter Ganges	9
		10
	2.5 Transmission and Recording System	0
	2.5.1 Wire Transmission System	12
	2.5.2 Radio Telemeter System	2
		13
		Ĭ,
SECTION 3	RESULTS AND CONCLUSIONS	5
	3.1 Data Obtained	15
	3.2 Conclusions	:5
APPENDIX A	PERSONNEL	27



ILLUSTRATIONS

SECTION 1	INT	RODUCTION	1
	1.1	Surface Shot Plan	2
	1.2	Underground Shot Plan	3
SECTION 2	DISC	CUSSION OF INSTRUMENTATION	4
	2.1	Damping Jig with Shock Tube (Upper Photos are Damp-	
		ing Jigs Alone)	5
	2.2	Surface Shot680-ft Station	6
	2.3	Pipe Probe	7
	2.4	Interferemeter Coffin	ġ
	2.5	Compling Unit	i
SECTION 3	RESU	TIAS AND CONCLUSIONS	5
	3.1	Zere-Time Hoise Burst	F
	3.2	Peak Overpressure vs Distance	7
	3.3	Time of Arrival vs Distance	÷
	3.4	Positive Phase Dureties we Distance	
	3.5	Surface Shot Pressure-Time Curve.	-
	3.6	Underground Shot Pressure-Time Curve	1
		TABLES	
SECTION 3	RESU	LTS AND CONCLUSIONS	5
	2.0	Pressure-Time-Distance Data, Surface Shet 1	0
	0.2	Pressure-Time-Distance Data, Underground Shot 1	0
	3.3	Indenter Gauge Data, Surface Shet	3
	3.4	Indenter Gauge Data, Underground Shot	4





ABSTRACT

Records of air overpressure versus time were made at essentially ground-level stations for both surface and underground atomic explosions of approximately one kiloton yield as part of Operation JAEGLE in Hovember 1951. For the surface shot several instruments were placed on a line extending from an overpressure region of 13 psi to a region of less than one psi; the air measurements for the underground shot ranged from 32 to 3 psi.





SECTION 1

INTRODUCTION

1.1 OBJECTIVE

The responsibility of Project 1.4 was to record the pressure-time wave form of the air blast at stations throughout the areas where structural damage was to be investigated; measuring stations were to be set up along a radius (the major blast line) from the predicted edge of the crater-throwout to a pressure region of approximately 2 psi. The measuring system was to have an over-all response of 500 cps or better and an accuracy of 5 per cent.

Although not a part of the mission assigned to Project 1.4, a rough examination of the symmetry of the divergent air shock wave was made by means of Naval Ordnance Laboratory indenter gauges.*

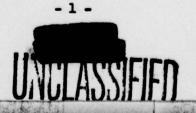
1.2 METHOD OF OBTAINING DATA

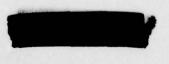
Free air pressure was measured along the ground from an over pressure region of 13 psi to a region of less than one psi on the surface shot and from 32 to 2 psi on the underground shot. All pressure measurements were made by means of Wiancko pressure gauges except that for the 4,200 foot station which was made by means of a self recording interferometer gauge.

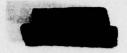
In general two Wiancko gauges were used at each instrument station to obtain duplicate pressure measurements. Data transmission from each gauge was effected either by a wire link or by a radio telemeter link. Unless otherwise noted, the data presented in Tables 3.1 and 3.2 were transmitted over a wire link.

All wire-link channels have an over-all system frequency response which is flat from 0-500 cps while the radio telemeter channels have an over-all system frequency response which is flat from 0 - 1,500 cps. The linearity of both systems was within 1 per cent. Signal amplitudes for the wire-link channels were approximately twice those of the radio telemeter channels.

Shafer, P. B., Operation SANDSTONE, Part II, Ch 9, Vol 21, 1948







At the time of detonation a burst of noise occurred on all channels (Figure 3.1), and the beginning of this burst of noise was used as zero for the time base.

To examine the symmetry of the divergent air shock wave five instrument stations consisting of four Naval Ordnance Laboratory indenter gauges each were placed on the circumference of a circle having a radius of 1,700 feet about ground zero. For the underground shot four instrument stations consisting of four indenter gauges each were placed on the circumference of a circle having a radius of 1,200 feet about ground zero.

locations of all instrument stations for the surface and underground shots with respect to ground zero are shown in Figures 1.1 and 1.2. Instrumentation is discussed in Section 2.

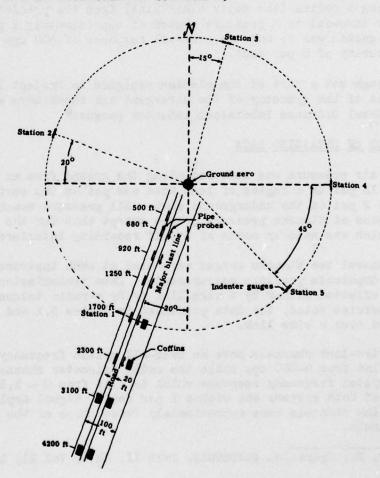
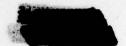


Fig. 1.1 Surface Shot Plan



PROJECT 1.4

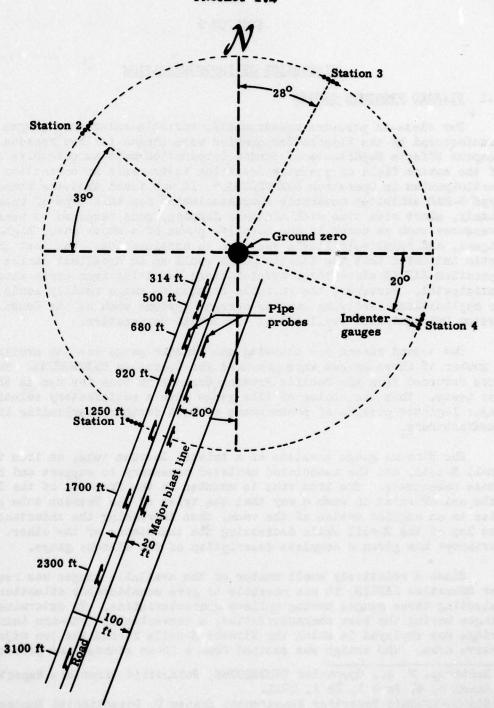


Fig. 1.2 Underground Shot Plan



SECTION 2

DISCUSSION OF INSTRUMENTATION

2.1 <u>VIANCEO PRESSURE GAUGES</u>

For close-in pressure measurements, variable-reluctance gauges manufactured by the Viancko Corporation were chosen for two reasons. The Weapons Effects Department of Sandia Corporation made an extensive survey of the entire field of pressure-measuring instruments in connection with participation in Operation GREENHOUSE.* It was found that the Viancko Type 3-PAD exhibited desirable characteristics for this type of operation, namely, short rise time with adequate damping, good response to near static pressures such as occur in the negative phase of a shock wave, high-level signal, and relatively little response to acceleration. The last characteristic indicated that the Viancko gauge would be an excellent choice for Operation JAMGLE since large accelerations resulting from earth shock were anticipated. Moreover, the variable-reluctance gauge readily lends itself to applications involving carrier current systems such as the Consolidated System D** equipment available at the Sandia Corporation.

The second reason for choosing the Wiancko gauge was its availability. A number of these gauges were procured for Operation GREENHOUSE. The gauges were returned from the Pacific Proving Grounds in time for use in the November tests. Thus the choice of this gauge gave a satisfactory solution to a major legistic problem of procurement without further overloading instrument manufacturers.

The Viancko gauge consists of a twisted Bourdon tube, an iron vane, a small B-coil, and the associated canister necessary to support and house these components. The iron vane is mounted on the free end of the Bourdon tube and oriented in such a way that the twist of the Bourdon tube gives rise to an angular motion of the vane, thus increasing the inductance of one leg of the B-coil while decreasing the inductance of the other.

Morthrop has given a complete description of the Wiancko gauge.

Since a relatively small number of the available gauges was required for Operation JANGLE, it was possible to give considerable attention to selecting those gauges having optimum characteristics. To determine the gauges having the best characteristics, a conventional four-arm inductance bridge was employed in which the Viancko E-coils formed the two adjacent active arms. The bridge was excited from a 10-kc source, and provision

^{**}Static-Dynamic Recording Measurement System D, Consolidated Engineering Corporation, Passdens, California.



[•] Morthrep, P. A., Operation GREENHOUSE, Scientific Directors Report, Annex 3, 4, Part 1, Ch 1, 1951.



PROJECT 1.4

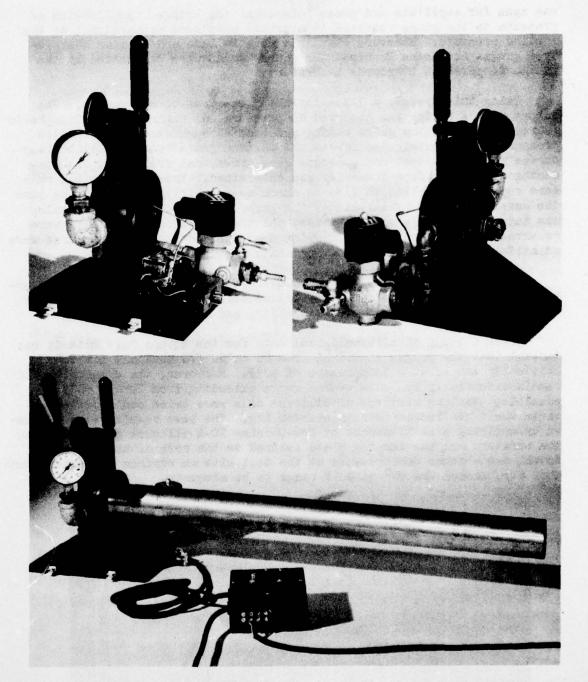
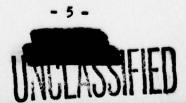


Fig. 2.1 Demping Jig with Shock Tube - Upper Photos are Damping Jigs Alone





was made for amplitude and phase balance of the bridge. Application of pressure to the gauge resulted in a bridge unbalance proportional to the applied pressure. Pressure standards were Wallace and Tiernan aneroid-type gauges and Heise Bourdon-tube gauges which were calibrated by the Sandia Corporation Standards Laboratory.

Using this system, a linearity check was made of all gauges. The eutput of the bridge was observed as pressure was changed from atmospheric (sero) to the maximum gauge rating and back through zero to a negative pressure approximately one fourth the maximum gauge rating. Calibration curves relating output and pressure were drawn, and from these the percentage deviation from linearity was determined. These calibration runs were repeated from time to time to check repeatability. At the same time the sensitivity and hysteresis of the gauge were determined. A catalog was made of the gauge sensitivities, and the most sensitive gauges were reserved for those positions in which the expected peak overpressures were relatively small (1/5 to 1/2 of the maximum gauge ratings).

In general all gauges were within the specified manufacturer's tolerances of less than 1.5 per cent of the measured pressure with respect to total hysteresis, drift, nonrepeatability, and nonlinearity.

After a study of climatological data for the Nevada Test Site it was decided that the gauges should be from 60 to 90 (75 nominal) per cent critically damped at a temperature of 40°F. Moreover, the damping should remain essentially the same over a range extending from 20° to 60°F if possible. Various mixtures of silicone oils were tried and rejected because their use led to extreme overdamping. The best results were obtained by applying a small amount of Dow-Corning DC-4 silicone grease between the armature and the damping plate secured to the core of the E-coil. Actual temperature measurements at the test site on surface and underground shot days showed the 20° to 60°F range to be adequate.

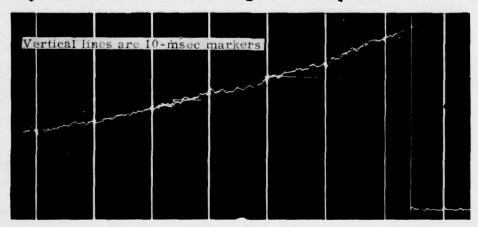
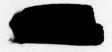


Fig. 2.2 Surface Shot-680-ft Station



To facilitate the damping adjustment, a special damping jig was constructed (Fig. 2.1) in which air under pressure is introduced into a reservoir enclosed by one or more sheets of cellophane. When the desired pressure is reached, the cellophane is punctured, and a rapid decrease of pressure results. The Bourdon-tube assembly is clamped in the jig in such a way that the reservoir pressure is applied to the tube while the armature and damping plate are accessible to the operator. Both rise time and damping can be determined from an analysis of the photograph of the gauge response as presented on an oscilloscope screen. Provision was made for the synchronization of the cellophane puncture with the start of the oscilloscope trace.

When DC-4 grease is used as the damping agent, a gauge properly damped at 40°F has an overshoot of about 15 per cent at 75°F. The gauge and damping jig were placed in a Bowser pressure-temperature chamber operated by the Electro-Mechanical Test Department of Sandia Corporation. The gauge response was examined at 10° steps from 70° to 0°F. Intervals varying from one-half to one hour were required for thermal equilibrium at each step. The relative humidity was held constant at 14 per cent. The shift in the balance point and changes in sensitivity were negligible over this temperature range.

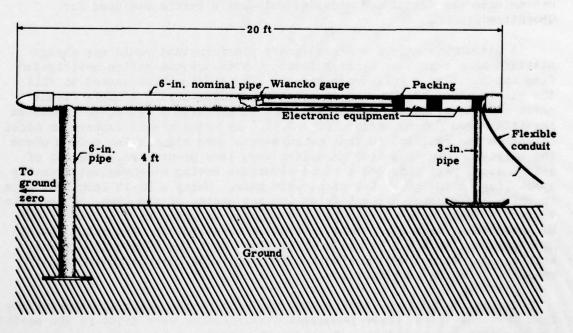
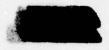


Fig. 2.3 Pipe Probe





Analysis of the oscillographs of the dynamic responses of the gauges at these temperatures showed that the gauges were somewhat overdamped at 20°F and somewhat underdamped at 50°F. When 10-psi gauges were checked dynamically in the Bowser chamber, the damping ranged between 10 and 80 per cent critical at 40°F, and a rise time of 0.40±0.10 msec to 95 per cent of the final pressure was observed. Thus it was concluded that this damping criterion was justified, i.e., the damping should allow a 15 per cent overshoot at 75°F.

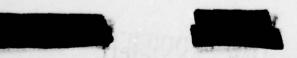
Figure 2.2 gives a representative trace from the oscillographic record of the surface shot. An average curve drawn through the overshoot and the noise envelope is superimposed on this record. The intersection of this curve with a vertical line drawn from the point of initial trace deflection was taken as the peak overpressure. Subsequent points were also obtained from the average curves on those channels in which the signal-to-noise ratio was low.

2.2 PIPE PROBE

The design of a baffle for measuring true 'free air' pressures was originally predicted on Operation WINDSTORM using a nominal A-bomb. For convenience the tested and accepted full-scale baffle was used for Operation JANGLE.

A search was made for a stationary platform that would not change attitude as a result of blast buffeting or the ground motion anticipated from the burst of a full-scale weapon. The baffle which seemed to fill the requirements best was a one-dimension baffle having a large fineness ratio and supported at the extreme ends to minimize pitch angle variation resulting from ground motion (Fig. 2.3). By using a 4-ft support an added advantage was realized in that measurements were made in the medium where the effects of surface-flow anomalies were less pronounced. The use of 6-inch steel pipe provided a rigid structure having a convenient mounting space (inside the pipe) for electronic gear. Using a 20-ft length of pipe in which the sensing element is at the top center of the span, calibration tests were made using high-explosive charges as great as 1.6 tons of TNT. No detectable discrepancy existed between measurements made using Wiancko gauges in the pipe baffle and mounted flush with the ground in a plane baffle. These data agreed within 1 per cent with interferometer gauge* readings from the same distance.

Choice of footings for the pipe was made on the basis of observations from previous tests, where permanent displacements were noted in the earth's surface near large craters. Consequently the front leg of 6-inch pipe was welded to a foot 18 inches in diameter and buried to a depth of 4 feet. The rear leg rested on the ground and terminated in a sled runner to permit surface motion.



AD-A078 577

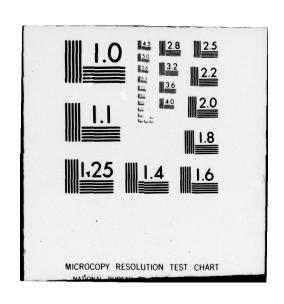
DEFENSE ATOMIC SUPPORT AGENCY WASHINGTON DC
OPERATION JANGLE. NEVADA PROVING GROUNDS, OCTOBER - NOVEMBER 19--ETC(U)
MAR 52

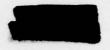
UNCLASSIFIED

AEC-WT-367

NL

END
DATE
FIRED
FIRED
FIRE
FIRED





The face of the Wiancko gauge was contoured to conform to the surface of the pipe. All gauges faced up since the pipe was more likely to change orientation because of yaw than because of pitch and since it was desirable to stay as far away from ground-roughness perturbations as possible.

2.3 INTERFEROMETER GAUGES

Self-recording interferometer gauges were installed at distances from surface-shot ground zero at which the anticipated radiation level was sufficiently low. To further minimize radiation effects and to provide air-baffling for such bulky equipment the gauges were buried flush with the earth (Fig. 2.4).

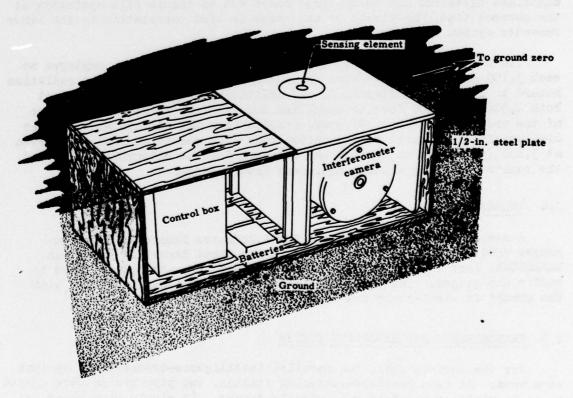
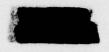


Fig. 2.4 Interferometer Coffin



Linegraph Ortho 35-mm film in 100-ft spools was chosen as the recording medium because of its high contrast, relative low sensitivity to radiation contamination, and availability. Sets conducted by the Bureau of Standards using 1,400-kv K-radiation indicate that data could be easily reduced after a 20-r radiation dose and could be reduced with some accuracy even after a 40-r dose.

Using quartz sensing elements having a maximum range of 3 to 5 psi and a recording speed of 30-40 ft/sec, a system response in excess of 2000 cps was assured.

The control system used for the interferometer received a turn-on signal and a 1000-cps timing pulse from the manned station, delivered over one pair of W-110-B wires serving all gauges. The coffin for each gauge contained batteries and delay-time relays set to insure film operation at the correct time. No tie-in to zero time or time correlation to the other recorder system was effected.

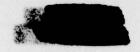
Two interferometer gauges were the only instrumentation employed at each 3,100 and 4,200-ft station for the surface shot. Since the radiation hazard to film was undetermined, one additional gauge was installed at both 2,300 and 1,700 feet to establish the marginal point for operation of the underground shot. However, results from the surface shot were so discouraging (extensive contamination made data reduction impossible even at 3,100 feet) that the system was scrapped for the underground shot and the remote-recording Wiancko equipment used throughout.

2.4 INDENTER GAUGES

A complete discription of the Naval Ordnance Laboratory indenter gauges used by this project is given in the Final Report of Operation SANDSTONE, Part II, Chapter 9, Volume 21, 1945. No attempt was made to baffle the gauges. The assembled instruments were installed flush with the ground on steel-stake mounts.

2.5 TRANSMISSION AND RECORDING SYSTEM

For the surface shot, two parallel intelligence-transmission systems were used. At each pressure-measuring station, two pipe probes were spaced so as to minimize the danger of missile damage. (A single pipe probe was located at 500 feet, but no record was obtained.) One probe was linked by radio telemetering equipment to a manned K35 trailer outfitted as a mobile recording laboratory. The other probe was linked to the same trailer by twisted-pair steel-copper telephone cables (Signal Corps W-110-B). Five such instrument stations were spaced logarithmically from 660-2, 300 feet. The positions of these stations relative to ground sero are given in Figure 1.1.



For the underground shot eight instrument stations were spaced logarithmically from 314-3, 100 feet. The positions of these stations relative to ground zero are given in Figure 1.2. Single pipe probes were used at each of the other stations. Radio telemetering was used only at the 1,700-ft station since preliminary evaluation of the surface shot data led to the conclusion that the wire link was more reliable. The pipe probe at 500 feet contained two Wiancko gauges in the wire link, one at 498 and one at 500 feet.

2.5.1 Wire Transmission System

A Static-Dynamic Recording Measurement System D. manufactured by the Consolidated Engineering Corporation, was used to excite the Wiancko gauge and demodulate the returning signal. The Consolidated equipment provides a 3000-cps carrier and a means of null-balancing the return carrier both in magnitude and phase. The Consolidated equipment was located in the K35 trailer, five miles west of the blast areas.

Signal Corps Type W-110-B field telephone cable was used to carry the carrier wave to the gauge and to return the modulated signal to the recording equipment.

The equipment, which was located in probes using this wirelinked system, consisted of the gauge and a coupling unit. A circuit diagram of this equipment is shown in Figure 2.5.

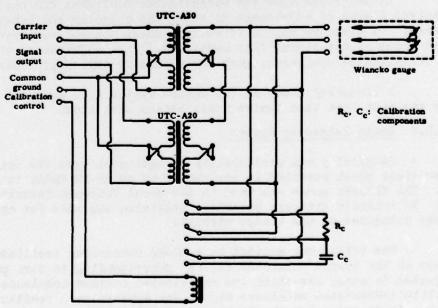
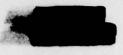


Fig. 2.5 Coupling Unit





Because of the unusually long lines used with the Consolidated equipment and the necessity of employing a carrier generator having very low output impedance, a 3000-cps 30-watt amplifier was used to deliver at least a 6-volt carrier to the gauge.

A simulated pressure was obtained for calibration purposes by means of a relay in the coupling unit. The relay inserted fixed electrical components into the bridge circuit and caused an unbalance equal to that which would result from a known applied pressure. The calibration pressures were based upon pressures predicted by Stanford Research Institute.

Following the original calibration in the instrument trailer, the coupling unit was installed in the probe and the calibration checked by applying pressure using a hand pump.

The decision to replace the telemetering system by the wire system for the underground shot required further modification of the measuring system. Four carrier lines supplied four gauges directly from the carrier amplifier. A second amplifier at 5000 feet from ground zero supplied the remaining eight gauges, each of which had a separate carrier line.

In addition, a single tube amplifier was placed in each signal return line at a distance of approximately 4000 feet from ground zero.

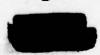
It was found that the Consolidated equipment did not provide a sufficient degree of adjustment to bring the outgoing and return carrier into phase. To overcome this difficulty a phase control was inserted in the grid input of the signal line amplifier. This adjustment, with that on the Consolidated equipment, gave the necessary degree of control.

A linearity check of the entire system from gauge to galvanometer was made less than twelve hours before each shot.

2.5.2 Radio Telemeter System

Simplicity and availability of equipment were the primary considerations which resulted in the choice of an AN-FN radio telemeter system. The Wiancko gauge was used in the usual four-arm inductance bridge. To indicate pressure polarity, provision was made for operation with some unbalance of the bridge circuit.

The bridge was excited by a 10-kc subcarrier oscillator. The magnitude of the bridge unbalance current corresponding to zero pressure was adjusted to about one-third the anticipated maximum unbalance current. The amplitude-modulated unbalance signal was applied to a reactance tube modulator, which modulated the frequency of a transmitter in the 70-90 maper-sec band.





The transmitter consisted of a Raytheon CK-5702 reactance tube, a CK-5702, 20-mc oscillator-doubler, and a CK-5702 40-mc buffer-doubler driving an RCA 5763 80-mc final amplifier. The r-f power output was approximately three watts. A quarter-wave vertical shunt-fed antenna was used.

The receiving antennas consisted of 3-element vertical Yagi arrays. The receivers were Navy Sonobouy RBF-3's whose audio amplifiers were modified to provide approximately 10 watts of a-f power. The 10-kc signal was fed to a full-wave bridge comprised of 1N39 germanium diodes. The demodulated signal was fed to the recorder through a 1,500 cps low-pass filter.

The Wiancko gauges used in the radio link were calibrated th through the entire radio telemeter system. Linearity of the system was within ± 1 per cent. Calibration signals were obtained by means of relays which shunted the bridge arms by suitable reactances which were chosen to simulate the maximum expected pressure.

The subcarrier oscillator, transmitter, calibration box, and battery power pack were located in the pipe probe. Power was applied to the electronic system by relays actuated by the -15-minute control, and the calibration relays were actuated by the -1-sec control signal. These control signals supplied by Edgerton, Germschausen, and Grier were transmitted from the recording trailer to the pipe probes by means of a 5-mile length of W-11-B cable.

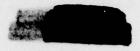
2.5.3 Recorder

All Wiancko gauge data were recorded using one Consolidated Engineering Corporation type 5-114P3 recording oscillograph. The 25-volt power supply for the oscillograph consisted of a bank of five 6-volt heavy-duty lead-acid storage batteries. Recording was initiated by the -1-sec control signal supplied by Edgerton, Germeshausen, and Grier.

Consolidated Engineering Corporation type 7-223 galvanometers were used to record the output of the wire-link system. These galvanometers have a flat (\pm 5 per cent) frequency response from 0 to 500 cps. The output of the radio telemetering system was recorded by Consolidated Engineering Corporation type 7-226 galvanometers having a flat (\pm 4 per cent) frequency response from 0 to 3000 cps and were 60 per cent critically damped.

To realize the higher frequency response inherent in the radiotelemeter system a recording speed of 75 in./sec was chosen. The recording medium was Kodak Linegraph Ortho film.



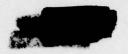


2.5.4 Critique of Data-Transmission Systems

The information-transmission system employing copper-steel field wire (M-110-B) proved reliable and practical although somewhat limited in frequency response. The cross-talk problem from a total of as many as 26 pairs buried in the same trench was insignificant. The use of field wire, which was procured from the military services, had the advantages of availability, economy, and mechanical strength. Splices and terminations were of the Stakon type. Therefore any lineman's crew could lay the 5-mile lengths of wire, and field terminations could be rapidly and efficiently made in adverse weather conditions without special equipment or techniques. Traffic, the blast wave, dust-control sprinkling, and weather proved to be no serious hazard to the wire since the most vulnerable portions were buried 1 to 3 feet below the surface. Further investigation of methods for transmitting high-frequency carrier signals on field wire will probably result in considerable improvement of the 500-cps resolution limit.

Frequency-modulated telemetering, despite the mediocre showing in this project, deserves some consideration. The system employed required on control line to each transmitter for turn-on and calibration. Even when using this system, but especially when using an all r-f setup (turn-on and calibration using a one-tube receiver), minimum preparation would be required to instrument a test. End instrument-transmitter packages could be placed in the test area as late as one day prior to the test, used, recovered, and stored for the next test.

However, it is doubtful that any atomic test will take place without last-minute unforeseeable radio interference that would seriously impair the reliability of a r-f system. Unless considerable attention is given to the problem of radio interference, the full advantage of a radio-telemetered system with respect to mobility and economy of time, expense, and personnel can not be realised.



SECTION 3

RESULTS AND CONCLUSIONS

3.1 DATA OBTAINED

Pressure-time-distance data for surface and underground shots are presented in Tables 3.1 and 3.2. Peak overpressure, time of arrival, and positive phase duration are plotted against distance from ground sero in Figures 3.2, 3.3 and 3.4. Pressure-time waveforms for the surface and underground shots are summarized in Figures 3.5 and 3.6.

Tables 3.3 and 3.4 contain indenter diameter data for the surface and underground shots. It is not necessary to rationalize indent-diameter with overpressure by determining the force constant for rapid rise time phenomena. The tabulation of diameters is sufficient to indicate that the measured phenomenon (regardless of its components) shows a marked symmetry. From analysis of the variants it is apparent that the symmetry of the measured phenomenon is greater than the precision of the measuring system.

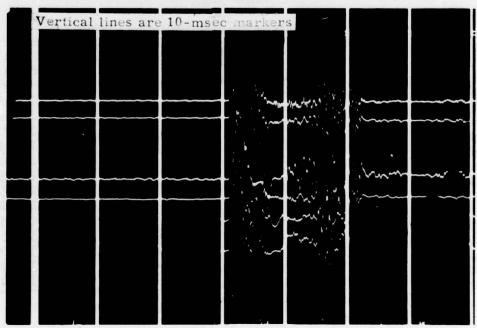
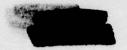


Fig. 3.1 Zero-Time Hoise Burst





PROJECT 1.4

TABLE 3.1

Pressure-Time-Distance Data, Surface Shot

Distance (ft)	2 ^t	Peak Overpressure (psi)	Time of Arrival (masc)	Positive Phase Duration (msec)
680	5.4	17.76	203	197
680(tel)		17.85	202	224
920(tel)	7.3	10.50	354	222
1250	7.3 9.95	7.02	593	303
1250(tel)		7.53	593 593•4	322.6
1700	13.5	4.07	947	381.5
1700(tel)		4.02	946	345.7
2300	18.2	5-144	1446	345.7 410.0
2300(tel)		2.64	1446	390.0
4200(int)	33-3	0.83	o treat	502.0

 $\dot{\tau} = \lambda$ based on a charge weight of 2 x 10⁶ lbs TMT

Tel - telemeter link Int - interferometer

TABLE 3.2

Pressure-Time-Distance Date. Under

Pressure-Time-Distance Data, Underground Shot				
Distance (ft)	λ [†]	Peak Overpressure (psi)	Time of Arrival	Positive Phase Duration (msec)
314 1498 500 6 60	2.5	32.39	122.5	100.2
498		13.57	228.2	170.8
500	3.96	13.57 14.39	229.0	160.0
680	3.96 5.4	9.90	348.7	206.8
680		10.09	348.0	201.0
920	7-3	7.30	520.5	238.5
920		7.07	521.5	287.5
1250	9-95	7.07 4.95 5.20	775.0	274.0
1250		5.20	774.5	254-5
1700	13.5	3.04	775.0 774.5 1134.5	314.5 335.0
1700(tel)		3.47	1134.0	335.0
2300	18.2	3.04 3.47 2.14	1636.3	363.0
3100	24.6	1.70	2322.0	387.0

+ = \lambda based on a charge weight of 2 x 10⁶ lbs THT Tel = telemeter link



AL TOMORY

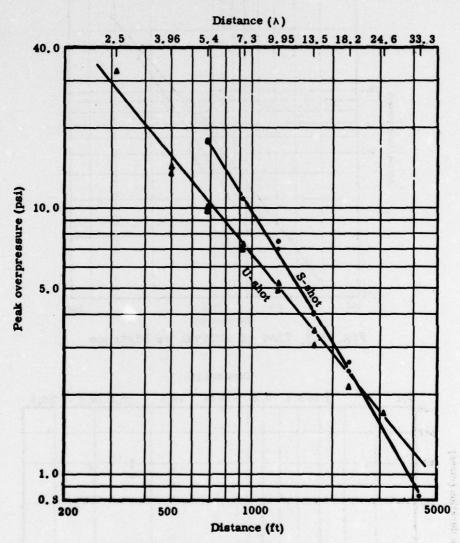


Fig. 3.2 Peak Overpressure vs Distance (Lines connecting data points are arbitrary.)

Ground acceleration may have introduced a systematic error into all readings of indenter gauges. However, a K-factor (force constant) of 50 psi/mm² can be derived from surface shot indenter data and the 1,700-ft peak air pressure, as measured by the Wiancko system. This same K-factor applied to the underground data resulted in agreement between indenter and Wiancko data at 1,250 feet, where ground accelerations were higher.



Distance ()

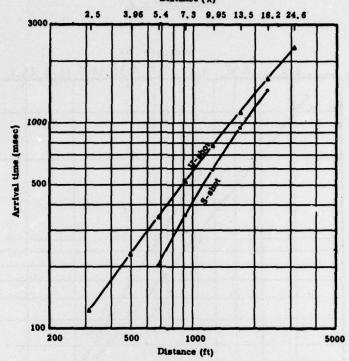


Fig. 3.3 Time of Arrival vs Distance

Distance (\(\lambda\)

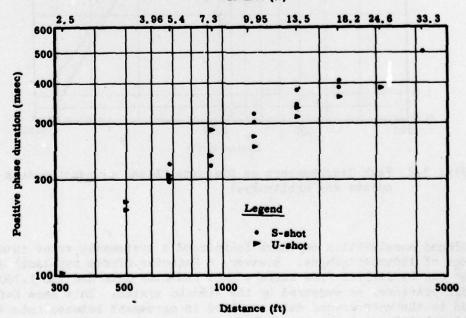
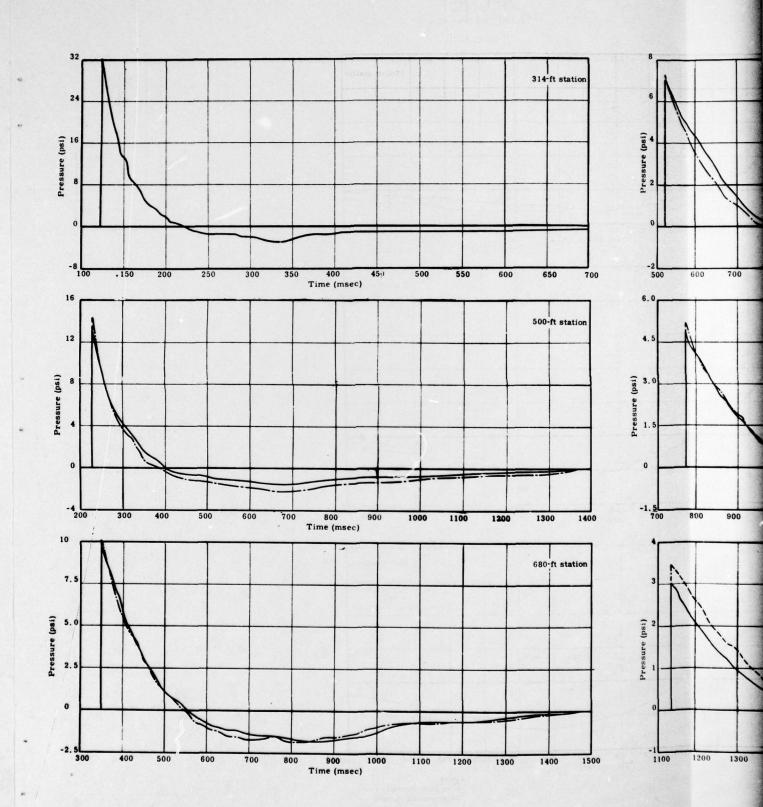
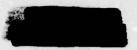


Fig. 3.4 Positive Phase Duration vs Distance











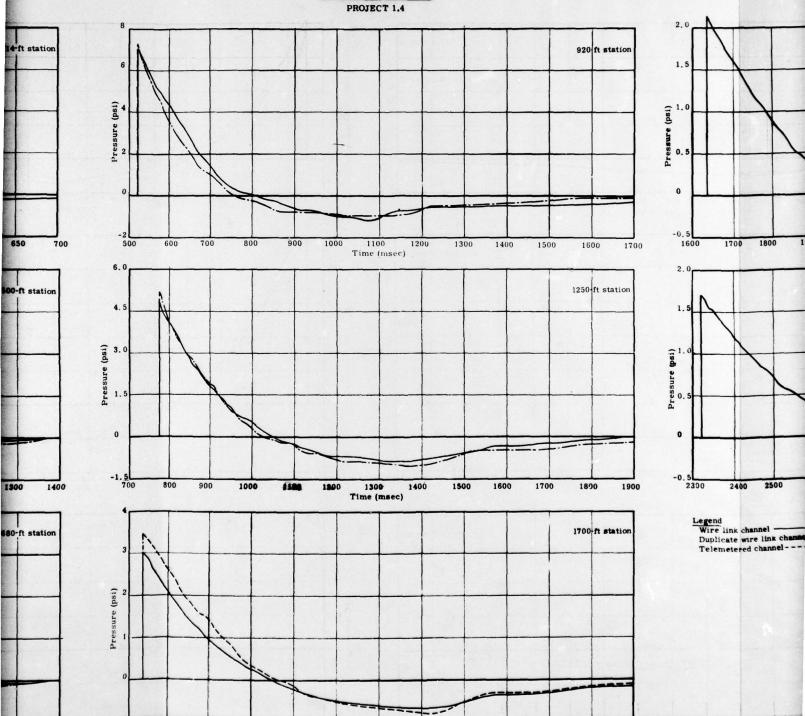
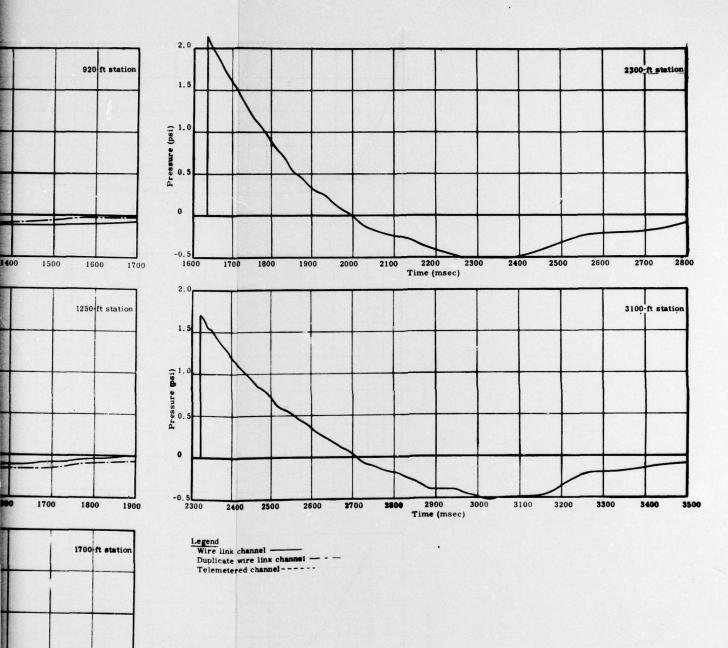


Fig. 3.6 Underground Shot Pressure-Time Curves

Time (msec)







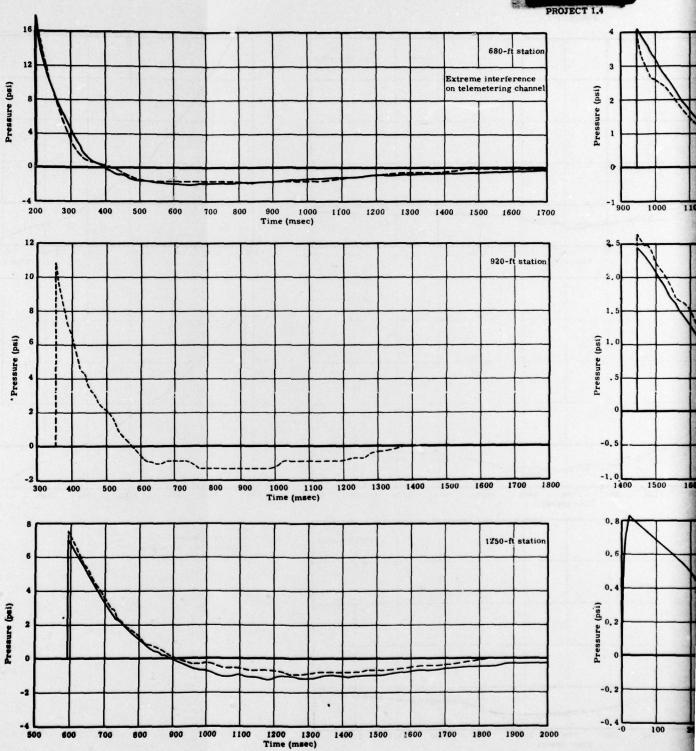


Fig. 3.5 Surface Shot Pressure-Time Curves



PROJECT 1.4 1700-ft statio rence channe Pressure (psi) 1600 170 Time (ssec) station 2300-ft station 2.0 1.5 Pressure (psi) -0.5 2100 2200 4200-ft station 0.6 Interferometer record (no time correlation) 0.4 Pressure (psi) -0.2 -0.4L Time (msec) Wire link channel
Telemetered channel Surface Shot Pressure-Time Curves

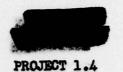


TABLE 3.3

Indenter Gauge Data, Surface Shot

Station	Gauge No.	Diameter (nm)	Diameter ²	Pressure (psi)
1	1 2 3 4	.255 .256 .306 .271	.0650 .0655 .0936 .0734	3.25 3.28 4.68 3.67 3.72 (ave)
2.	1 2 3 4	.280 .290 .237 .274	.0784 .0841 .0562 .0751	3.92 4.21 2.81 3.76 3.68 (ave)
3	1 2 3 4	.263 .273 .296 .298	.0691 .0745 .0876 .0888	4.00 (ave)
4	1 2 3 4	.304 .288 .268 .302	.0924 .0829 .0718 .0912	4.62 4.15 3.59 4.56 4.23 (ave)
5 10 1 s - 1	2 3 4	.292 .284 .297 .299	.0853 .0807 .0882 .0894	4.27 4.04 4.47 4.30 (ave)

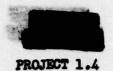
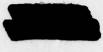


TABLE 3.4 Indenter Gauge Data, Underground Shot

Station	Gauge No.	Diameter (mm)	Diameter ²	Pressure (psi)
1	1 2 3 4	•336 •307 •339 •337	.113 .094 .115 .114	5.65 4.70 5.75 5.70 5.45 (ave)
2	1 2 3 4	•340 •341 •342 •346	.116 .116 .117 .120	5.80 5.80 5.85 6.00 5.86 (ave)
3	2 3 4	•337 •340 •353 •343	.114 .116 .125 .118	5.70 5.80 6.25 5.90 5.91 (ave)
1	2 3 4	•332 •334 •339 •332	.110 .112 .115 .110	5.50 5.60 5.75 5.50 5.59 (ave)

The data gathered are useful for correlating blast strengths with observed damage to structures of Program Three, for distinguishing airinduced ground sheaks from true ground phenomena (air-to ground coupling, and as source material for any application study.



3.2 CONCLUSIONS

It is apparent from the pressure-time curves for both underground and surface shots that the shape of the shock wave conforms generally to the classic form as described in The Effects of Atomic Weapons.*

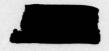
The system (including data reduction) permitted time resolution to 0.5 macc. Within this limitation the pressure discontinuity at the shock front appears instantaneous in most instances. *

Pressure-distance data were within 10 per cent of anticipated values, based on Stanford Research Institute extrapolations from scaled TMT blasts at DUGWAY and early JANGLE tests.** Extrapolation of air shock data from surface and underground TMT tests appears valid for surface and underground atomic blasts.

^{*} The Effects of Atomic Weapons, Section 3.11, Los Alamos Scientific Laboratory, U. S. Government Printing Office, 1950.

^{*} For a discussion rise-time phenomena from other atomic blasts see Murphey, B. F., Operation BUSTER - Some Measurements of Overpressure-Time vs Distance for Airburst Bombs, Sandia Corporation report No. SC-2142 (tr) (to be published).

^{**} Doll, E. B. Interim Report - Part II HE tests - Operation JANGLE, Stanford Research Institute, October 1951, Figs. 5 and 6.



APPENDIX A

PERSONNEL PARTICIPATING IN PROJECT 1.4

From Sandia Corporation, Albuquerque, N. N.

G. W. Burnside

W. J. Howard

J. C. Hughes

R. D. Jones

F. W. Loomis

D. G. Palmer

1. J. Vulgan

H. E. Waldorf

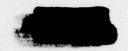
From Armed Forces Special Weapons Project, Washington D. C.

Lt. Col. L. F. Lawson

From 1st Tactical Support Squadron, Sandia Base, Albuquerque, M. M.

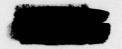
M/Sgt. B. R. Smith Sgt. L. F. Roberson

- 25 -



DISTRIBUTION

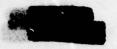
	Copy	MO.
ARMY ACTIVITIES		
Aset. Chief of Staff, G-1, Department of the Army, Washington 25, D. C.		1
Asst. Chief of Staff, G-2, Department of the Army, Washington 25, D. C.		2
Asst. Chief of Staff, G-3, Department of the Army, Washington 25, D. C.	3-	6
Asst. Chief of Staff, G-4, Department of the Army, Washington		11
25, D. C. Chief of Ordnance, Department of the Army, Washington 25, D. C. Chief Chemical Officer, Temp. Bldg. T-7, Room G-522, Gravelly	12-	
Point, Va. Chief of Engineers, Temp. Bldg. T-7, Room G-425, Gravelly	15-	18
Point, Va.	19-	21
The Quartermaster General, Second and T Sts. SW, Room 1139A, Washington 25, D. C.	22-	26
Chief of Transportation, Temp. Bldg, T-7, Room G-816, Gravelly Point, Va.	27-	28
Chief Signal Officer, Department of the Army, Washington 25, D. C.	29-	31
The Surgeon General, Main Navy Bldg., Room 1651, Washington 25, D. C.	32-	34
Provost Marshal General, Main Navy Bldg., Room 1065, Washington 25, D. C.	35-	
Chief, Army Field Forces, Fort Monroe, Va. President, Army Field Forces Board No. 1, Fort Bragg, N. C.	38-	41
President, Army Field Forces Board No. 2, Fort Knox, Ky. President, Army Field Forces Board No. 3, Fort Benning, Ga.		43
President, Army Field Forces Board No. 4, Fort Bliss, Tex. Commandant, The Infantry School, Fort Benning, Ga.	46-	45
Commandant, The Armored School, Fort Knox, Ky. President, The Artillery School Board, Fort Sill, Okla.	48-	49
Commandant, The AA&GM Branch, The Artillery School, Fort Bliss,	52-	
Commandant, Army War College, Carlisle Barracks, Pa. Commandant, Command and General Staff College, Fort Leaven-	54-	
worth, Kans. Commandant, Army General School, Fort Riley, Kans.	56-	57 58



DISTRIBUTION (Continued)	Copy No.
Commendation Commend Telephone Commendation Toland New York	
Commanding General, First Army, Governor's Island, New York 4,	59- 60
N. Y.	61- 62
Commanding General, Second Army, Fort George G. Meade, Md.	63- 64
Commanding General, Third Army, Fort McPherson, Ga.	65- 66
Commanding General, Fourth Army, Fort Sam Houston, Tex.	07- 00
Commanding General, Fifth Army, 1660 E. Hyde Park Blvd., Chicago 15, Ill.	67- 68
Commanding General, Sixth Army, Presidio of San Francisco,	
Calif.	69- 70
Commander-in-Chief, European Command, APO 403, c/o Postmaster,	
New York, N. Y.	71- 72
Commander-in-Chief, Far East, APO 500, c/o Postmaster, San	
Francisco, Calif.	73- 74
Commanding General, U. S. Army, Pacific, APO 958, c/o Post-	
master, San Francisco, Calif.	75- 76
Commanding General, U. S. Army, Caribbean, APO 834, c/o Post-	
master, New Orleans, La.	77- 78
Commanding General, U. S. Army, Alaska, APO 942, c/o Post-	
master, Seattle, Wash.	79- 80
Director, Operations Research Office, 6410 Connecticut Ave.,	
Chevy Chase, Md.	81- 83
Commanding Officer, Ballistic Research Laboratories, Aberdeen	
Proving Ground, Aberdeen, Md.	84- 85
Commanding Officer, Engineer Research and Development Labora-	THE STATE OF THE
tory, Fort Belvoir, Va.	86- 87
Commanding Officer, Signal Corps Engineering Laboratories, Fort	10 70 10
Monmouth, N. J.	88- 89
Commanding Officer, Evans Signal Laboratory, Belmar, N. J.	90- 91
Commanding General, Army Chemical Center, Md. ATTN: Chemical	
and Radiological Laboratory	92- 93
NAVY ACTIVITIES	
Chief of Naval Operations, Department of the Navy, Washington	
25, D. C. ATTN: Op-36	94- 95
	34- 37
Chief, Bureau of Ships, Department of the Navy, Washington 25, D. C.	96- 99
Chief, Bureau of Ordnance, Department of the Navy, Washington	
25, D. C.	100
Chief, Bureau of Medicine and Surgery, Department of the Navy,	
Washington 25, D. C.	101-102
Chief, Bureau of Aeronautics, Department of the Navy, Wash-	
ington 25, D. C.	103-104
Chief, Bureau of Supplies and Accounts, Department of the Navy,	
Washington 25, D. C.	105-106
Chief, Bureau of Yards and Docks, Department of the Navy,	
Washington 25, D. C.	107-109



DISTRIBUTION (Continued)	Coly No.
Chief of Naval Personnel, Department of the Navy, Washington 25, D. C.	110
Commandant of the Marine Corps, Washington 25, D. C.	111-113
Commander-in-Chief, U. S. Pacific Fleet, Fleet Post Office,	
San Francisco, Calif.	114
Commander-in-Chief, U. S. Atlantic Fleet, Fleet Post Office,	
	115
New York, N. Y.	116
President, U. S. Naval War College, Newport, R. I.	
Commandant, Marine Corps Schools, Quantico, Va.	117-118
Chief of Naval Research, Department of the Navy, Washington	
25, D. C.	119-120
Commander, U. S. Naval Ordnance Laboratory, Silver Spring 19,	
Md.	121
Commander, U. S. Naval Ordnance Laboratory, Silver Spring 19,	
Md. ATTN: Aliex	122
Director, U. S. Naval Research Laboratory, Washington 25, D. C.	123
	25
Commanding Officer and Director, U. S. Naval Electronics	201
Laboratory, San Diego 52, Calif.	124
Commanding Officer, U. S. Naval Radiological Defense Labora-	
tory, San Francisco 24, Calif.	125-128
Commanding Officer and Director, David Taylor Model Basin,	
Washington 7, D. C.	129
Commander, Naval Material Laboratory, New York Naval Shippard,	
Naval Base, New York 1, N. Y.	130
Officer-in-Charge, U. S. Naval Civil Engineering Research and	
Evaluation Laboratory, U. S. Naval Construction Battalion	121 120
Center, Port Hueneme, Calif.	131-132
Commanding Officer, U. S. Naval Medical Research Institute,	
National Naval Medical Center, Bethesda 14, Md.	133
Commander, U. S. Naval Ordnance Test Station, Inyokern, China	
Lake, Calif.	134
AIR FORCE ACTIVITIES	
Assistant for Atomic Energy, Headquarters, United States Air	
	125-126
Force, Washington 25, D. C.	135-136
Director of Operations, Headquarters, United States Air Force,	
Washington 25, D. C. ATTN: Operations Analysis Division	137-138
Director of Plans, Headquarters, United States Air Force,	
Washington 25, D. C. ATTN: AFOPD-P1	139
Director of Requirements, Headquarters, United States Air	
Force, Washington 25, D. C.	140
Director of Research and Development, Headquarters, United	
States Air Force, Washington 25, D. C.	141-142
Director of Intelligence, Headquarters, United States Air Force,	
Washington 25, D. C. ATTN: Phys. Vul. Branch, Air Targets	162-161
Division	143-144



DISTRIBUTION (Continued)

	Copy No.
Director of Installations, Headquarters, United States Air	
Force, Washington 25, D. C.	145
Asst. for Development Planning, Headquarters, United States Air	
Force, Washington 25, D. C.	146
Asst. for Materiel Program Control, Headquarters, United States	
Air Force, Washington 25, D. C.	147
The Surgeon General, Headquarters, United States Air Force,	
Washington 25, D. C.	148
Commanding General, Strategic Air Command, Offutt Air Force	
Base, Nebr.	149-151
Commanding General, Air Research and Development Command, P.O.	
Box 1395, Baltimore 3, Md.	152-161
Commanding General, Air Materiel Command, Wright-Patterson Air	
Force Base, Dayton, Ohio	162-163
Commanding General, Air Materiel Command, Wright-Patterson Air	ARTER P. C.
Force Base, Dayton, Ohio. ATTN: Air Installations Division	164-165
Commanding General, Tactical Air Command, Langley Air Force	
Base, Va.	166-168
Commanding General, Air Defense Command, Ent Air Force Base,	
Colo.	169-171
Commanding General, Air Proving Ground, Eglin Air Force Base,	TOTAL CO.
Fla.	172-173
Commanding General, Air Training Command, Scott Air Force Base,	3-1 3-6
Belleville, Ill.	174-176
Commanding General, Air University, Maxwell Air Force Base,	300 300
Montgomery, Ala.	177-179
Commanding General, Special Weapons Center, Kirtland Air Force	100 100
Base, N. Mex.	180-182
Commanding General, 1009th Special Weapons Squadron, 1712 G St.	183
NW, Washington 25, D. C.	103
Commanding General, Wright Air Development Center, Wright-	184-187
Patterson Air Force Base, Dayton, Ohio	104-101
Commanding General, Air Force Cambridge Research Center, 230	188-189
Albany St., Cambridge 39, Mass.	100-109
Commanding General, U. S. Air Forces in Europe, APO 633, c/o	100 101
Postmaster, New York, N. Y.	190-191
Commanding General, Far East Air Forces, APO 925, c/o Post-	192-193
master, San Francisco, Calif.	192-193
Commanding General, Air Force Missile Center, Patrick Air Force	194
Base, Cocoa, Fla.	194
Commandant, USAF School of Aviation Medicine, Randolph Air	105
Force Base, Randolph Field, Tex. Asst. to the Special Asst., Chief of Staff, United States Air	195
	196
Force, Washington 25, D. C. ATTN: David T. Griggs The RAND Corporation, 1500 Fourth St., Santa Monica, Calif.	197-198
The Man Corporation, 1900 Fourth St., Santa Montea, Call.	T3 (-T30



DISTRIBUTION (Continued)

AFSWP ACTIVITIES	Copy No.
Chief, Armed Forces Special Weapons Project, P.O. Box 2610, Washington 13, D. C.	199-207
Commanding General, Field Command, Armed Forces Special Weapons Project, P.O. Box 5100, Albuquerque, N. Mex.	208-213
OTHER ACTIVITIES	
Chairman, Research and Development Board, Department of De-	214
fense, Washington 25, D. C. Director, Weapons System Evaluations Group, Office of the	
Secretary of Defense, Washington 25, D. C. Executive Director, Committee on Atomic Energy, Research and	215
Development Board, Department of Defense, Washington 25, D. C. ATTN: David Beckler	216
Executive Director, Committee on Medical Sciences, Research and Development Board, Department of Defense, Washington 25,	
D. C.	217
U. S. Atomic Energy Commission, Classified Document Room, 1901 Constitution Ave., Washington 25, D. C. ATTN: Mrs. J. M.	
O'Leary	218-220
Los Alamos Scientific Laboratory, Report Library, P.O. Box 1663, Los Alamos, N. Mex. ATTN: Helen Challenger	221-223
Sandia Corporation, Classified Document Division, Sandia Base,	
Albuquerque, N. Mex. ATTN: Wynne K. Cox	224-243